AN ABSTRACT OF THE DISSERTATION OF

Timothy M. Lewis for the degree of Doctor of Philosophy in
Electrical and Computer Engineering presented on March 18, 2014.

Title: A Remotely Operated, Autonomous Wave Energy Converter System

Abstract approved: _____
Annette R. von Jouanne

The potential for electric energy generation from ocean waves is substantial and much research is being conducted on the conversion process as a renewable, grid-connected, power source. Some of the same attributes that make wave energy harvesting attractive as a grid-connected source also make it attractive as a remote, or isolated, ocean energy source. The advantages for autonomous applications such as energy persistence and energy density, as well as challenges such as system complexity, maintainability, and cost, will be explored. First, a survey of wave energy fundamentals, generation, conversion devices, and converter control will be completed. Then remote ocean applications that require electrical power will be reviewed. The requirements for an isolated, or remote, wave energy generation device will be summarized and a candidate set of ocean power device requirements chosen. Ocean wave energy options will be generated and their use as a remote ocean power source will be explored. A potential solution will be proposed, designed, fabricated, and tested in a wave energy laboratory. Control methods to attempt to maximize power will be designed and implemented and then compared to classical damping control.

A Remotely Operated, Autonomous Wave Energy Converter System

by

Timothy M. Lewis

A DISSERTATION

submitted to

Oregon State University

in partial fulfillment of
the requirements for the
degree of

Doctor of Philosophy

Presented March 18, 2014
Commencement June 2014

Doctor of Philosophy dissertation of Timothy M. Lewis presented on March 18, 2014.

APPROVED:

_____

Major Professor, representing Electrical and Computer Engineering

_____

Director of the School of Electrical Engineering and Computer Science

_____

Dean of the Graduate School

I understand that my dissertation will become part of the permanent collection of Oregon State University libraries. My signature below authorizes release of my dissertation to any reader upon request.

_____

Timothy M. Lewis, Author

ACKNOWLEDGEMENTS

I would first like to thank my committee members Dr. Annette von Jouanne, Dr. Ted Brekken, Dr. Raviv Raich, Dr. Thinh Nguyen, Dr. Ethan Minot, and Dr. Roberto Albertani. I want to give special thanks to Dr. von Jouanne for the opportunity, steady guidance, and patience. I also thank fellow student Bret Bosma who assisted with mooring design, wave energy converter fabrication, and collaboration in the final integration and wave lab testing. Manfred Dittrich was also instrumental for fabrication support and ideas, and constant enthusiasm.

I acknowledge support for this work from the US Department of Energy (Award Number DE-FG3608GO18179) for the Northwest National Marine Renewable Energy Center (NMMREC).

Finally I would like to thank all family and friends who provided support and encouragement over these four years.

TABLE OF CONTENTS

Page

TABLE OF CONTENTS (Continued)

TABLE OF CONTENTS (Continued)

TABLE OF CONTENTS (Continued)

TABLE OF CONTENTS (Continued)

TABLE OF CONTENTS (Continued)

Page

TABLE OF CONTENTS (Continued)

TABLE OF CONTENTS (Continued)

TABLE OF CONTENTS (Continued)

LIST OF FIGURES

Figure Page

LIST OF FIGURES (Continued)

LIST OF FIGURES (Continued)

Figure Page

LIST OF FIGURES (Continued)

Figure Page

LIST OF FIGURES (Continued)

LIST OF TABLES

1 Introduction

1.1 Background

Ocean waves have a tremendous potential for electric energy generation, both as a renewable, grid-connected, power source; and as an energy harvesting source for use onboard a remote ocean platform. These remote ocean platforms can utilize ocean wave energy for all or some of the onboard energy needs. Some uses for these platforms are weather or tsunami buoys, ocean surveillance buoys, or potentially unmanned sea platform charging stations. This work is concerned with remotely generating and utilizing the energy onboard these remote, or autonomous, ocean platforms. This remote ocean wave energy converter throughout this research is referred to as the Autonomous Wave Energy Converter (AWEC).

The selected solution for the AWEC was a two-body point absorber. A detailed analysis of the prospective operating location and conditions was performed and a design was completed, fabricated, and tested – both on a land based test fixture and in an ocean wave laboratory. The goal of the research was to link the design, and specifically, the use of linked hydrodynamic and power generating finite element analysis (FEA), to actual wave tank performance data to validate the design and the modeling techniques.

This thesis contains six (6) chapters in manuscript format that contain the bulk of the work. They cover the literature research, system engineering and basic conceptual analysis through detailed wave energy converter design through actual wave tank testing.

1.2 Wave Energy Conversion System for Remote and Autonomous Applications (Chapter 2)

This paper utilized for the qualification examination first presents wave energy fundamentals and the derivation of the power per unit width for a wave. It presents an overview of the regional and climatic variation of ocean wave energy around the

world. Due to the variability and storm conditions a set of operating regions for a wave energy device are discussed. A review of the general classification of wave energy devices is discussed, and then a detailed description of prior direct drive wave energy converters is presented. The first order impedance matching methods for control of the power take-off (PTO) are reviewed, and then additional potential control and analysis methods are discussed. A review of the potential uses for a remote wave energy converter is presented and from this a list of general requirements are formulated. These requirements are then given nominal quantitative numbers that will be used for this future research. From these requirements device characteristics are presented and then formulated into a concept design for future work.

1.3 Per-Unit Wave Energy Converter Analysis (Chapter 3)

This work first provides a more detailed formulation of the Morison linearized hydrodynamic model that will be used later to characterize and control the wave energy converter. A detailed free body diagram of the concept point absorbing converter is given which includes the rotating inertias and the linear-to-rotational roller screw arrangement. Since the AWEC is still conceptual at this point analysis can be performed in a generalized, or per-unit, manner. This allows for the comparison of different geometries for general characteristics while abstracting the scale of the device. A previous design geometry was utilized, along with a specific ocean location's wave characteristics, to then run a series of Simulink simulations to compare different control methods. The term 'resonance ratio' was used to quantify the difference between the natural resonance of wave energy converter and the ocean spectra's dominant frequency. It was validated that optimal control which adds a reactive control term in addition to the power absorbing control term yields greater average power output but requires a power take-off with a much larger power, or kVA, capacity. Also significant was the result that the larger the resonance ratio, or the farther the natural resonating frequency of the converter is from the wave being tuned to, required much more power take-off capacity. A comparison with damping

only control resulted in less power output but a much smaller power take-off capacity requirement.

1.4 Wave Energy Converter with Wideband Power Absorption (Chapter 4)

This paper first presented wave spectra from three different world-wide locations to demonstrate the fairly different wave spectra that are present in the world. Some spectra may be fairly narrowband but other spectra have either a wider bandwidth, or in some cases multiple dominant frequencies. This paper formulated the term 'power capture bandwidth' to describe and quantify the frequency range in which a wave energy converter can effectively absorb power. The first order bandwidth of a previous wave energy converter using optimal control was derived and plotted. This converter was then simulated with Simulink using the different wave spectra to highlight the result that a significant amount of the wave's energy cannot be absorbed due to the limited bandwidth of the wave energy converter. Based on matching and filter design techniques two proposed controller architectures were presented. The L-section matching filter actually yields a smaller bandwidth than the baseline optimally controlled converter. The resonating Cauer filter yielded a wider bandwidth and could be pursued though it did cause resonating velocities in the time domain.

1.5 Modeling and Control of a Slack-Moored Two-Body Wave Energy Converter with Finite Element Analysis (Chapter 5)

This paper first presents a more detailed summary of United States near-coastal wave conditions. Since an AWEC must provide the specified power even in low wave conditions, this focused on the summer month averages from these locations. From this a candidate condition of a wave spectra with a significant wave height of 0.65 m and a dominant period of 6 seconds was used for the preliminary design of the AWEC. Details of the physical design were derived and a finite element model of the design was constructed. Since the design has two moving bodies an equivalent circuit was

constructed that extended the single-body equivalent circuit. A method using the finite element analysis program was constructed to be able to derive all of the terms of the equivalent circuit. The methodology utilized was to fix one body to the ocean floor then tune for maximum power. That, and the knowledge of accurate physical modeling, allows one to extract the parameters. The resulting two-body equivalent circuit is then formulated from the single-body parameters. Again tuning for maximum power the two-body Thevenin equivalent circuit is within 5% of the damping term and 20% for the reactive term as compared to the FEA analysis model. The paper concluded with a parameter sweep in wave height and period comparing the equivalent circuit with the FEA analysis.

1.6 Modeling of a Two-Body Wave Energy Converter Driven by Spectral JONSWAP Waves (Chapter 6)

This paper extended the FEA design analysis and performance assessment from monochromatic to spectral waves. In addition the two-body equivalent circuit was implemented in SPICE for use in comparison with the FEA analysis. First a monochromatic wave was used to compare both damping and binary optimal control between SPICE and the FEA analysis. Power output using damping control was approximately 50% that of binary optimal control. Spectral waves were then described and an equivalent for the target environment of Galveston, TX was utilized. FEA analysis results were then obtained using both damping and binary optimal control with these spectral waves and compared to the monochromatic output. Under both control methods the power output with spectral waves was approximately 50% of that with monochromatic waves. A ternary control method (using two reactive series control components) was formulated to potentially provide a more wideband control. It is shown with spectral plots that due to the complexity of the two-body converter this does not materialize in a significant way. Also if any significant power take-off losses are incorporated, the minor benefit of the proposed ternary controll tends to zero. Also with the included power take-off damping losses any optimal, or reactive,

control should be reassessed in view of the disadvantages (increased power take-off kVA requirements and increased physical differential travel).

1.7 Hinsdale Wave Research Laboratory Testing and Results (Chapter 7)

The testing and instrumentation of the O.H. Hinsdale Wave Research lab is discussed. Results are shown for damping control, binary (2 term – real and reactive) control, and ternary control (3 term) control. Correlation to prior finite element modeling is completed. Conclusions are discussed in this section since it was the culmination of the full research into AWECs.

1.8 Conclusions and Future Research (Chapter 8)

Lessons learned and possibilities for future research are discussed.

Note

With the manuscript format the paper are being kept in their original form. Any realized corrections are listed below:

- When the term power absorption spectrum is used it has a transfer function that is termed as an impedance. As graphed it is really and admittance so it should be Y_{WEC}.

A REMOTELY OPERATED, AUTONOMOUS WAVE ENERGY CONVERTER SYSTEM

Timothy M. Lewis

School of Electrical Engineering and Computer Science

1148 Kelley Engineering Center

Oregon State University

Corvallis, USA

lewisti@eecs.oregonstate.edu

Oregon State University Qualification Exam

February 2, 2010

2 A Remotely Operated, Autonomous Wave Energy Converter System

Abstract - The potential for electric energy generation from ocean waves is substantial and much research is being conducted on the conversion process as a renewable, grid-connected, power source. Some of the same attributes that make wave energy harvesting attractive as a grid-connected source also make it attractive as a remote, or isolated, ocean energy source. The advantages such as energy persistence and energy density, as well as challenges such as system complexity, maintainability, and cost, will be explored. First, a survey of wave energy generation, description, wave energy conversion devices, and converter control will be completed. Then remote ocean applications that require electrical power will be reviewed. The requirements for an isolated, or remote, wave energy generation device will be summarized and a candidate set of ocean power device requirements chosen. Ocean wave energy options will be generated and their use as a remote ocean power source will be explored (future). A potential solution will be proposed with suggested future work.

Symbol Definitions (units)—

a: Wave amplitude (m)

A : Area (m^2)

B_b*:* Buoy hydrodynamic damping (N·s/m)

B_g*:* Apparent generator hydrodynamic dampening (N·s/m)

g: Gravitational acceleration (9.81 m/s^2)

H_s*:* Significant wave height, peak to trough (m)

λ*:* Wavelength (m)

K_b*:* Buoy buoyancy (N/m)

K_g: Apparent generator buoyancy (N/m)

M_b: Mass of buoy (kg)

M_g: Apparent generator mass (kg)

P : Power (W)

ρ: Density of sea water (kg/m^3)

T: Wave period (s)

v_g : Wave group velocity (m/s)

v_p : Wave phase velocity (m/s)

W: Width of a wave crest (m)

Z_b: Impedance of buoy (Ω)

Z_g: Impedance of incident wave (Ω)

Index Terms— Ocean wave energy, remote power generation, direct drive generator, linear generator, rotary generator.

2.1 Introduction

Wave energy is recognized as a potential source for energy harvesting. Direct energy from the immediate ocean environment may be of particular interest for remote or isolated ocean applications since the local wave energy source is persistent and maintains a minimum power level in most ocean environments. Waves have several advantages over other forms of localized energy to harvest such as wind and solar, since the energy is more persistent, predictable, and offers a higher energy density. Wave energy converters can then extract more power from a smaller volume at a

consequential lower cost and reduced visual impact. These initial qualitative advantages make wave energy worthy of analysis as a remote ocean power source. This paper will explore a particular wave energy converter (WEC) device solution, the point absorber, for use in a remote, or isolated, application.

2.2 Wave Energy Creation

Waves are created by wind blowing across a large body of water. Once troughs start to form they are further accentuated by the increased surface tension on the peaks and the decreased surface tension in the troughs. A washboard effect occurs and the wave created moves in the direction of the wind. Fig. 2 shows a simplified representation of a mono-chromatic (single frequency) wave. Waves generated over large area of water will have large differences in potential energy, with the maximum energy at the end of a prevailing wind travel. An example is the high amount of wave energy in the Pacific Northwest coast from the usual west-to-east prevailing winds in that region of the world.

2.3 Wave Phase and Group Velocity

can be characterized by two distinct velocities that can be described by generalized wave theory. These velocities are the wave velocity and the group velocity. Wave velocity is the amount of movement per time from the peak to the following peak set up as a standing wave. This wave velocity is the same as the standing velocity set up on a constrained string. The velocity of an ocean wave is [1]:

$$v_p = \sqrt{\frac{g\lambda}{2\pi}} \tag{1}$$

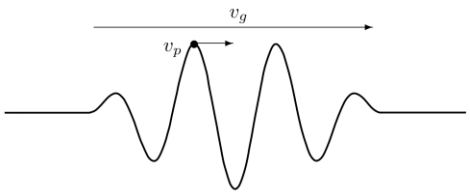

Fig. 1. Wave Energy Packet

Group velocity is the velocity of a packet of waves as they move across the body of water. This group velocity is the speed that energy is transmitted across the water surface. For water waves it is defined as [1]:

$$v_g = \frac{1}{2} v_p = \frac{1}{2}\sqrt{\frac{g\lambda}{2\pi}} \ \left[\frac{m}{s}\right] \tag{2}$$

The relationship between phase and group velocity is shown in Fig. 1.

2.4 Monochromatic Wave Assumption

The rate of wave energy accumulation will increase and decrease due to the wind speed and other effects as it moves in its direction of travel. Water is a dissipative medium so at one extreme the wave energy would dissipate to zero if the wind speed decreased accordingly. For example, a wave's energy moving outward from a stone being dropped in a pond decreases to zero.

For analysis of a wave energy device that is fixed in location, the assumption will be that the wave is a simple sinusoid and that its wavelength and amplitude may vary over large time frames (see later section with respect to climatic variability). This variability is the subject of wave energy prediction which is outside of the scope of this survey paper.

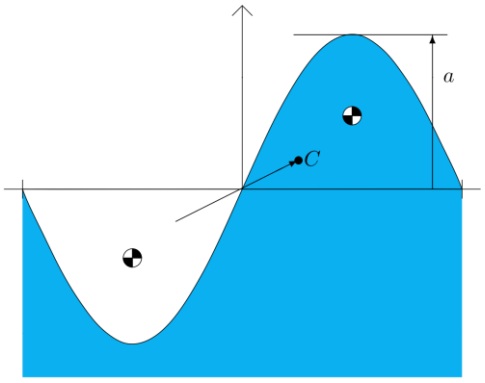

Fig. 2. Monochromatic Wave Dimensions

2.5 Wave Energy Derivation

Fig. 2, again, shows a monochromatic wave to use for analysis [2]. The potential energy of the wave per single wavelength and per unit along the length of the wave would be:

$$E_p = \left(\frac{1}{\lambda}\right) \rho g \int_0^{\lambda} \int_0^{a \sin(2\pi x/\lambda)} z \, dz \, dx \tag{3}$$

which has the solution:

$$E_p = \frac{1}{4} \rho g a^2 \ \left[\frac{J}{m^2}\right] \tag{4}$$

At a time of quasi-equilibrium, the wave potential energy is equal to the kinetic energy of the wave so the total energy is twice the potential energy or:

$$E = \frac{1}{2} \rho g a^2 \ \left[\frac{J}{m^2}\right] \tag{5}$$

The power of the wave per unit length of the wavefront is the energy times the rate of travel of the wavefront which is the group velocity.

$$P = Ev_g = \frac{1}{4}\rho g a^2 \sqrt{\frac{g\lambda}{2\pi}} \quad \left[\frac{W}{m}\right] \tag{6}$$

A conclusion from this is the wave energy is proportional to the square of the wave height [2].

2.6 Wave Energy Examples

Annual average wave power along the edge of North America's eastern continental shelf ranges from 10 to 20 kW/m. By comparison, shelf-edge wave power off the exposed western coasts of the British Isles averages 60 to 70 kW/m, decreasing farther south, to about 30 kW/m off central Portugal. A similar pattern occurs off Taiwan and Japan, wave power averages 5 to 15 kW/m. On the opposite side of the Pacific Ocean on the coast of Northern California, wave power ranges from 25 to 35 kW/m. [3]

2.7 Climatic Variation

Wave energy has variability over several time scales:

Wave to wave (seconds)

Wave group to wave group (minutes)

Sea state to sea state (hours to days)

Season to season (months)

Power plant service life (years)

Sea state has two statistical parameters: significant wave height and a peak wave period. Significant wave height is defined as the average height of the highest one-third of the prevailing waves. This historically approximates the height that a shipboard observer will report from visual observation of the sea state. Peak wave period is the harmonic frequency component having the greatest amount of energy in a

given sea state. Variability of the significant wave height and peak wave period is more random in seas generated by strong local winds and less random in swells that arrive from far distant storms.

Waves often occur in successive groups of alternately high and low waves. If these can be smoothed by storage on the minute time frame it can enable the use of lower capacity electrical equipment. This has been demonstrated with mechanical and fluid energy storage systems.

Wave energy levels can also change over periods of hours to days. Developing long-term statistics associated with the day-to-day variability of wave energy levels is important, since it is this variability that governs conversion equipment rating. A system designer must make a trade-off between under-utilization of installed capacity and excessive shedding of absorbed power.

Seasonal variability in wave energy can be fairly wide ranging also. Seasonal variability has been measured on the order of 3:1 to 5:1 [3]. Though fairly variable, this is much less than wind power in all but the best wind harvesting locations.

In another example there was a variation ranging from (T = 6.5 sec, Hs = 0.75m) to (T=12 sec, Hs = 5m) [4]. These correspond to power per meter differences of 3.6 kW/m and 300 kW/m respectively.

Year-to-year variability in wave energy levels must be considered, particularly in projecting long-term power plant performance but this is not in the scope of this survey.

If optimizing a generator, linear or otherwise, to accommodate two orders of magnitude in power variation may be financially impractical. Thus some means should be considered to equalize this variation in power input to the generator. In the same way that wind turbines pitch their blades to reduce the power input to the system

[2], wave energy devices may need to reduce the power input to the direct drive mechanism.

Regions of operation

Similar to wind energy extraction, there are usually four regions of operation depending on the energy input and the capability of the energy capture system.

Typical Regions of Operation

Off – Energy Input Too Low

No wave-to-low wave conditions. The generator is shutdown and awaits more favorable wave conditions.

Optimal Region

Low to medium wave conditions. The generator is controlled according to optimal control. Power extraction is maximized.

Limiting Region

High wave conditions. The generator continues to operate. However, the raw wave energy available exceeds the capacity of the system. The generator is controlled according to sub-optimal control, and the excess power is spilled.

Off – Survival Region

Storm conditions. The generator is shut down and the system reverts to survival mode.

Remote WEC Regions of Operation

Since the remote wave energy device must continuously produce power for the application load there really should not be any *Off* modes because energy is

continuously required to power the application package. The regions of operation for a remote WEC are then:

Black Start

Minimal wave input. The generator awaits the minimum amount of wave movement to allow for the boot-strap start to occur. The system is designed to at least provide some trickle energy at the low extreme of wave energy content.

Optimal Region

Low-to-medium wave conditions. The generator is controlled according to optimal control. Power extraction is maximized.

Limiting Region

High wave conditions. The generator continues to operate. However, the raw wave energy available exceeds the capacity of the system. The generator is controlled according to sub-optimal control, and the excess power is first used to charge any on-board storage, then it is spilled.

Off – Survival Region

Storm conditions. The generator is shut down and the system reverts to survival mode. The shutdown requires a mechanical disconnect from the excessive wave energy. The system enters a low-power mode and monitors for the conditions required to re-engage the mechanical linkage to the wave energy to transition back to the Limiting Region.

Linearized wave equation

Wave action can be approximated by using a linearization of the Morrison wave equations [4,5]. This linearization is summarized as:

$$F_e = A \cdot \ddot{z}_w + C \cdot \dot{z}_w + k \cdot z_w \tag{7}$$

where:

F_e is the excitation force from the wave

A is the added mass

C is the viscous damping

k is the hydrostatic stiffness

z_w is the elevation of the water at the device

The added mass is a concept introduced to include the water surrounding a submerged body that moves with the body, effectively increasing its mass in terms of the force required to accelerate it.

This linearization is the standard first order approximation in the literature. It yields a linear differential equation that is suitable for simpler analysis techniques than the partial differential equations that usually result from wave theory.

2.8 Overview of wave energy extraction

2.8.1 WEC Extraction Methods

Several different methods have been utilized for ocean energy extraction methods for a wave energy converter (WEC). Extraction methods are of four major types:

- Oscillating Water Columns (OWC)
- Wave Activated Contour Devices
- Overtopping
- Point Absorbers

Oscillating water columns are chambers where the water level rises and falls with the waves. The air coming into and going out of this chamber drives a well turbine connected to a generator [7].

Wave activated contour devices consist of different floaters that move with respect to each other when waves pass. From this motion, energy is extracted, mostly with hydraulic pumps [8].

Overtopping devices are water reservoirs which are filled by waves via some kind of wave concentrator which increases the wave height. The water leaves the reservoir via a water turbine driving a generator [9].

Point absorber moored devices that have a floater that is moved by the waves. Energy is extracted from this motion. The motion may be up and down or around an axis [10].

Fig. 3 provides a simplified schematic of each.

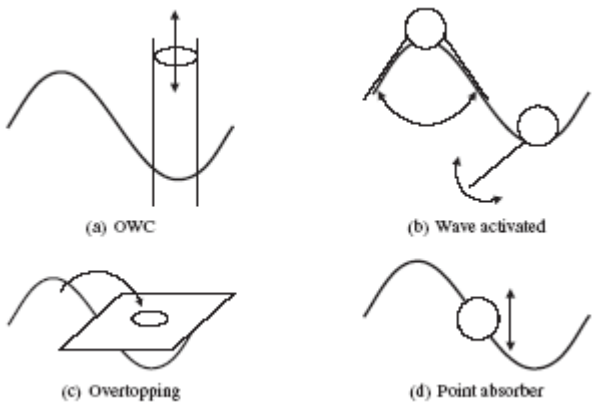

Fig. 3. Wave Energy Extraction Methods

2.9 WEC Locations

WEC locations can be generally described by three main geographical areas with corresponding types of WECs broadly utilized in each area by: Inshore, near-shore, and off-shore. The inshore WEC installations are usually oscillating water columns or overtopping devices which can be large, and with the majority of the mechanical structure fixed to the shore. Near-shore devices can be also oscillating water columns, point absorbers, or wave activated devices. Off-shore devices, and the focus of this future research, are typically point absorbers, either moored with a long cable and riding the top of the water, or submerged in the water.

2.10 Wave Energy Conversion (WEC) Devices

Since wave energy is a new field numerous concepts have been brought forward and no particular architectures dominate the field yet. At this early stage of development there has not been a consensus as to how best to approach this problem.

This study is concentrating on the application of remote WEC utilization. For this application the important criteria are:

Low cost, which implies minimizing the utilization of permanent magnets and other expensive components. Also the utilization of the expensive permanent magnet components in the active flux transfer area should be high.

Lower power, which implies that the magnitude of forces applied to the mechanical components may not be as high as a WEC used for a utility power generating application. Also, off-the-shelf mechanical components may be able to be utilized.

Single remote applications lead to the use of lower power point absorber WECs

Contact-less Force Transmission Systems

For WECs, the conclusion has been that most applications benefit for a contact-less force transmission system (CTFS) due to reliability and maintainability reasons in the

ocean environment. Polinder [11] addressed converting linear motion from wave energy to electrical energy by summarizing that the energy could be practically extracted by converting the linear motion into rotating motion and by using a rotating generator. He concluded that it appears to be extremely difficult to build a robust, maintenance-free gear for such a conversion, and provide a sealed interface. Therefore, in [11], he sued a linear generator, which converts the energy from the linear motion directly into electrical energy.

2.11 Research at Oregon State University

Langeliers [12] describes a permanent magnet, rack and pinion gearbox WEC system. It consists of a contact-less force transmission based on the permanent magnet rotary magnetic gears. It has two magnetic sections. The translator has an alternating assembly of Nd-Fe-B permanent magnets. The flux is transferred over the contact-less interface, through flux guides to the PM rotary gears. One disadvantage with this architecture though is that the full amount of electromagnetic flux must cross two air-gap interfaces for force transmission. Also at any given time, on a fractional amount, only one magnetic section on the translator is being used.

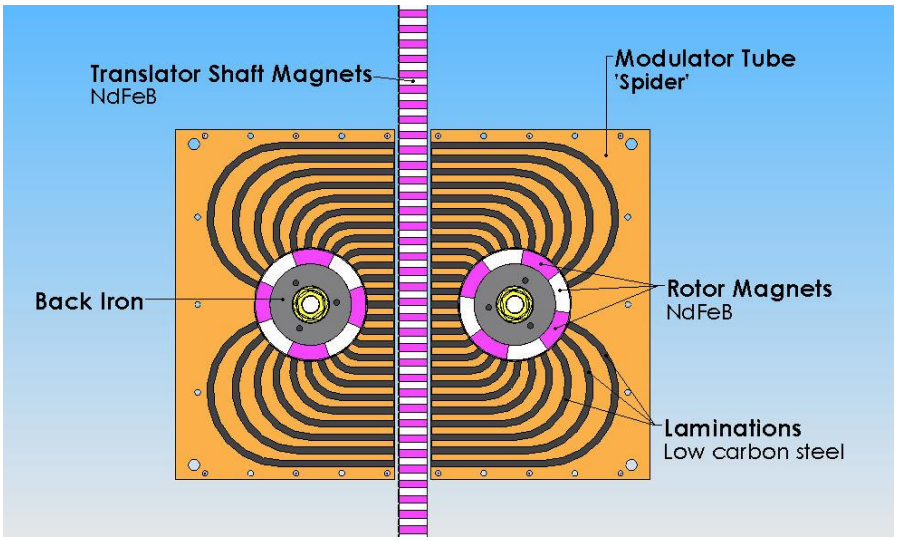

Fig. 4. Arrangement of the Translator Shaft, 'Spider', and Rotors for Rack and Pinnion

Rhinefrank [13] employed a contact-less force transmission system (CFTS) by putting an alternating assembly of Nd-Fe-B permanent magnets on the translator with the flux passing to coils on a stationary stator assembly. See Fig. 5. A full wave rectifier with bulk capacitance was used for smoothing the DC output. A disadvantage with this system is that portions of the active PM area is not utilized at all times time. Also there is no sensing of the PM field position, so more advanced control may be difficult.

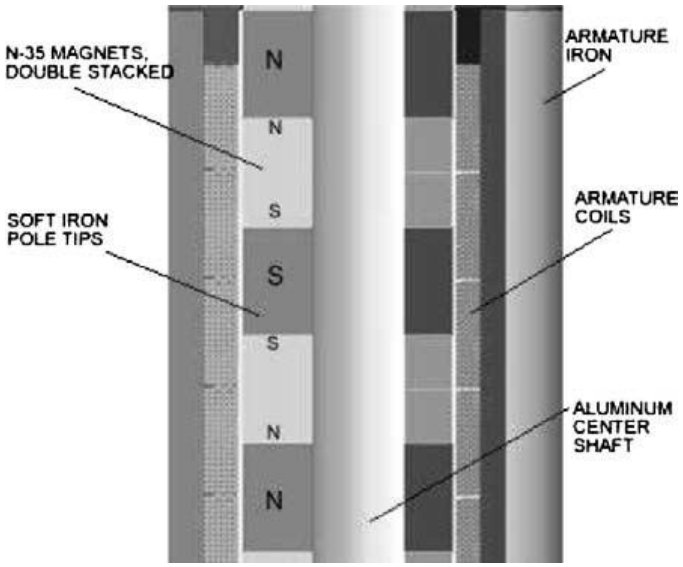

Fig. 5. Arrangement of PM Contact-Less Force Transmission System (CFTS)

Agamloh [14] designed a CFTS WEC that used a vertical center spar with outer cylindrical float. A steel ring was attached to the float and served as the back-iron for a PM structure that is in the spar. The force that is developed when the buoy moves up and down is transmitted across the buoy/spar interface to the PM structure in the spar via the magnetic reluctance path. The center spar PM structure is attached to the ball screw which then drives the screw rotationally. Permanent magnets are used for the magnetic contact-less force transmission which can be a high cost solution.

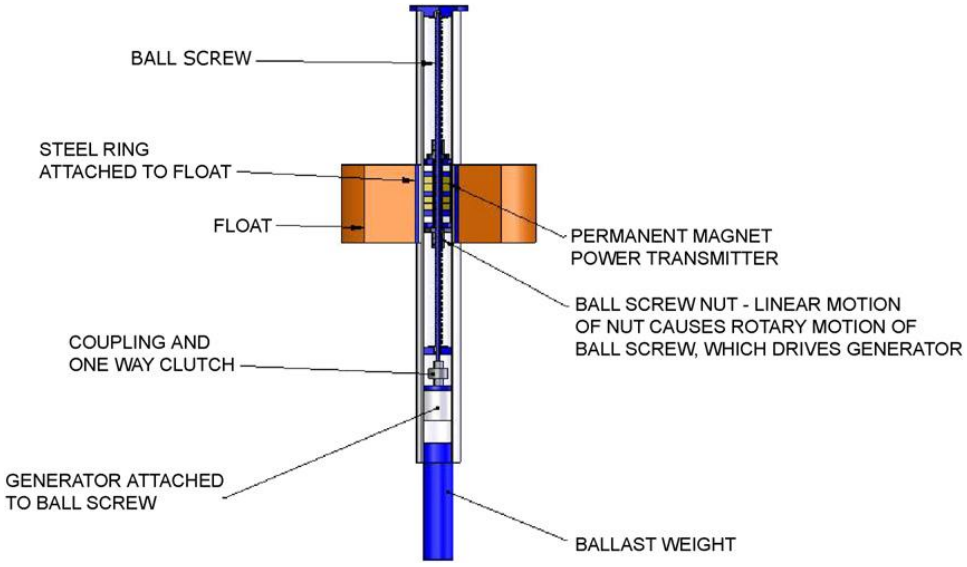

Fig. 6. Arrangement of PM Spar CFTS WEC

Prudell [15] designed a WEC, named the SeaBeav1, that has a magnet section on the outer floating buoy, an armature on the spar, with the spar being taut-wire tethered. The heavier magnet section is in the higher buoyancy buoy. Also, high density foam is added to the float for added buoyancy. This has emerged as a robust buoy systems though electromagnetically there is still a lot of unused PM flux at any given time for a large portion of the duty cycle.

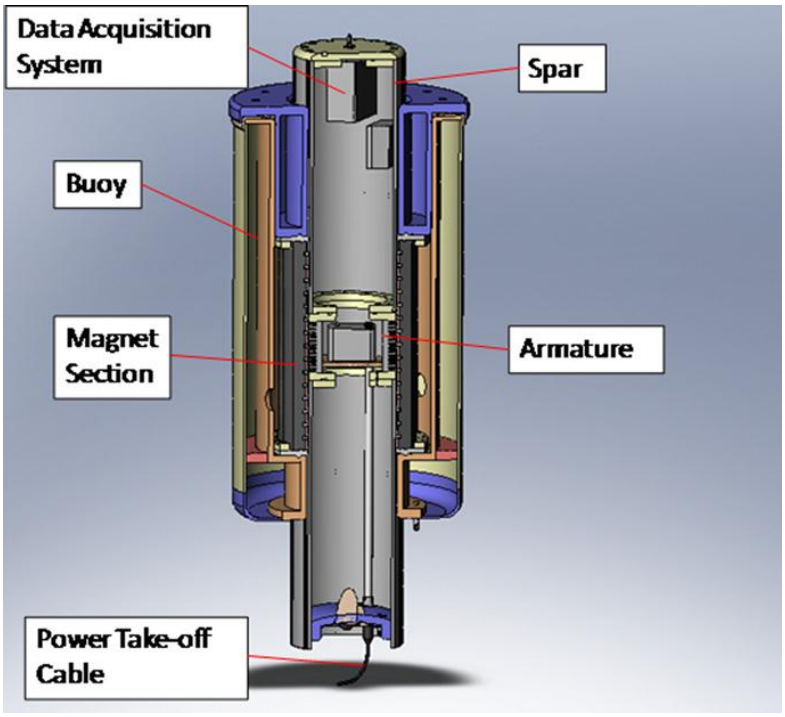

Fig. 7. SeaBeav1 Spar and Buoy Arrangement

2.12 Other Research Initiatives

Mueller [16] surveyed many WEC projects and summarized some of the challenges with using a linear, direct drive generator. They concluded that with velocities on the order of 0.5 – 2 m/s the direct drive machine has to react to large forces, with typical airgap shear stresses in the region of 20-40 kN/m^2. His example is that a 2 MW electric machine at 2 m/s would require an airgap surface area of 25 m^2 approximately. Direct drive machines, therefore, could be very large and heavy.

McDonald [17] has shown that for direct drive rotary machines the inactive part can be greater than 60% of the total mass. This inactive component is required principally to overcome Maxwell Stress force which acts normal to the airgap surface. This can be mitigated by double sided, or cylindrical machines, but potentially due to

manufacturing tolerance there will be some differences in airgap along the length of the machine.

Polinder [18] described the machine and inverter in the Archimedes Wave Swing (AWS) which was composed of a PM linear synchronous generator with a current source inverter (CSI). It is a double sided linear PM machine with the PMs on the translator. It is large and rectangular in nature. One reason a CSI was used is because it does not require an accurate translator position sensor. They arrived at the design conclusion that balancing forces in these machines was a necessity for a large mechanical direct drive structure. They also addressed the need to study where sensor placement, needed for control, can be on the machine.

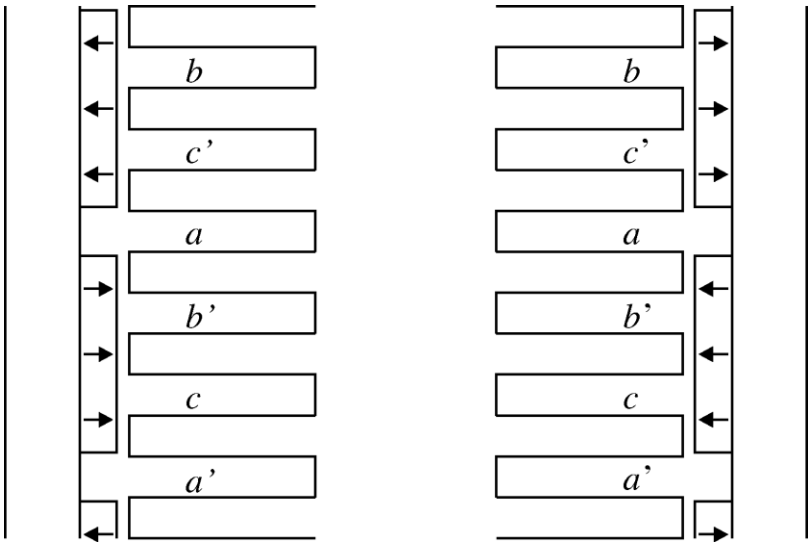

Fig. 8. Double-sided Linear PM Machine for AWS

After designing the conventional linear PM synchronous machine for the AWS, Polinder [11] compared a number of different machine topologies: including, the

linear induction machine, PM synchronous machine, both iron and air-cored, and the switched reluctance machine, with the final result showing that the iron-cored PM machine designed and built for the AWS was superior in terms of cost/kW. A novel high force traverse flux machine introduced in the paper also looked promising but it suffered from core loss effects. The comparison was just on the active components and did not take into account mechanical aspects, with the TFM being mechanically more difficult to construct. Mueller also discussed the possible use of a TFM in [19].

Mueller [20] studied an air-cored concept to counteract the challenge of the magnetic attraction forces impact on structural and bearing design. The design has a translator with a PM structure and a cylindrical armature. Mueller emphasized that the most efficient electromagnetic machine will not be the optimum solution, but it will be a solution that is optimized for both electrical and mechanical design, thus the reason for his investigation into an air-cored machine to lessen the requirements on the mechanical aspects of the total structure.

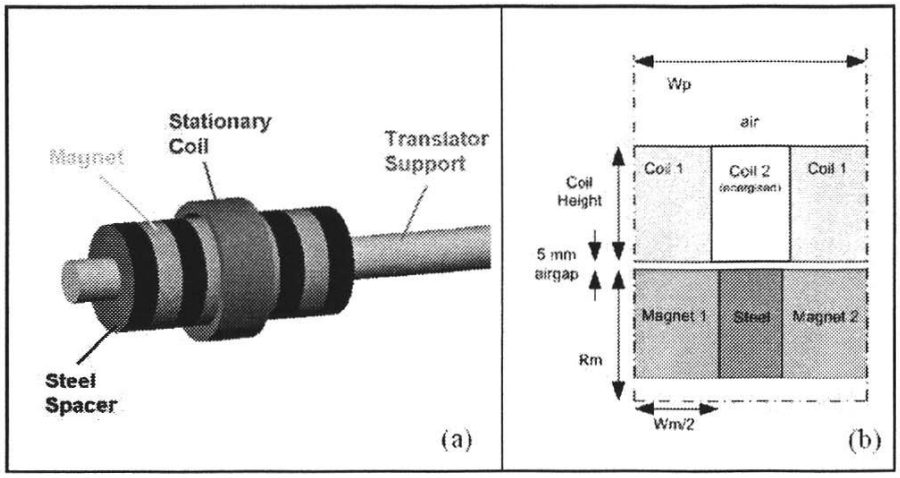

Fig. 9. Air-cored Stator, PM Translator WEC

Blanco [21] has proposed using a switched reluctance machine and unidirectional 3-switch converter for a linear direct-drive WEC application. It consists of a rectangular back-iron movement with two rectangular armatures symmetrically on each side. It would have a qualitative advantage of less active material (no non-utilized permanent magnets over the travel path, or duty cycle) though it seems that the natural need for a small airgap for a switched reluctance machine would be counter to design for a contact-less WEC solution. The concept has been simulated and mocked-up with a rotary switched reluctance machine but has not be experimental verified yet as a linear drive.

Cancelliere [22] designed an interior PM spar with an outer cylindrical armature. Buried PMs were used so the machine had a salient structure. The control was chosen to not utilize the salient structure since the d-axis command was set to zero. This concept was also tested with a land-based facility, and was not contact-less since a linear encoder was used on the inner PM spar.

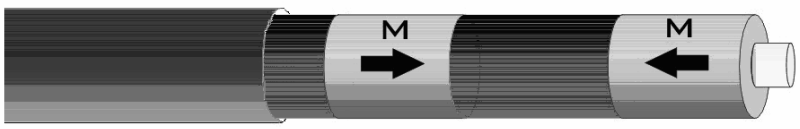

Fig. 10. Salient PM Translator

2.13 Previous Research Conclusions

Rhinefrank [23] summarized the comparison between linear generators well concluding that:

The low speed of wave energy devices puts linear generators at a disadvantage. If a highly efficient mechanism could reliably transform the high-thrust, low-speed, wave action from the buoy into a high-speed, low-thrust rotary output, then a standard rotary generator with a much lower cost could be used for power generation.

Power factor correction and varying speed issues emphasize the need for external generator excitation (or an advanced control method with more sensors).

The highest cost contributor to the linear generators evaluated is the permanent magnets. These costs are on the order of 50% to 75% of the material costs of the machines.

2.14 Wave energy converter control

2.14.1 WEC Control

Nie [24] provides a summary of two major types of control 1) simple diode rectification, and 2) active bridge control. In the first case the unidirectional topology can potentially be used to save cost. The electric machine though must have a high intrinsic power factor and the mechanical power take-off system can achieve the desired response to input waves without the need for bidirectional power flow from the converter. For the second case of active bridge control, he concluded that this level of complexity was required for machines with a naturally high self inductance and low power factor like the TFM. Also tuning of a resonant mechanical power take-off was less necessary. With a linear generator the power factor can be upwards of 0.95 to 1.0 since the speed is slow and the usual speed-voltage terms are of a lesser effect. Nie surprisingly measured only a 52.3% vs. 51.6% efficiency gain when using an H-bridge converter vs. passive rectification. His tuning of the mechanical system

and the control forcing function level is unclear and it is not know if this was the reason for the limited performance.

2.14.2 Impedance Matching for Maximum Power Transfer

Since the hydrodynamic solution of the Morison model is similar to a mass-spring-damper system with a periodic input, the concept of formulating a generator equivalent is used to extract power. This is because the solution for power extraction can be arrived at by matching the impedance of the incident hydrodynamic input with that of the generator. When matched the maximum amount of power can be extracted. For a 1 dimensional heave system, this maximum is 50%.

The equivalent circuit is shown in Fig 11.

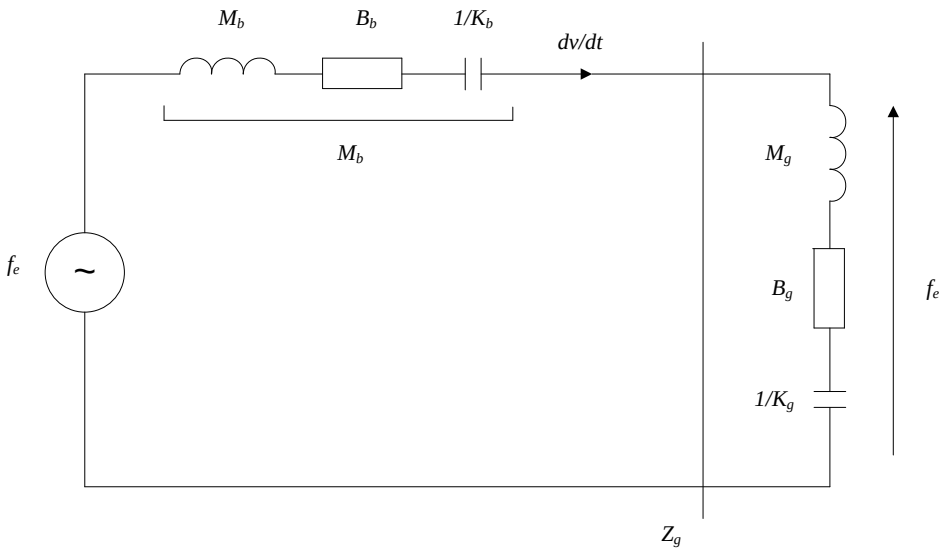

Fig. 11. Wave Physics Equivalent Electrical Circuit

In this electrical equivalent, for the inputs and state variables, force is analogous to voltage and buoy velocity is analogous to current. For the system characteristics, the masses are analogous to inductance, the dampening is analogous to resistance, and the buoyancy is analogous to capacitance. The generator force is proportional to current for a current controlled WEC.

The inner current loop control can be accomplished with different machines, converters, and control schemes, actively adjusted to change the torque and speed capability of the generator.

Most authors proceed with this formulation as the foundation of the system description and control.

If the buoy was to just be mechanically tuned to match with a passive converter, the resonant frequency for the maximum power transfer would be:

$$\omega_0 = 2\pi \cdot \sqrt{\frac{K_b}{M_b}} \tag{8}$$

This, though, typically leads to a heavy buoy for the resonance frequency to be in the approximate range for an ocean point absorber.

Impedance Matching Control

Under matched impedance control the generator coefficients are controlled such that these parameters are the complex conjugate of the hydrodynamic input. The generator's complex conjugate output should then equate the real part (dampening) and provide the opposite polarity reactive control (mass and buoyancy equivalents). The matching of the reactive force components means that the generator must deliver power to the water at certain points of the periodic cycle. This power may be too large to be practical due to the low frequency wavelength.

Schacher [25] constructed a unitary control that drove the dampening of the generator and matched that to the hydrodynamic impedance. His nomenclature was c_{gen} for the generator dampening and it is termed c^*_{gen} control.

$$c_{gen} = |\overline{Z_b}| \tag{9}$$

Shek [26,27] implements a binary control term into the generator current. Under this control scheme, the dampening and hydrodynamic generator terms are controlled and the mass term is set to zero. With the mass term set to zero, it turns out that the generator has to provide less reactive energy to the ocean but power is not perfectly maximized (similar to the c_{gen} control above).

The control is set up such that:

$$B_g = B_b \tag{10}$$

and

$$K_g = M_b \cdot \omega^2 - K_b \tag{11}$$

There will therefore be two components of the generator current command: a dampening force proportional to the velocity which provides amplitude control and the conversation of real power, and a hydrodynamic stiffening force proportional to displacement that provides phase control. It is planned to investigate both of these control schemes to compare and find the limitations versus alternate control schemes.

The resonance of this scheme is:

$$\omega = 2\pi \cdot \sqrt{\frac{K_b + K_g}{M_b}} \tag{12}$$

In comparison with the resonance equation using only mechanical tuning, it can be seen that active generator control can lead to a smaller buoy and adjust for different resonant frequencies.

2.15 Summary of Complex Conjugate Control [2,25]

Under complex conjugate control, significant amounts of energy must be driven into the ocean at times. There either may be no on-board energy storage sufficient to drive the machine for several seconds or the energy storage may not be optimized for power delivery and it may have power cycling limitations.

Complex conjugate control assumes unrealistic monochromatic waves. Some work [25] is starting to use more stochastic wave stimulus that was found to be more realistic of waves in the Pacific Northwest. It uses a spectrum of wave amplitudes and frequencies based on a Pierson-Moskowitz distribution.

It can have excessive speeds and range of travel. Optimal control can lead to control buoy stokes of up to 4 times that of the incident wave. Climatic variation may also exacerbate this and the design range required for travel could be very large. This speed variation may be mitigated by the machine and converter utilized. A choice that can support a wide speed range could be used. This area could be investigated.

Complex conjugate control may impose higher maximum current and power limits for a WEC design. The generating machine and power electronics (usually current limited) form a constraint. This may be mitigated by a machine/converter choice with a wide power range with respect to speed. This too will be investigated.

2.16 Latching Control

Latching control, Spooner [28] is a method of holding the buoy at the end of travel location and releasing if for rapid translation. This can potentially put velocity and force in phase. Many references qualitatively discuss this type of control but it is not apparent that it would yield better results. For a passive rectifier system, though, this

could potentially yield some better performance but the control of it would seem to be empirical and would be hard to consistently achieve with changing wave conditions.

2.17 State Space Realization and Optimization

Another method of control formulation is to cast the linear equations into a state space realization. For the linearized Morison model, the first order system could be written using the states of displacement (x) and displacement rate ($\dot{x}$).

A state space realization may be more useful to describe the system for the following reasons:

A system with multiple inputs (force input with two components) leads to Multiple Input, Multiple Output (MIMO) natural state space control realizations.

Additional degree of freedom (DOF) linear equations can be easily added. For example, wave surge forces could be added to the first order heave forces.

More formalized methods of analysis for observability and controllability can be used to address limits of control and sensor recommendations.

State space control or system description also leads to the control engineering view of optimal control. This optimal control constructs several weighting criteria and a minimization is performed to arrive at a 'best fit' controller. For example, the weighting criteria could be defined and a minimization performed to minimize loss of resonance, spar translator travel, and spar translator speed.

2.18 Wavelet Analysis

If there are time gaps between waves that are finite due to the energy naturally dissipating to zero or the WEC not being able to extract useful energy, other mathematical tools for multiple waveform control or analysis could used. Wavelet analysis may be appropriate. The wavelet transform is the similar to the Fourier transform in which signals are represented by a sum of sinusoids. Wavelets though

are localized in both time and frequency unlike the Fourier transform which is localized in frequency only. The appropriateness of this analysis could also be investigated.

2.19 WEC System analysis

2.19.1 System Analysis

Many of the literature references deal with the control at the hydrodynamic and mechanical power take-off level, referencing the generator control as a system input. This is sufficient for the slower power transfer, or impedance matching, part of the control since the time-constant for that aspect of the control is on the order of seconds. The small signal inner loop current control of the generator can be handled as a separate control entity. But if the generator/converter entity can be controlled in such a way as to influence the limits of the displacement range or displacement velocity, it should be included any system analysis or simulation. This is proposed for future work.

2.19.2 Per Unit Analysis

It is also proposed that to compare control strategies, relative types of buoys shapes, and controller power limitations, a system needs to be constructed that will allow for the comparison of different designs or strategies in a relative sense. A per-unit system will allow this comparison. Instead of WEC parameters that are scaled with the WEC size if the parameters are scaled to a per-unit system, using an orthogonal set of state variables, then the relative merits of WEC designs can be compared.

2.20 Remote ocean power applications

A search was performed for current remote ocean applications that could use local wave energy. These applications have been condensed to form one set of requirements for future work, Table 1.

2.20.1 Marine Observation Buoys

Coastal – Marine Automated Network

Coastal – Marine Automated Network (C-MAN) buoys are buoys that are a part of the National Data Buoy Center (NDBC) program. These buoys measure and transmit ocean and meteorological conditions for weather and navigational purposes.

Deep-Ocean Assessment and Reporting of Tsunamis

Deep-Ocean Assessment and Reporting of Tsunamis (DART) buoys ring the Pacific Ocean to monitor for and report possible tsunami conditions. The buoy system is made up of a bottom pressure recorder (BPR) and a companion moored surface buoy for real-time communication. An acoustic link transmits data from the BPR on the seafloor to the surface buoy. For this application an energy generator would be needed for both the seafloor and surface buoy component.

Tropical Atmospheric Ocean Array

Tropical Atmospheric Ocean (TAO) array buoys are a system of buoys for detection, understanding, and prediction of El Nino and La Nina. The buoys are laid out in a large grid in the Pacific Ocean.

2.20.2 Military/Homeland Security Surveillance Buoys

Deep Water Active Detection System

Deep Water Active Detection System (DWADS) is a proposed system of buoys used for the monitoring of ship traffic. Several SBIR (Small Business Innovation Research) contracts through ONR (Office of Naval Research) have been let to test various DWADS concepts. Some initial prototypes that use wave energy converters have been installed off of the coast of Kaneohe, Oahu, Hawaii and off of the coast of New Jersey.

AUV Charging Stations

Several concepts and demonstrations have started with respect to Autonomous Underwater Vehicles, their operations, and their infrastructure (power, for one). Hagerman [3] developed a notional power budget for a dock-based URFC (Unitary Regenerative Fuel Cell) storage system charging AUVs designed for North Atlantic under-ice surveys.

The AUV Laboratory at the Massachusetts Institute of Technology (MIT) has developed a docking system capable of supporting the development of Autonomous Ocean Sampling Networks. It started sea trials in May 1997.

In May 2001, Maridan A/S, with partners, completed sea trials of the Eurodocker project in Kiel Harbor, Germany.

2.21 Remote ocean power generation requirements

A draft set of requirements has been selected for investigating a remote WEC. These requirements are:

2.21.1 Generalized Requirements

Continuous Power Rating

The continuous power rating is the power output from the WEC required to support the on-board payload.

Voltage Output Level

The voltage output level is the level that can support all payload electronics and sensors.

Steady State Voltage Range

The steady state voltage range is the range over which all of the payload electronics can operate with indefinitely.

Transient Voltage Range

The transient voltage level is the range over which the payload electronics can operate with for a defined amount of time.

Burst Power Level

The burst power level is the amount of burst power that the WEC can deliver to meet payload electronics burst power needs.

Energy Storage Equivalent

The energy storage equivalent is the amount of equivalent energy that would be provided by an equivalent battery system.

Voltage Sag Energy Storage

The voltage sage energy storage is the amount of energy that would be required to hold-up the payload electronics operating in an emergency, low-power mode.

Speed Input Range

The speed input range is the ratio of maximum mechanical speed input to minimum speed input to the WEC.

Duty Cycle

The duty cycle is a power vs. time plot that can be used for an overall efficiency calculation.

Black Start

Black start is the ability of the WEC to start, or restart, with zero stored energy and just from mechanical input to the WEC.

Operating Depth

The operating depth is the minimum to maximum ocean depth that the WEC shall be able to operate over if it is submerged.

Electromagnetic Environmental Effects

The electromagnetic effects requirements are minimum requirements for the WEC to operate successfully in a complete electronics systems without degrading other electronics system components or being susceptible to other electronic system components.

Operating and Storage Temperature

The operating and storage temperature requirements are the temperature range, in deg C, which the WEC must be able to operate within in ocean, and in any type of storage or transport environment.

Vibration and Shock Environment

The vibration and shock environmental requirements are the amount of mechanical agitation that the WEC must be able to endure when operating, in storage, or in transport.

Humidity

The humidity requirement is a both a moisture and sealing requirement for a submerged device.

Wind Speed

The wind speed requirement is the maximum over ocean wind speed that the WEC must tolerate when operating of the ocean surface.

Minimum Deployment Duration

The minimum deployment duration requirement is the amount of time the WEC shall operate continuously in the operating environment.

Service Life

The service life is the expected lifetime for the WEC.

Time Between Service

The time between service duration requirement is the amount of time the WEC shall operate between maintenance periods.

Volume

The volume requirement is the maximum spatial dimensions that WEC can fill.

Weight

The weight requirement is the maximum weight of the mechanical structure for energy production, linkages, gears, generator, power and control electronics.

Cost

The cost requirement is the amount per-unit, or recurring cost for the WEC.

Fault Handling

The fault handling requirement is the minimum amount of functionality the control electronics must be able to sense and contend with to safely operate the WEC and provide status about it.

Fault Recording

The fault recording requirements are the minimum number and type of fault and status messages the WEC shall be able to store.

Diagnostics

The diagnostic requirement is the amount of predictive fault handling that the WEC must possess.

2.22 Selected Study Requirements

The selected requirements for a study remote WEC are as follows:

Table 1. WEC Requirements for Remote Applications

Continuous Power Rating	500 W
Voltage Output Level	42 VDC
Steady State Voltage Range	+/- 10% (46.2 VDC to 37.8 VDC)
Transient Voltage Range	+/- 20% (50.4 VDC to 33.6 VDC for 0.1 sec.)
Burst Power Level	Two time (2x) continuous power level for 1 sec.
Energy Storage Equivalent	500 W-hrs
Voltage Sag Energy Storage	30 minutes. This requirement is based on allowing for two (2) passes of the Iridium satellite for possible communication of a status message.
Speed Input Range	60% of the continuous power rating over an 6:1 speed range.
Duty Cycle	TBD power vs. time profile
Black Start	The wave energy device shall be able to start from the mechanical input of wave motion with no electrical energy remaining.
Operating Depth	100 ft to 5000 ft
Electromagnetic Environmental Effects	MIL-STD-461G (CE102, RE101, CS101, RS101)
Operating and Storage Temperature	-30 deg C to 50 deg C (75 deg C for storage)

Vibration and Shock Environment	Vibration: 5G's MIL-STD-202 Test Condition B, Method 204 Shock: 75G's MIL-STD-202F Test Condition H, Method 213B
Humidity	MIL-STD-202F Test Condition B, Method 103B
Wind Speed	Up to 140 knots for a surface utilized device
Minimum Deployment Duration	2 years
Service Life	2 to 20 years
Time Between Service	2 years
Volume	The volume shall be minimized since for a remote application the payload shall take precedence.
Weight	The weight shall be minimized since for a remote application the payload shall take precedence.
Cost	The cost shall be minimized since for a remote application the payload shall take precedence.
Fault Handling	The WEC shall be able to handle faults and be able to shutdown without damage.
Fault Recording	The WEC shall be able to record up to 128 faults locally with an externally supplied time-stamp.
Diagnostics	The WEC shall have TBD diagnostic capabilities.

2.23 Remote wave energy device characteristics

From the literature search and the requirements specific to a remote wave energy generation system, there are several keys areas where a trade-off can be made with the architecture. These characteristics, and the chosen solutions, will form the initial proposed system. Future work could more quantitatively validate the selected features.

2.23.1 Force Transmission System

The buoy force can be either directly coupled or indirectly coupled to the generating system. Although for a small WEC it may be possible to directly couple and seal the transmission system, the bulk of the literature uses some sort of an indirect, or contactless force transmission system. Also for a safe oscillatory operational range, the buoy may also need to be physically disconnected from the generation system at times. Therefore a contract-less force transmission system will be proposed.

2.23.2 Generator Speed

The designed generator could be either low speed or high speed. The input forcing function has a low velocity input so for systems that are designed to maximize efficiency direct drive has been used. For a small remote application, there is an advantage to increasing the speed to decrease the generator size. If this is done a more economical generator can be used. Also the small size of a remote WEC allows the use of mechanical speed changing components that are reasonable in size. A high speed generator WEC system will be proposed.

2.23.3 Generator Speed Range

The hydrodynamic forcing function to the WEC system also varies over a quite a wide speed range. Some control methods also increase the required speed range. A mechanical system could be utilized, such as a variable speed gearbox, to accommodate this wide speed range, or the electric machine and converter could be chosen to meet this requirement. For this application that requires a ‘black start’ a PM machine will be chosen so that movement will produce and electromotive force without external excitation. Also, the PM machine and its controller will be designed to accommodate a wide speed range.

2.23.4 Control Electronics

The control electronics could be of a simpler passive design or a more complex active design. Even though a more simple rectified control may seem attractive for a small

device, it is qualitatively felt that all of the WEC requirements will not be able to be met without active control. An active control system will also allow for an optimization of WEC characteristics and design parameters.

2.23.5 Control Method

Several differential control methods have been reviewed and suggested for future work. This design characteristic is still undermined. A greater understanding and review of the real-world energy input characteristics, matched to a validated hydrodynamic buoy design, needs to be amassed before control simulations for compare performance and can be analyzed.

2.24 Proposed Remote Wave Energy Devices

From a review of the prior research, and based off of the specific requirements for this application, a proposed remote WEC would try to:

- Minimize cost, use common mechanical components, maximize the use of active PM or active airgap area
- Operate over a wide speed range
- Allow for the ability of complex control for the extraction of the maximum amount of energy possible.

2.25 Proposed Wave Energy Converter Device

The proposed WEC device consists of an outer buoy around a cylindrical spar. The inner cylindrical spar is taut-moored, see Fig. 12. Similar to Agamloh, the outer buoy would contain back-iron for a contact-less force transmission system (CFTS). The CFTS is used to couple the outer moving buoy to an internal spar mechanism. The internal spar mechanism first consists of a structure with a cylindrical electromagnet which is rigidly attached to a central ball screw nut. The electromagnet is energized to

make this inner spar structure move vertically which turns the roller lead screw mechanism.

A roller screw mechanism is used since it uses multiple threaded helical rollers for transmitting forces. This arrangement allows it to carry heavy loads in arduous conditions so it is a good choice for this demanding, continuous-duty application.

At the end of the roller screw a PM machine is mounted which is controlled in a generating mode. The machine is directly coupled to the lead screw so the electric machine rotates in a bidirectional manner with the vertical oscillatory motion of the spar. The machine is a 3-phase interior PM machine with saliency. The control electronics consists of a 6-switch AC/DC converter to rectify and condition the DC output power.

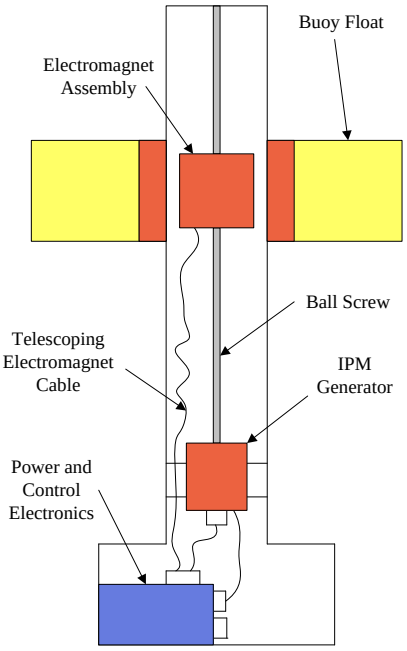

Fig. 12. Proposed Remote WEC Architecture

2.26 Proposed Wave Energy Device Advantages

The proposed WEC has the following advantages for use with this application:

2.26.1 Lower Cost

Unit cost can be lowered by utilizing less, or more fully utilizing the costly permanent magnets. For this concept the permanent magnets are only used in the rotary electric machine. As opposed to a linear machine, the permanent magnets are used more efficiently there since there is no unused section of the active magnetic material during the oscillatory duty cycle.

2.26.2 Fail-safe Shutdown Feature Using Electromagnet

Since the CFTS electromagnet is just used to couple to the outer buoy it does not need high dynamic control. This allows for a low-current, higher inductance electromagnet to be used. Using an electromagnet also provides a mechanism for WEC shut-down due to high wave height. When that condition occurs the electromagnet is de-energized to uncouple the outer buoy from the inner spar movable structure.

2.26.3 Wide Speed Range Electric Machine and Converter

The use of a higher speed rotary IPM machine provides a more compact volume for a given machine power rating since the speed is higher. Also less mechanical structure is required to contain it. The active magnetic path will be used more efficiently, and in a radial flux electric machine it is easier to use a salient PM structure. The salient PM structure will allow the machine to operate over a wider speed range for maximum power output. The wider constant power area may be useful for reactive control at certain reciprocating stroke positions.

2.26.4 Use of a Position Sensor

The use of a rotary machine allows for the use of a commutation resolver to provide better phase control of the generator. Also since the machine is coupled to the roller

screw which has a set relationship to the outer buoy, it will also be able to sense the wave group velocity and position.

2.27 Proposed Wave Energy Device Analysis

Future work would entail the analysis of the proposed concept. It would include the simulation of the wave and buoy input function, the sizing of components, and the control system analysis necessary to meet the state requirements for a remote WEC.

2.28 Conclusions

Wave energy has the potential for use with remote or isolated application and it has the advantage of harvesting continual, renewable power locally so that other energy type sources do not have to be used, energy sources that may have higher maintenance or storage requirements.

This survey paper has reviewed wave energy generation, power production, wave energy conversion devices, control schemes, remote ocean energy requirements, and a proposed system.

2.29 References

[1] Andrews, Jelley, Energy Science: Principles, Technologies, and Impacts, Oxford University Press, 2007.

[2] T. Brekken and A. von Jouanne “ECCE Wave Energy Tutorial”, Energy Conversion Conference and Exposition, Sept 2009

[3] G. Haggerman, “Wave Energy Systems for Recharging AUV Supplies,” Workshop on Autonomous Underwater Vehicles, June 2002, pg. 75-84.

[4] N.J. Baker, “Linear Generators for Direct Drive marine Renewable Energy Converters”, University of Durham, PhD. Thesis, 2003

[5] J. Falnes, Ocean Waves and Oscillating Systems: Linear Interactions Including Wave-Energy Extraction, Cambridge University Press, 2002.

[6] M. Patel, "Dynamics of offshore structures," Butterworth and Co. Ltd., 1980.

[7] K. Thorburn, "Electric Energy Conversion Systems: Wave Energy and Hydropower," Digital Comprehensive Summaries of Uppsala Dissertations from the Faculty of Science and Technology 202, Uppsala University, 2006.

[8] H. Polinder and M. Scuotto, "Wave Energy Converters and their Impact on Power Systems," in 2005 International Conference on Future Power Systems, Nov. 2005.

[9] M. Previsic, "Wave Power Technologies", IEEE Conference Proceeding Power Engineering Society General Meeting, 12-16 June 2005, Vol. 2, pg. 2011-2016.

[10] M. Leijon, H. Bernhoff, O. Agren, J. Isberg, J. Sundberg, M. Berg, K. E. Karlsson, and A. Wolfbrandt, "Multiphysics Simulation of Wave Energy to Electric Energy Conversion by Permanent Magnet Linear Generators," in IEEE Transaction on Energy Conversion, Vol. 20, Issue 1, pp. 219-224, Mar 2005.

[11] H. Polinder, B.C. Mecrow, A.G. Jack, P.G. Dickinson, M.A. Mueller, "Conventional and TFPM Linear Generators for Direct-Drive Wave Energy Conversion", IEEE Trans. on Energy Conversion, Vol. 20, No.2, June 2005

[12] M. Langeliers, E. Agamloh, A. von Jouanne, A. Wallace, "A Permanent Magnet, Rack and Pinion Gearbox for Ocean Energy Extraction," 44th AIAA Aerospace Science Meeting and Exhibit, Reno, NV, Jan. 2006, AIAA-2006-999.

[13] K. Rhinefrank, E.B. Agamloh, A. von Jouanne, A.K. Wallace, J. Prudell, K. Kimble, J. Aills, E. Schmidt, P. Chan, B. Sweeny, A. Schacher, "Novel Ocean Energy Permanent Magnet Linear Generator Buoy", *Elsevier Renewable Energy* Journal, Vol. 31, Issue 9, July 2006, pg. 1279-1298

[14] E.B. Agamloh, A.K. Wallace, and A. von Jouanne, "A Novel Direct-Drive Ocean Wave Energy Extraction Concept with Contact-Less Force Transmission System," Renewable Energy, Vol. 33, 2008, pp. 520-529.

[15] J.H. Prudell, “Novel Design and Implementation of a Permanent Magnet Linear Tubular Generator for Wave Energy Conversion,” Master’s Thesis. Corvallis, OR: Oregon State University, 2007.

[16] M.A. Mueller, “Current and Novel Electrical Generator Technology for Wave Energy Converters,” International Electric Machine and Drive Conference, May 2007, pg. 1401-1406.

[17] M.A. Mueller, A.S. McDonald & D.E. Macpherson “Structural Analysis of Low Speed Axial Flux Permanent Magnet Machines”, IEE Proceedings on Electric Power Applications, Vol 152, No. 6, pp. 1417-1426, November 2005, ISSN 1350-2352

[18] H. Polinder, M. Damen, and F. Gardner, “Linear PM Generator System for Wave Energy Conversion in the AWS,” IEEE Transactions on Energy Conversion, Vol. 19, Issue 3, Sept. 2004, pg. 583-589.

[19] M.A. Mueller, “Electrical generators for direct drive wave energy converters,” in Proc. Inst. Elect. Eng. Generation, Transmission and Distribution, vol. 149, 2002, pp. 446–456.

[20] N.J. Baker, M.A. Mueller, E. Spooner, “Permanent magnet air-cored tubular linear generator for marine energy converters”’ University of Durham, University of Edinburgh, IEE, 2004

[21] M. Blanco, G. Navarro, M. Lafoz, “Control of Power Electronics Driving a Switched Reluctance Linear Generator in Wave Energy Applications,” 13th European Conference on Power Electronics and Applications, Sept. 1009, pg. 1-9.

[22] P. Cancelliere, F. Marignetti, V. Delli Colli, R. Di Stefano, M. Scarano, “A Tubular Generator For Marine Energy Direct Drive Applications”, DAEIMI-Department of Automation, Faculty of Engineering, University of Cassino, 2005

[23] K. Rhinefrank, T. Brekken, B. Pasch, A. Yokochi, and A. von Jouanne, “Comparison of Linear Generators for Wave Energy Applications,” 46th AIAA Aerospace Science Meeting and Exhibit, Reno, NV, Jan. 2008, AIAA-2008-1335.

[24] Z. Nie, P.C.J. Clifton, Y. Wu, and R.A. McMahon, “Emulation and Power Conditioning of Outputs from a Direct Drive Wave Energy Converter,” International Conference on Sustainable Energy Technologies, Nov. 2008, pg. 1129-1133.

[25] A. Schacher, A.V. Meulen, D. Elwood, P. Hogan, K. Rhinefrank, T. Brekken, A. von Jouanne, S. Yim, “Novel Control Design for a Wave Energy Generator,” 46th AIAA Aerospace Science Meeting and Exhibit, Reno, NV, Jan. 2008, AIAA-2008-1305.

[26] J.K.H. Shek, D.E. Macpherson, M.A. Mueller, "Phase and Amplitude Control of a Linear Generator for Wave Energy Conversion" 4th conference on Power Electronics, Machines, and Drives, April 2008, pg. 66-70.

[27] J.K.H. Shek, D.E. Macpherson, M.A. Mueller, J. Xiang, "Reaction Force Control of a Linear Electrical Generator for Direct Drive Wave Energy Conversion", lET Renewable Power Generation, 2007,1, (1), pp. 17-24.

[28] E. Spooner, P. Tavner, M.A. Mueller, N.J. Baker, "Vernier Hybrid Machines for Compact Drive Applications". lEE Int. Conf. Power Electronics, Machines and Drives, Edinburgh, UK, 2004, pp. 452-457.

PER UNIT WAVE ENERGY CONVERTER SYSTEM ANALYSIS

Timothy M. Lewis, Annette von Jouanne, Ted K.A. Brekken

School of Electrical Engineering and Computer Science

1148 Kelley Engineering Center

Oregon State University

Corvallis, USA

lewisti@eecs.oregonstate.edu

Energy Conversion Conference and Exposition

Phoenix, AZ

September 17-22, 2011

3 Per Unit Wave Energy Converter System Analysis

Abstract -A wave energy converter (WEC) system is composed of hydrodynamic, mechanical, and electrical elements, along with the associated control. An integrated design approach that can optimize the attributes between design elements is desired, especially for a smaller WEC device that has size and cost constraints. This paper presents a per-unit analysis system for a point absorber WEC topology. The goal of the per-unit system is to provide insight into the complete system design regardless of the power scale and to assist in the sizing and specification of the disparate components. Empirical characteristics from a WEC are used in the per-unit system and electrical sizing results from an integrated WEC design that uses optimal and other control schemes are presented.

3.1 Introduction

Since wave energy is persistent, predictable, has a high power density, and maintains a minimum power level in most ocean environments it may be of particular interest for energy harvesting for remote or isolated ocean applications [1,2]. Being able to harvest energy in-situ would also lower the need for periodic maintenance for a remote ocean system with some sort of payload that requires power. For such a system it would be desired to minimize the size of the power generating section to maximize the space for the payload and also to make the power system as simple as possible to minimize potential failures.

Since such systems could potentially be very different sizes it would be best to assess system attributes in a generic sense, not tied to the specific physical dimensions of a point-solution design. To that end this paper proposes a per-unit analysis method and then performs some system sizing analysis to reach some general conclusions for such a remote, autonomous WEC system.

3.2 Autonomous Wave Energy Converter System

The device that is proposed for this application as a remote, autonomous WEC is shown in Fig. 13.

The WEC device consists of an outer buoy around a cylindrical spar. The inner cylindrical spar is taut-moored. The outer buoy contains the back-iron for a contact-less force transmission system (CFTS). The CFTS is used to couple the outer moving buoy to an internal spar mechanism. The internal spar mechanism consists of a structure with an electromagnet system that provides contact-less holding torque with the outer float in addition to minimizing the dampening between the float and spar. The electromagnet system is rigidly attached to a central roller screw nut. The electromagnet is energized to make this inner spar structure move vertically which turns the roller lead screw mechanism. On the cylindrical electromagnet assembly an accelerometer is mounted and is used for potential future compensation schemes.

At the end of the roller screw a PM machine is mounted which is controlled in a generating mode. The machine is directly coupled to the lead screw so the electric machine rotates in a bidirectional manner with the vertical oscillatory motion of the float. The machine is a 3-phase PM machine. The control electronics consists of a 6-switch AC/DC converter to rectify and condition the DC output power. Heave acceleration is sensed with an accelerometer on the inner spar cylindrical assembly. Heave position is derived from the sensed commutation resolver position and lead screw pitch. Generator force is sensed through the controlled quadrature current in the PM machine.

This work extends the previous research for an axi-symmetric, heave-only, power absorber in [3,4].

This WEC is currently being designed with the system component requirements being determined with this per-unit analysis which allows for an optimization across the hydrodynamic, mechanical and electrical domains.

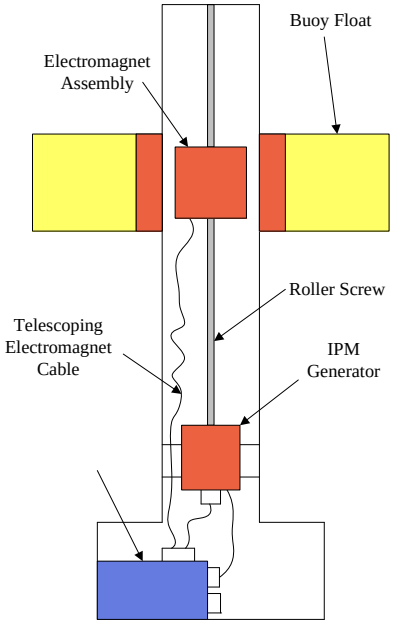

Fig. 13. Proposed WEC Device

3.3 Linearized Wave Equation

For a WEC system the force balance is described by:

$$F_e + F_r + F_b + F_{gen} = m\ddot{z}_B \tag{1}$$

in which F_e is the excitation force, F_r is the radiation force generated by the object in the water, F_b is the buoyancy force of the object in the water, F_{gen} is the generator force, m is the mass of the object, and $\ddot{z}_B$ is the acceleration in the heave (vertical) direction for a one dimensional WEC converter.

Wave action can be approximated and is typically described in the literature by using a linearization of the Morrison wave equation [5]. The hydrodynamic equations involving an object moving at velocity v, in a flow with velocity u, is:

$$(\dot{u} - \dot{v})A + (u - v)^2\hat{B} + F_{ext} = m\dot{v} \tag{2}$$

A dampening term, *B*, is used to linearize $(u-v)^2$ for small $(u-v)$ or $(\dot{z}_w - \dot{z}_b)$ for a heave reference system. With the definition of the added mass term, *A*, the linearization is:

$$(\ddot{z}_w - \ddot{z}_b)A + (\dot{z}_w - \dot{z}_b)B + (z_w - z_b)K + F_{gen} = m\ddot{z}_b \tag{3}$$

Grouping:

$$F_e = A\ddot{z}_w + B\dot{z}_w + Kz_w \tag{4}$$

$$F_r = -A\ddot{z}_b - B\dot{z}_b \tag{5}$$

$$F_b = -Kz_b \tag{6}$$

yields the system linearization:

$$F_e + F_{gen} = M\ddot{z}_b + B\dot{z}_b + Kz_b \tag{7}$$

where F_e is the excitation force from the wave; *M* is the system mass, *m*, plus the added mass, *A*; *B* is the viscous damping of the mechanical system, *K* is the hydrostatic stiffness, and z_w is the elevation of the water at the device.

This linearization is the standard first order approximation in the literature. It yields a linear differential equation that is more suitable for analysis and control techniques than the partial differential equations that usually result from wave theory.

Since the hydrodynamic solution of the Morison model is similar to a mass-spring-damper system with a periodic input, the concept of formulating a generator equivalent is often used to extract power with active control. This is because the solution for power extraction can be arrived at by matching the impedance of the incident hydrodynamic input with that of the generator control system. When matched the maximum amount of power can be extracted. For a one dimensional heave system, this maximum is 50% [2].

3.4 Equivalent Circuit

For this family of matching strategies an equivalent electrical representation can be formulated and it is shown in Fig. 14. In this equivalent, the input force is analogous to voltage and the buoy velocity state variable ($\dot{z}_b$) is analogous to current. For the system linear time-invariant coefficients, the mass (*M*) terms are analogous to inductance, the dampening (*B*) terms are analogous to resistance, and the hydrostatic stiffness (*K*) terms are analogous to inverse capacitance. The generator impedance is the summation of forces proportional to buoy heave acceleration ($\ddot{z}_w$), velocity ($\dot{z}_b$), and position (z_b).

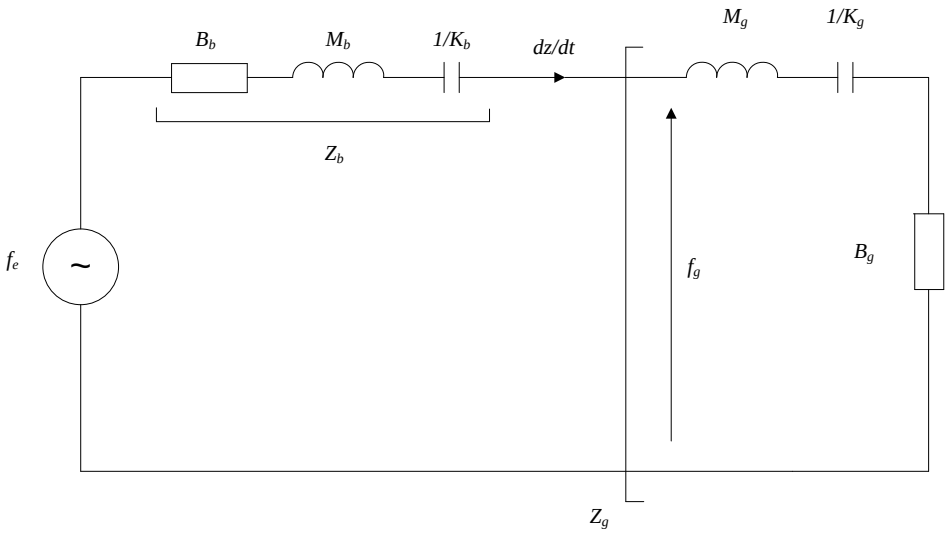

Fig. 14. Equivalent Circuit with Matching Control

3.5 Autonomous Wave Energy Converter Modeling

The Morison model for the hydrodynamic representation for the ocean dynamics is similar to a mass-spring-damper system with a periodic input. The combined coefficients of the hydrodynamic and mechanical system are derived from the free-body diagram, Fig. 15. The mass and dampening term both need to be modified due to the coupled CFTS, roller screw, and generator system.

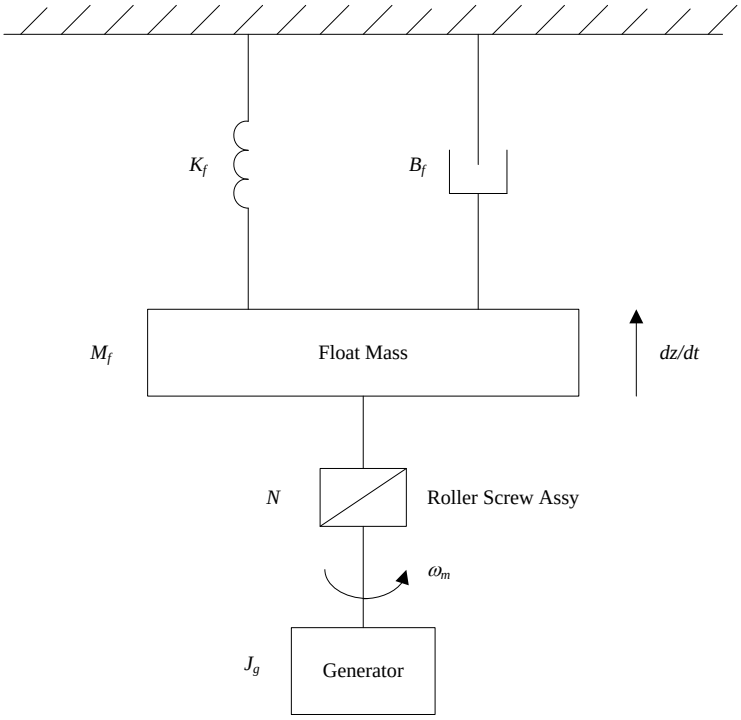

Fig. 15. WEC Free-Body Diagram

The addition of the roller screw assembly and generator alter the system coefficients via the lead screw turns-to-distance pitch. The coefficients are reflected to the buoy side with the following equations.

$$M = M_f + M_a + N^2 J_g \quad [kg] \tag{8}$$

$$B = B_f + B_{cfts} + B_{trans} + NB_g \quad [\frac{kg}{s}] \tag{9}$$

M Total mass of system [kg]

M_f Physical mass of buoy float [kg]

M_a Added mass of water [kg]

N Linear roller screw pitch [m/rev]

J_g Inertia of the electric machine [kg·m2]

K_f Hydrodynamic stiffness of the system [N/m]

B Total dampening of the system [N·s/m]

B_{cfts} Dampening of the contact-less force transmission system [N·s/m]

B_{trans} Dampening of the roller screw transmission [N·s/m]

B_g Dampening of the electric machine [N·s/m]

This unique feature will be utilized to increase the 'apparent' mass of the mechanical system and lower the buoy's natural resonating frequency. The WEC mechanical resonance result of this reflected inertia scheme would then be:

$$\omega_m = \sqrt{\frac{K}{M_f + M_a + N^2 J_g}} \tag{10}$$

3.6 Control Strategies Utilized in Study

In this study, two different control strategies will be utilized to assess the effects of purposely changing the WEC's natural mechanical frequency. Each of the strategies has different overall purposes. The reason for using two different strategies is to ensure that the conclusions regarding the use of the reflected inertia are not obscured

due to the use of one control method. The strategies utilized were Binary Optimal Control and Matched Impedance Control. The details of the strategies are in [6] but are summarized below.

For power absorption to occur in a WEC the control essentially makes the WEC system's controlled plus natural mechanical frequency match the natural frequency of the ocean wave from which power is extracted. The control compensates for if the natural mechanical frequency does not match the wave, controlling the generator to extract power and keep the WEC system in resonance with the ocean wave.

3.6.1 Binary Optimal Control

Under optimal control the generator coefficients are controlled such that these parameters are the complex conjugate of the hydrodynamic input. Under this control scheme as realized in [7,8] the dampening and hydrodynamic generator terms are controlled and the mass term is set to zero. The control is set up such that:

$$B_g = B_b \tag{11}$$

$$K_g = M_b \cdot \omega^2 - K_b \tag{12}$$

There will therefore be two components, or binary, control of the generator current command: a dampening force proportional to the velocity which provides amplitude control and the conservation of real power, and a hydrodynamic stiffening force proportional to displacement that provides phase control.

Matched Non-Reactive Control

Matched Non-Reactive Control is detailed in Ref. [9]. (Some literature cites this as C_{gen} control). Only the dampening term is utilized and the control is set up as:

$$B_g = |\bar{Z}_b(j\omega)| = \left|B_b + j\omega \cdot M_b + \frac{K_b}{j\omega}\right| \tag{13}$$

The goal of this control is to limit the velocity and reactive control swing by ensuring power is always absorbed and not regenerated. (Add wideband control and note – use in analysis)

3.6.2 Per-Unit Wave Energy Converter Analysis

Per-unit scaling is used extensively in power system analysis. Traditionally this has been done to eliminate the effects of step-up and step-down transformers from the numerical analysis. For power flow analysis this eliminates the additional cumbersome transformers turns-count ratios. Also most per-unit systems normalize parameters of particular interest to unity then comparisons to these values can be identified as "normal" or "rated" [10]. As an example, for power systems when the system is converted to per-unit quantities a base quantity of unity apparent power (VA) is often selected [11].

Per-unit systems can also be used for scaling. Often in hydrodynamics this is done using the dimensionless Froude number. The Froude number is based on the ratio of a body's inertia to gravitational forces and that results in scaling based on the square root of the length of the body. This type of scaling, or per-unit system, is useful for extrapolating experimental results from scale models, for example, in hydrodynamic tank testing.

The per-unit system used for this analysis is based on deriving near-unity values that span the systems so that a more complete hydrodynamic-to-mechanical-to-electrical system analysis can occur.

The reasons for using a per-unit analysis for this work are:

The elimination of the 'transformer' effect, albeit it could also be mechanical in nature (gearbox or lead-screw).

Normalization will demonstrate relative power levels in a mixed-physics analysis. The wave energy system and environment will include power devices that have

alternating current terminal conditions, direct current terminal conditions, and mechanical force, velocity, and displacement terminal conditions.

The chosen per-unit base values for this study are 1.0 N (rms) for the wave forcing function (F_e) and a 0.5 Ω impedance for the buoy mechanical dampening (B_b). If a heave-only WEC is perfectly matched (B_g = 0.5 Ω) this will yield a wave power of 1 W, a heave velocity ($\dot{z}_b$) of 1 m/s, and an absorbed WEC power of 0.5 W. (The maximum power absorbed with a heave-only WEC is 50%). To eliminate the frequency term in the buoy impedances and to normalize all ocean spectra, a base value of 1.0 rad/sec is chosen for the dominant ocean wave frequency ($\hat{\omega}$). This is summarized as:

$$\frac{\langle F_e^2 \rangle}{F_{e,base}} = 1.0 \tag{14}$$

$$\frac{B_b}{Z_{base}} = 0.5 \tag{15}$$

$$\frac{\hat{\omega}}{\omega_{base}} = 1.0 \tag{16}$$

3.7 Per-unit WEC Simulations

To analyze the effect of the reflected inertia term, simulations were performed utilizing the real-world buoy parameters from [9] and the Buoy 51101 (NW Hawaii) ocean spectra utilized in [6].

For the study a resonance ratio is defined to quantify how different the buoy's natural mechanical resonance is from the ocean spectra's dominant frequency, or the frequency that the WEC is tuned to. The resonance ratio is then:

$$N_r = \frac{\omega_m}{\hat{\omega}} \tag{17}$$

The resonance ratios compared were 1.05, 1.94 (the resonance ratio of the mechanical buoy with the Buoy 51101 dominant wave frequency), and 3.0.

3.8 Power and Heave Velocity Comparison

Fig. 16, Fig. 17, and Fig. 18 show the power absorbed for each of the two control methods for each of the three resonance ratio conditions. As expected the Matched Non-Reactive Control does not have bidirectional power flow since it is tuning with just the dampening (resistive) term and the power absorbed is consistent as the resonance ratio increases. The Binary Optimal Control will absorb a greater amount of power but it also is bidirectional, returning power to the sea over parts of the time-series. Since the power flow is bidirectional the use of Binary Control necessitates the need for some amount of energy storage on the WEC. As the resonance ratio increases it can be seen that the magnitude of the bidirectional power flow increases greatly. This would increase the amount of energy storage required if maintaining optimal control and resonance as the resonance ratio increases.

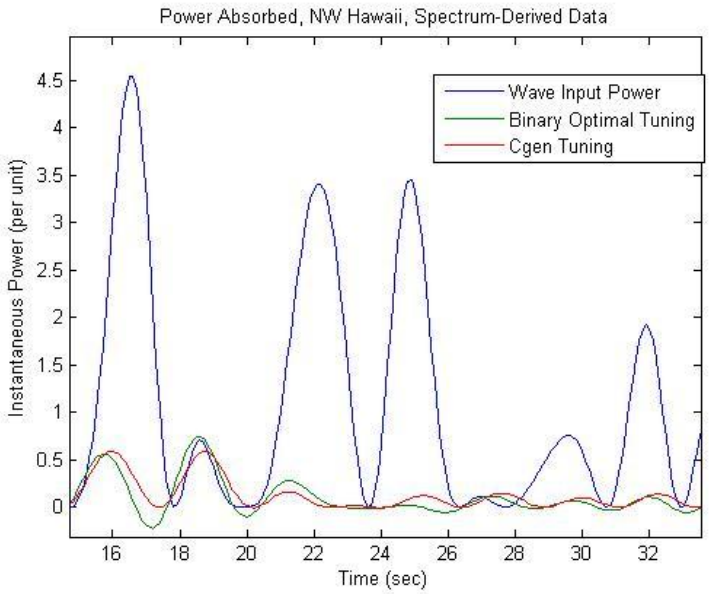

Fig. 16. Power Absorbed, 1.05 Resonance Ration

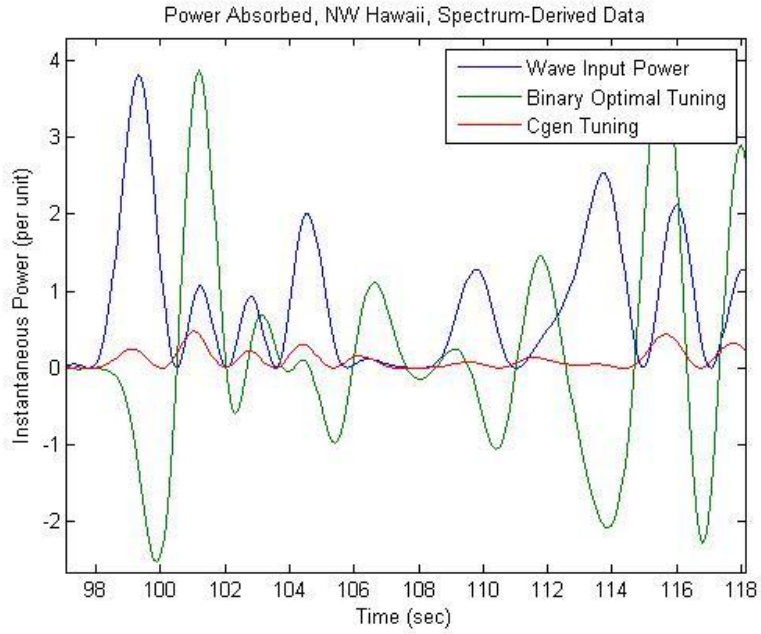

Fig. 17. Power Absorbed, 1.94 Resonance Ratio

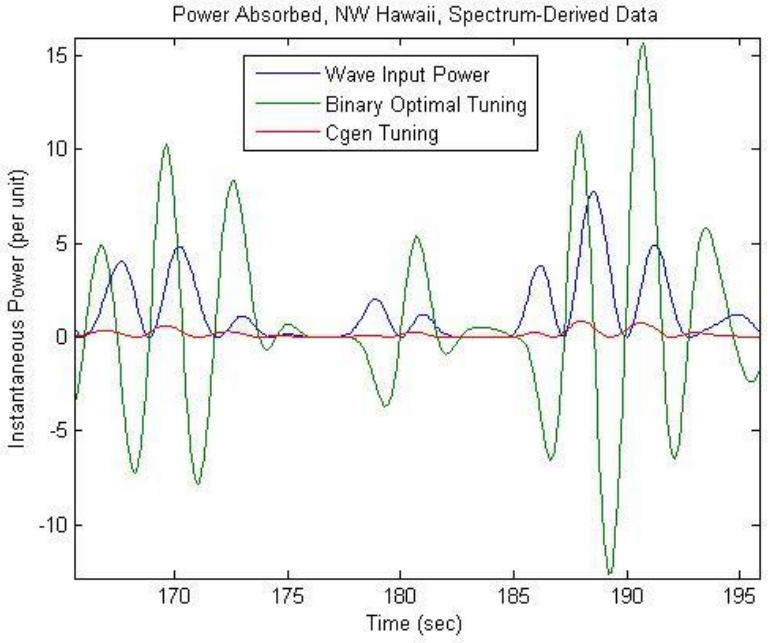

Fig. 18. Power Absorbed, 3.0 Resonance Ratio

Fig. 19, Fig. 20, and Fig. 21 show the WEC heave velocities with the different resonance ratios. In Fig. 19. Heave Velocity, 1.05 Resonance Ratio

when the resonance ratio is near unity the heave velocity using Binary Optimal Control is nearly the same as the heave velocity resulting from the dampening-only Matched Non-Reactive Control.

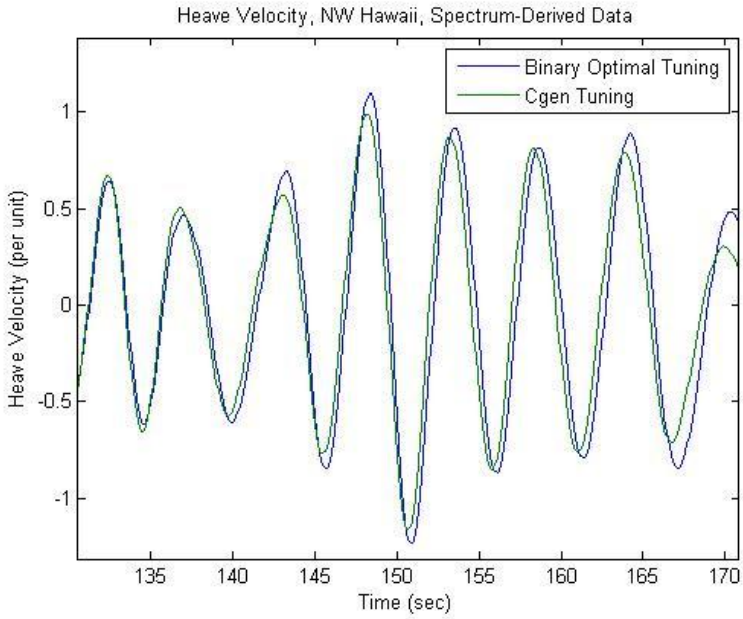

Fig. 19. Heave Velocity, 1.05 Resonance Ratio

But as the resonance ratio increases the heave velocity increases greatly when using Binary Control. This would necessitate a WEC with a longer active travel area to accommodate the greater speeds or some sort of end-of-travel limiting to contain this. The use of end-of-travel limiting though would reduce the power absorbed once that supervisory control is activated.

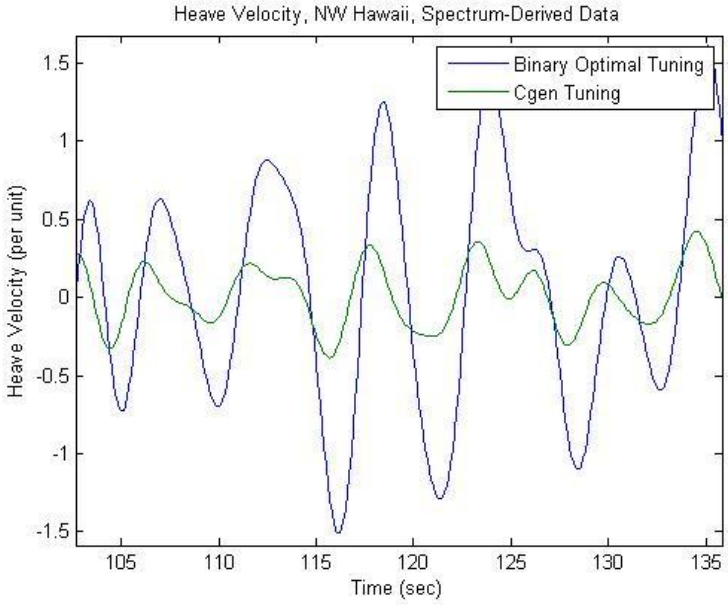

Fig. 20. Heave Velocity, 1.94 Resonance Ratio

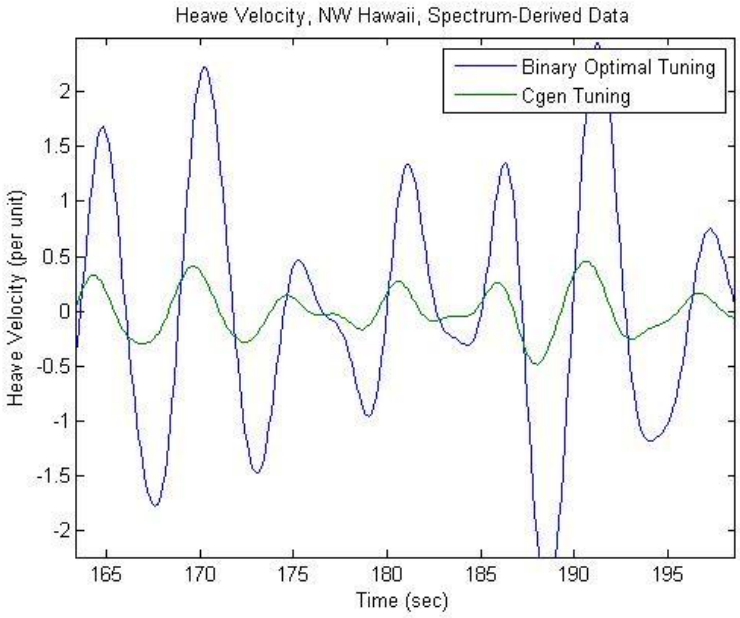

Fig. 21. Heave Velocity, 3.0 Resonance Ratio

3.9 Binary Optimal Control Force vs. Velocity Results

To analyze the imposed requirements on the electrical power system when the resonance ratio changes, plots of the generator force vs. velocity were also generated. For Binary Optimal Control it can be seen, Fig. 22, that the required force is approximately 0.5 per-unit and the required velocity is approximately 1.0 per-unit which is to be expected since very little control is being exerted. As the resonance ratio increases though the force and velocity requirements increase greatly,Fig. 23, and Fig. 24. This translates to an increased rating for the generator system power electronics and a generator with a large torque vs. speed curve.

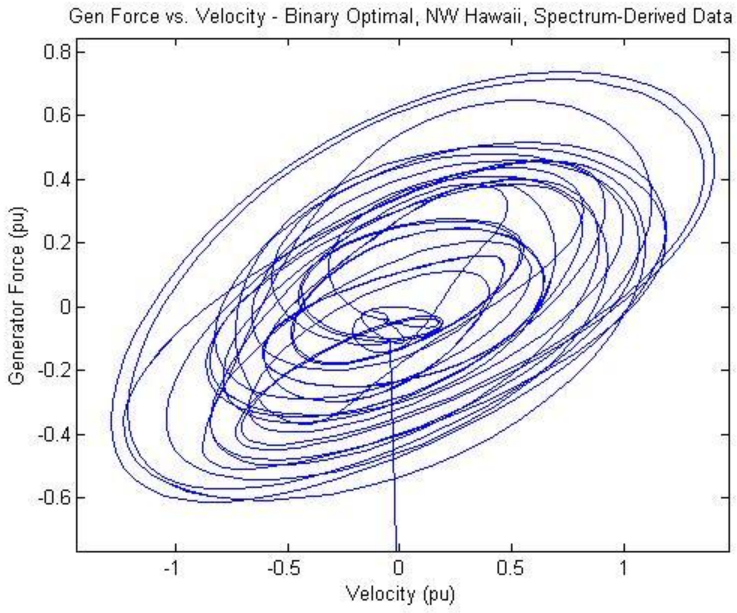

Fig. 22. Force vs. Velocity, 1.05 Resonance Ratio

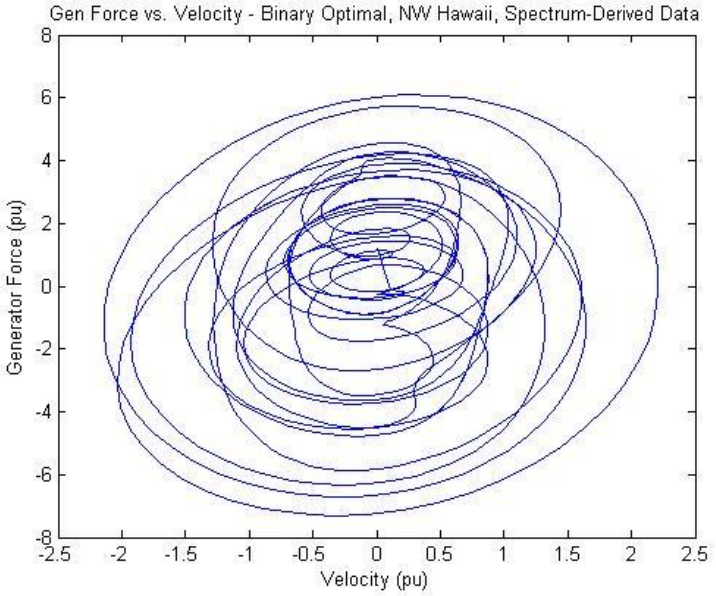

Fig. 23. Force vs. Velocity, 1.94 Resonance Ratio

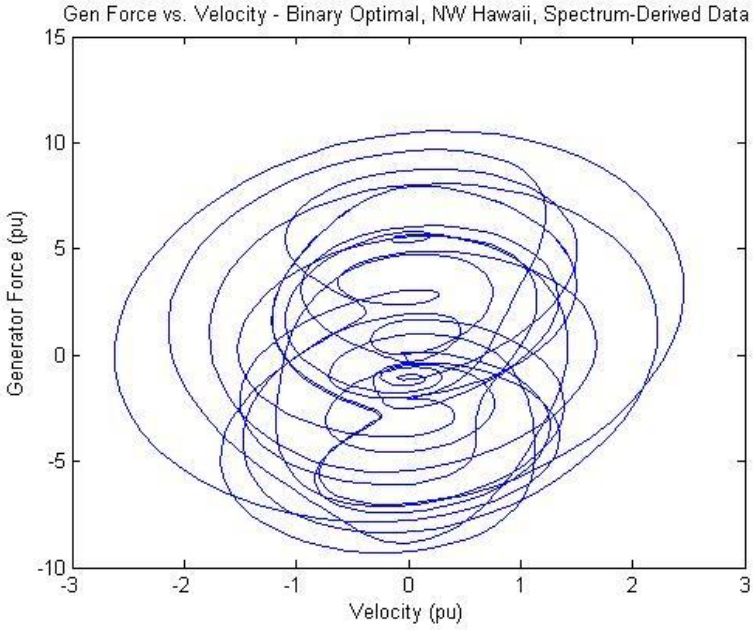

Fig. 24. Force vs. Velocity, 3.0 Resonance Ratio

3.10 Matched Non-Reactive (Cgen) Control Force vs. Velocity Results

The Matched Non-Reactive Control results are shown in Fig. 25, Fig. 26, and Fig. 27. Since this is just dampening control the generator force is directly proportional to velocity and any deviation from that is due to the changing slope of that ratio due to the changing input wave frequencies. Even when using this control scheme the force requirements of the generator increase as the resonance ratio increases. Though the velocity requirement seems to diminish it is felt that this is due to the non-matched, and loss of power absorption ability.

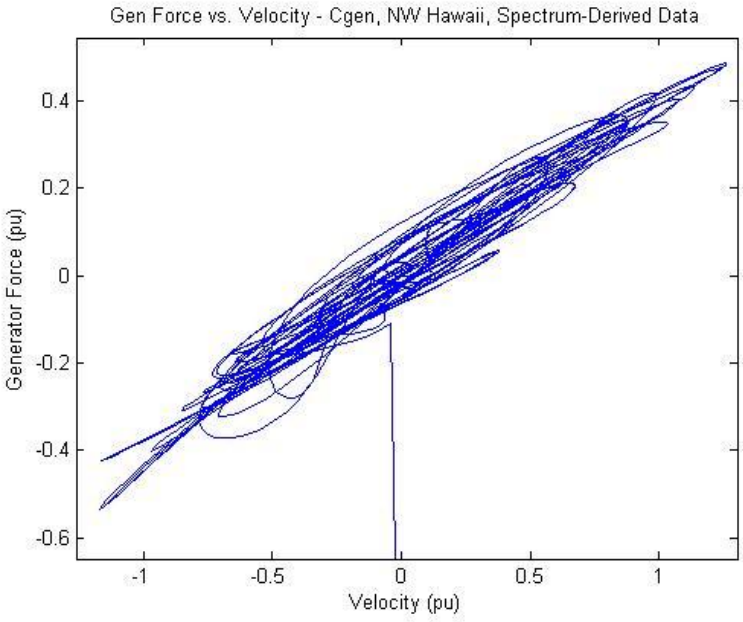

Fig. 25. Force vs. Velocity, 1.05 Resonance Ratio

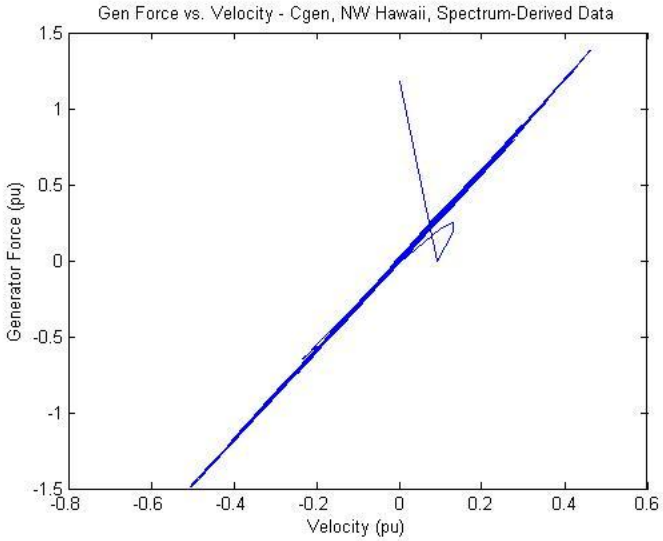

Fig. 26. Force vs. Velocity, 1.94 Resonance Ratio

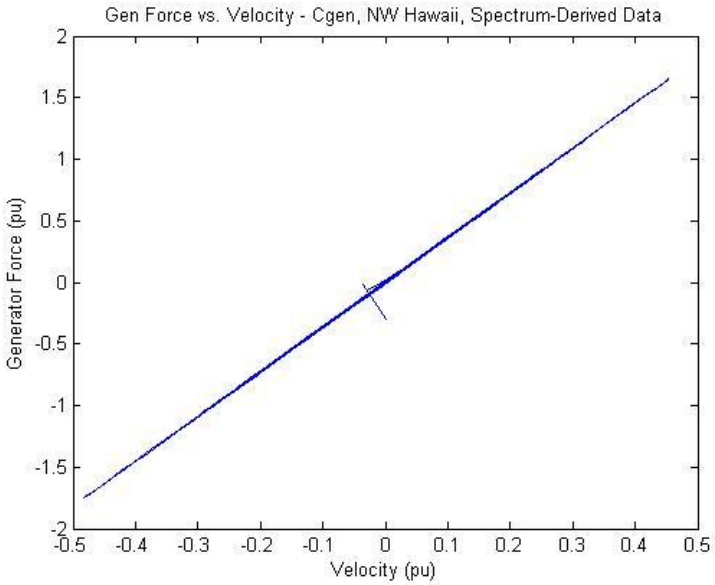

Fig. 27. Force vs. Velocity, 3.0 Resonance Ratio

3.11 Conclusions

This paper has described a per-unit analysis system for wave energy converters (WEC) to allow for the quantitative assessment of devices with different physical

dimensions. The purpose of this was to analyze generalized features and concepts that affect the system design.

One analyzed trade-off was assessing the impact of the resonance ratio on the required sizing of the electrical components. It was found that having a wide mechanical-resonance-to-wave frequency ratio greatly increased the required rating of the power take-off generator and power electronics. A concept for reducing this ratio through the use of a reflected inertia was presented.

Future work will involve the physical implementation of the WEC system and testing to validate the concepts presented.

3.12 References

[1] T. Brekken and A. von Jouanne "ECCE Wave Energy Tutorial", Energy Conversion Conference and Exposition, Sept 2009

[2] J. Falnes, Ocean Waves and Oscillating Systems: Linear Interactions Including Wave-Energy Extraction, Cambridge University Press, 2002.

[3] M. Langeliers, E. Agamloh, A. von Jouanne, A. Wallace, "A Permanent Magnet, Rack and Pinion Gearbox for Ocean Energy Extraction," *44th AIAA Aerospace Science Meeting and Exhibit*, Reno, NV, Jan. 2006, AIAA-2006-999.

[4] K. Rhinefrank, E.B. Agamloh, A. von Jouanne, A.K. Wallace, J. Prudell, K. Kimble, J. Aills, E. Schmidt, P. Chan, B. Sweeny, A. Schacher, "Novel Ocean Energy Permanent Magnet Linear Generator Buoy", *Elsevier Renewable Energy Journal*, Vol. 31, Issue 9, July 2006, pg. 1279-1298

[5] M. Patel, *Dynamics of Offshore Structures*. Butterworth-Heinemann, 1989.

[6] T. Lewis, A. von Jouanne, T. Brekken, "Wave Energy Converter with Wideband Power Absorption," Digest for *IEEE Energy Conversion Congress and Exposition 2011*.

[7] J.K.H. Shek, D.E. Macpherson, M.A. Mueller, "Phase and Amplitude Control of a Linear Generator for Wave Energy Conversion" *4th Conference on Power Electronics, Machines, and Drives*, April 2008, pg. 66-70.

[8] J.K.H. Shek, D.E. Macpherson, M.A. Mueller, J. Xiang, "Reaction Force Control of a Linear Electrical Generator for Direct Drive Wave Energy Conversion", *lET Renewable Power Generation*, 2007,1, (1), pp. 17-24.

[9] Schacher, A.V. Meulen, D. Elwood, P. Hogan, K. Rhinefrank, T. Brekken, A. von Jouanne, S. Yim, "Novel Control Design for a Wave Energy Generator," *46th AIAA Aerospace Science Meeting and Exhibit*, Reno, NV, Jan. 2008, AIAA-2008-1305.

[10] C.A. Gross, S.P. Melipoulos, "Per-Unit Scaling in Electric Power Systems", *Transactions on Power Systems*, Vol. 7, No. 2, May 1992.

[11] P.C. Krause, O. Wasynczuk, S.D. Sudhoff, *Analysis of Electric Machinery*, McGraw Hill, 1986

WAVE ENERGY CONVERTER WITH WIDEBAND POWER ABSORPTION

Timothy M. Lewis, Annette von Jouanne, Ted K.A. Brekken

School of Electrical Engineering and Computer Science

1148 Kelley Engineering Center

Oregon State University

Corvallis, USA

lewisti@eecs.oregonstate.edu

Energy Conversion Conference and Exposition

Phoenix, AZ

September 17-22, 2011

4 Wave Energy Converter with Wideband Power Absorption

Abstract - Wave energy possesses a wide frequency range for many real-world ocean locations compared to the power absorption or capture range for some proposed Wave Energy Converter (WEC) systems. Many ocean sites possess waves with a rich frequency content due either to random sea or in-shore effects. This paper first demonstrates the potential missed energy extraction opportunities at three different ocean sites using the buoy parameters from a previously built WEC that utilizes an optimal control scheme. It then introduces several control strategies in the literature, in addition to a proposed wide bandwidth control strategy, and compares the amount of relative power absorption of the WEC. The proposed controller does not require acceleration feedback and can be realized with only position feedback. The design of the proposed controller is discussed and then the power absorption results are compared to optimal and other wave energy capture schemes.

4.1 Introduction

Wave energy is recognized as a potential source for energy harvesting. Direct energy from the immediate ocean environment may be of particular interest for remote or isolated ocean applications since the local wave energy source is persistent, predictable, has a high power density, and maintains a minimum power level in most ocean environments [1,2]. Wave energy converters can then extract more power from a smaller volume at a consequential lower cost and reduced visual impact. This paper will explore a particular wave energy converter (WEC) device solution, a heave-only point absorber, for use in a remote, or isolated, application with a control method to further increase the amount of energy captured. The work extends the previous research for an axisymmetric, heave-only, power absorber [3,4]

4.2 Ocean Wave Spectra

WEC power absorption estimates are complicated by the stochastic nature and wide frequency range of the wave energy. The frequency range of the wave energy can be due to random sea or in-shore effects. Some work [5] is starting to use more stochastic wave stimulus that was found to be more realistic of waves in the ocean environment. This frequency range effect is well understood and predicted spectra have been empirically derived by Pierson and Moskowitz [6]. The Pierson-Moskowitz distribution were defined for deep water conditions but also in-shore (close to shore) effects can increase the frequency range of the wave energy spectra. Since proposed power absorbing WECs for renewable energy are mostly proposed to be close to the shore, these effects should be understood.

Calculation for the potential power in waves is typically derived from a monochromatic wave assumption or using the equivalence of significant wave height and energy period derived from the generated moments of a wave spectral density. Only some of the energy represented by the spectral density is available to the WEC, as dictated by its frequency response.

Since this paper will address the power capture ability of WECs viewed from the frequency domain, knowledge of the wave energy density is required. Real ocean energy spectra data of wave energy in different locations is captured by NOAA buoys and this information will be used in this study to quantitatively assess the impact on power absorption due to the wave frequency spectra and power capture bandwidth.

The three ocean sites that will be used for this study are Buoy 51101, 170 NM north-west of Kauai, Hawaii (Fig. 28); Buoy 46050, 20 NM west of Newport, Oregon (Fig. 29); and Buoy 52200 near Ipan, Guam (Fig. 30).

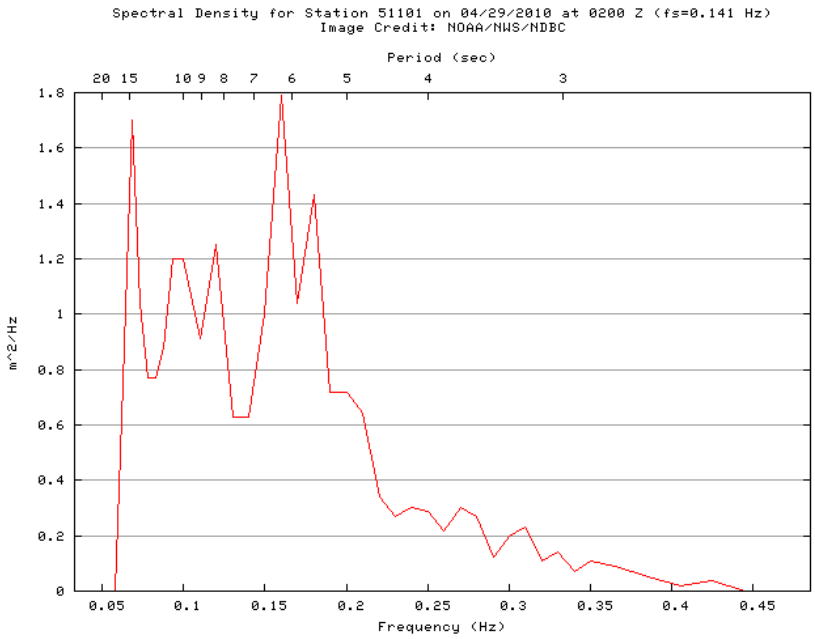

Fig. 28. NW Hawaii

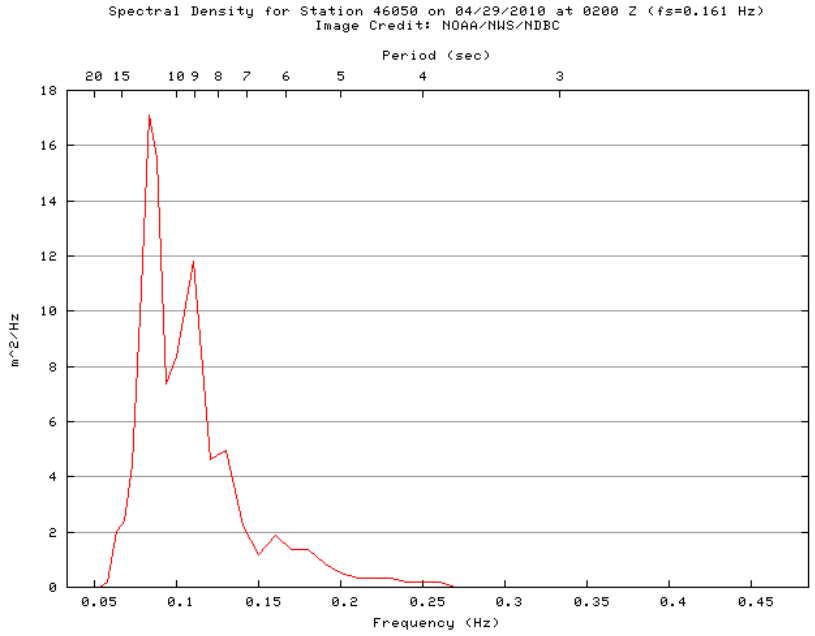

Fig. 29. Stonewall Banks

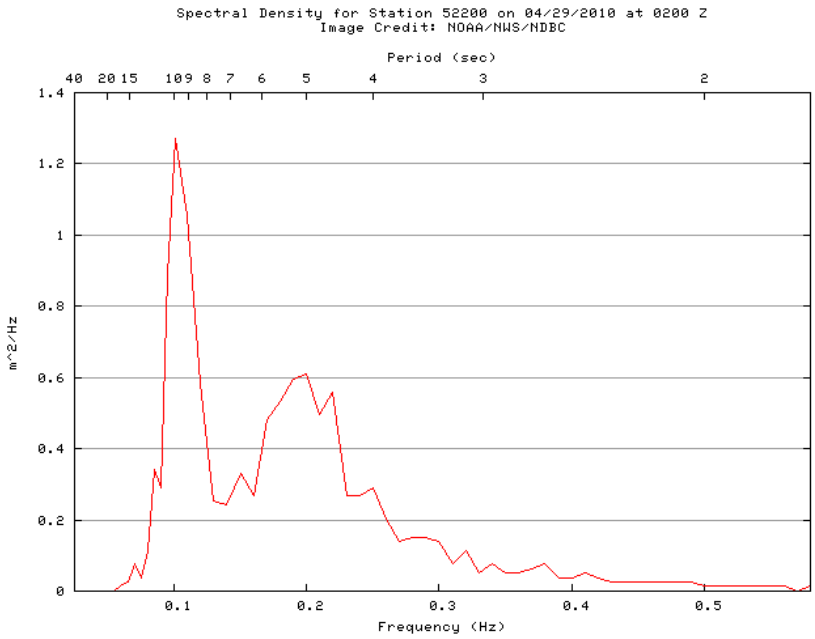

Fig. 30. Ipan, Guam

Notable for these ocean locations is that the ocean spectra does not have a single dominant frequency. The NW Hawaii spectra has significant energy content with both 6 second and 15 second waves and the Guam spectra has narrowband energy at the dominant frequency (10 second waves) and a more frequency distributed energy content around the second dominant frequency (5 second waves).

4.3 Linearized Wave Equation

For a WEC system the force balance is described by:

$$F_e + F_r + F_b + F_{gen} = m\ddot{z}_B \tag{1}$$

in which F_e is the excitation force, F_r is the radiation force generated by the object in the water, F_b is the buoyancy force of the object in the water, F_{gen} is the generator force, m is the mass of the object, and $\ddot{z}_B$ is the acceleration in the heave (vertical) direction for a one dimensional WEC converter.

Wave action can be approximated and is typically described in the literature by using a linearization of the Morrison wave equation [7]. The hydrodynamic equations involving an object moving at velocity *v*, in a flow with velocity *u*, is:

$$(\dot{u} - \dot{v})A + (u - v)^2\hat{B} + F_{ext} = m\dot{v} \tag{2}$$

A dampening term, *B*, is used to linearize $(u - v)^2$ for small $(u - v)$ or $(\dot{z}_w - \dot{z}_b)$ for a heave reference system. With the definition of the added mass term, *A*, the linearization is:

$$(\ddot{z}_w - \ddot{z}_b)A + (\dot{z}_w - \dot{z}_b)B + (z_w - z_b)K + F_{gen} = m\ddot{z}_b \tag{3}$$

Grouping:

$$F_e = A\ddot{z}_w + B\dot{z}_w + Kz_w \tag{4}$$

$$F_r = -A\ddot{z}_b - B\dot{z}_b \tag{5}$$

$$F_b = -Kz_b \tag{6}$$

yields the system linearization:

$$F_e + F_{gen} = M\ddot{z}_b + B\dot{z}_b + Kz_b \tag{7}$$

where F_e is the excitation force from the wave; *M* is the system mass, *m*, plus the added mass, *A*; *B* is the viscous damping of the mechanical system, *K* is the hydrostatic stiffness, and z_w is the elevation of the water at the device.

This linearization is the standard first order approximation in the literature. It yields a linear differential equation that is more suitable for analysis and control techniques than the partial differential equations that usually result from wave theory.

Since the hydrodynamic solution of the Morison model is similar to a mass-spring-damper system with a periodic input, the concept of formulating a generator equivalent is often used to extract power with active control. This is because the

solution for power extraction can be arrived at by matching the impedance of the incident hydrodynamic input with that of the generator control system. When matched the maximum amount of power can be extracted. For a one dimensional heave system, this maximum is 50% [4]. Control is summarized by Nie [5] but expanded on later in the detailed explanation of control strategies.

4.4 Equivalent Circuit

For this family of matching strategies an equivalent electrical representation can be formulated and it is shown in Fig. 31. In this equivalent circuit, the input force is analogous to voltage and the buoy velocity state variable ($\dot{z}_b$) is analogous to current. For the system linear time-invariant coefficients, the mass (*M*) terms are analogous to inductance, the dampening (*B*) terms are analogous to resistance, and the hydrostatic stiffness (*K*) terms are analogous to inverse capacitance. The generator impedance is the summation of forces proportional to buoy heave acceleration ($\ddot{z}_b$), velocity ($\dot{z}_b$), and position (z_b).

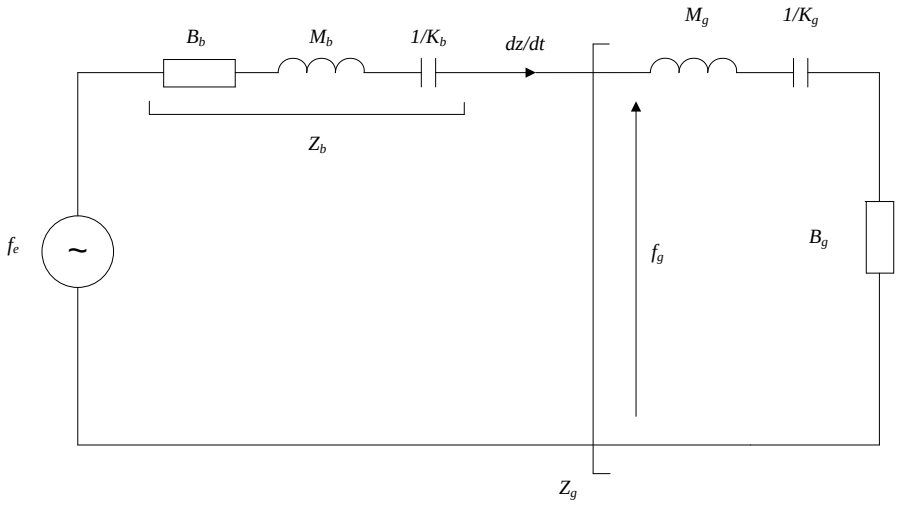

Fig. 31. Equivalent Circuit

4.5 Previous Controller Architectures

4.5.1 Binary Optimal Control

Under matched impedance, or what is termed optimal, the generator coefficients are controlled such that these parameters are the complex conjugate of the hydrodynamic input. The generator's complex conjugate output should then equate the real part (dampening) and provide the opposite polarity reactive control (mass and buoyancy equivalents). The matching of the reactive force components means that the generator must deliver power to the water at certain points of the periodic cycle.

Shek [8,9] implements a binary control term into the generator current, which is proportional to the amount of generator force exerted or absorbed in the WEC. Under this control scheme, the dampening (B_g) and hydrodynamic generator (K_g) terms are controlled and the mass term is set to zero. The control is set up such that:

$$B_g = B_b \tag{8}$$

$$K_g = M_b \cdot \omega^2 - K_b \tag{9}$$

There will therefore be two components of the generator current command: a dampening force proportional to the velocity which provides amplitude control and the conservation of real power, and a hydrodynamic stiffening force proportional to displacement that provides phase control.

Advantages

The advantages of this control scheme are that it does not require acceleration feedback (only velocity and position feedback are required), it does provide perfect matching, and it is relatively simple.

Disadvantages

The disadvantages of this control scheme are that though it does provide for perfect matching, that only occurs at a single designated frequency. For perfect matching and maximum power capture, this frequency must line up with the ocean spectra's dominant frequency necessitating some sort of maximum power point tracking algorithm. Also, for the non-dominant frequency spectra that is either due to a non-alignment of the assumed dominant frequency or the frequency spread of the ocean power, perfect matching does not occur and the maximum power is not absorbed.

4.5.2 Ternary Optimal Control

Another version of complex conjugate control could be formulated by setting:

$$B_g = B_b \tag{10}$$

$$K_g = -K_b \tag{11}$$

$$M_g = -M_b \tag{12}$$

This control scheme is termed ternary optimal control since all three sensed or estimated system states (acceleration, velocity, and position) are used to form the dampening term for maximum power transfer and for perfect complex conjugate matching by matching each reactive term individually. Since there is no assumed dominant wave frequency used in matching and each of the three linearized buoy dynamic terms are matched or cancelled with this feedforward approach, the WEC would theoretically have perfect matching regardless of ocean spectra frequency content.

Advantages

The advantage of this control scheme is that it can theoretically provide perfect matching regardless of wave frequency.

Disadvantages

The disadvantages of this control scheme are that it requires acceleration sensing and its feedforward effectiveness is dependent on the accuracy of the Morison linearization.

Analysis of this controller, and a proposed control scheme, is performed in [10] but this paper focuses on the analysis of control solutions without acceleration sensing and proposed solutions of achieving a wide frequency response without it.

4.5.3 Matched Non-Reactive Control

A by-product of the optimal control schemes above is that the resonance of the WEC is increased and WEC velocities can increase greatly. Often some sort of limit control must be placed into the control scheme to protect the WEC. To accomplish this limit control and also to limit the amount of 'reactive' power flow a matched dampening control was proposed in [11]. This scheme is sub-optimal and is termed Matched Non-Reactive Control. (Some literature cites this as C_{gen} control). With this control scheme only the dampening term is controlled and it is controlled to match the buoy's total impedance:

$$B_g = |\bar{Z}_b(j\omega)| = \left|B_b + j\omega \cdot M_b + \frac{K_b}{j\omega}\right| \tag{13}$$

The frequency selected for the compensation is assumed to be the dominant wave frequency.

Advantages

The advantages of this control scheme are that it is simple; utilizing one control term for both matching and end-limit control, and that it requires only velocity sensing. This control scheme also does not require passive energy storage since it is not actively cancelling the buoy reactive dynamics with reactive control.

Disadvantages

Though the scheme utilizes an assumed dominant wave frequency, the scheme will never match perfectly since it is not canceling the 'reactive' components. It also does not have a frequency response that matching the ocean spectra (seen later).

4.6 Bandwidth and Power Capture

When the response of the WEC buoy/controller system is viewed in the frequency domain, it can exhibit a bandpass filter type of response with several of the control schemes.

When the buoy and controller mass (*M*), dampening (*B*), and hydrostatic stiffness (*K*) terms are lumped together the equivalent Laplace formulation of the impedance is:

$$Z_{WEC}(s) = \frac{\left(\frac{1}{M}\right)s}{s^2+\left(\frac{B}{M}\right)s+\frac{K}{M}} \tag{14}$$

This is the form of a bandpass filter with the characteristics:

$$Z_{WEC}(s) = \frac{C\prime s}{s^2+\left(\frac{\omega_0}{Q}\right)s+\omega_o^2} \tag{15}$$

Using binary optimal control described above, there would be a second order response with the characteristics of:

$$BW = \frac{B_b+B_g}{M_b} \tag{16}$$

$$\omega_o = \sqrt{\frac{K_b+K_g}{M_b}} \tag{17}$$

Fig. 32 shows the response of a 1 kW buoy [9] using binary optimal control.

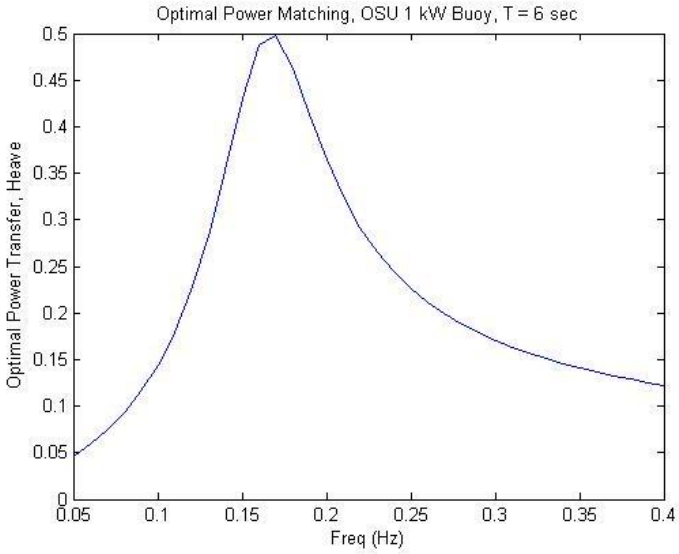

Fig. 32. Binary Optimal Control Bandwidth Response

Even when the optimal control center frequency is perfectly matched to the wave, a significant part of the wave's energy spectrum is not absorbed. Fig. 33 shows the energy absorption response of an optimally tuned buoy with empirical wave data from NW Hawaii buoy 51101.

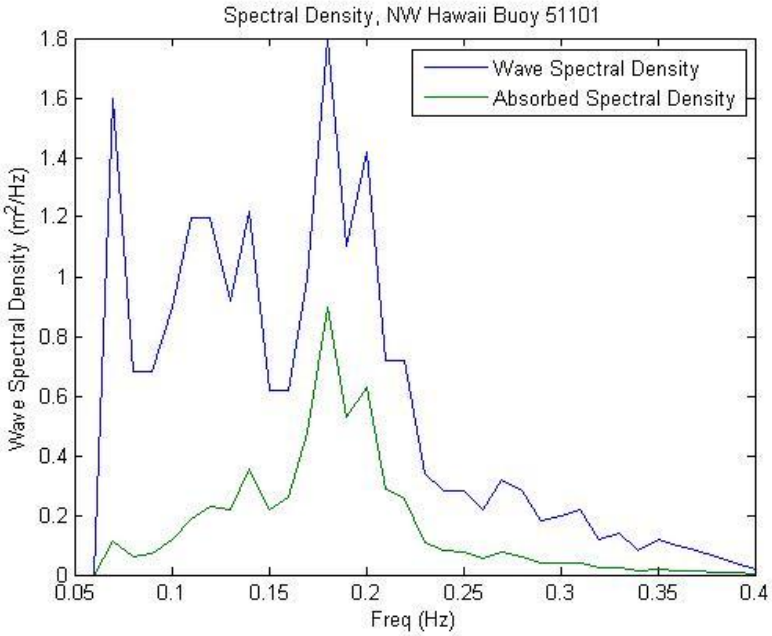

Fig. 33. Absorbed Spectrum, NW Hawaii

Fig. 34 and Fig. 35 then show the frequency domain response and the qualitative loss of power captured, for the Stonewall Banks, OR and the Ipan, Guam ocean locations with their spectral conditions.

Also note that for these plots the dominant wave frequency is assumed to be known. If the tracking algorithm to derive this is off, the optimal tuning would occur for the wrong dominant frequency and the spectral capture would be even less.

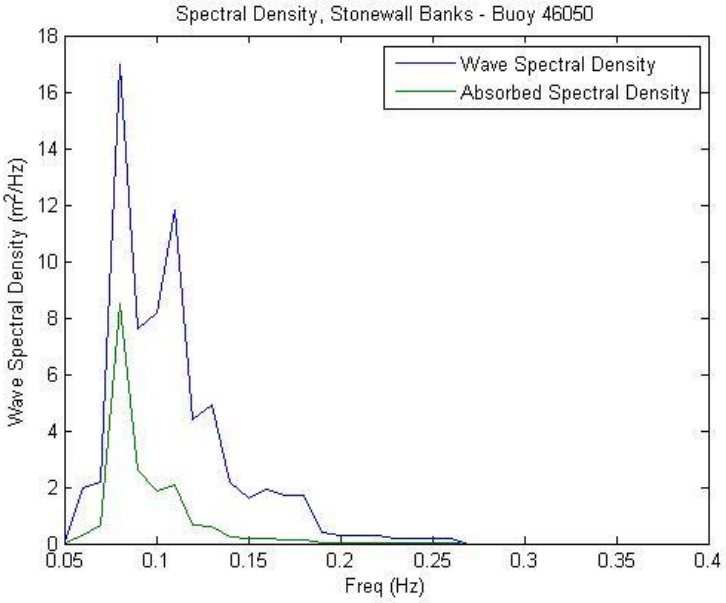

Fig. 34. Absorbed Spectrum, Stonewall Banks, OR

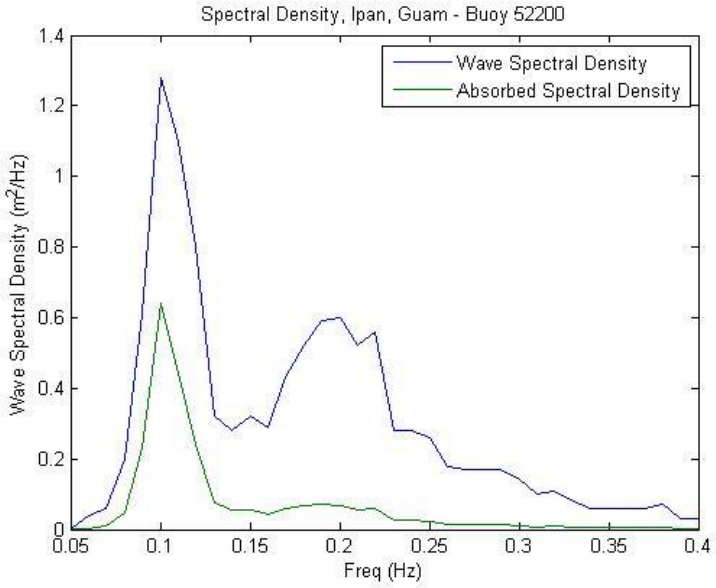

Fig. 35. Absorbed Spectrum, Ipan, Guam

4.7 Proposed Controller Architectures

4.7.1 L-Section Controller

L-section Control is leveraged from electromagnetic matching at RF frequencies that allow for lumped parameter circuits. It uses only reactive elements (inductors or capacitors) to conjugately match any load impedance to any source impedance. One idea of this control was to investigate whether it would mitigate the increased heave velocities that result from optimal control. A 'reverseed L-section' is used to match a load with a larger load resistance than source resistance. See Fig. 36.

Details for the design are derived in Ref. [12] but the result for the reversed solution is:

$$X_1 = \frac{X_g \pm B_g Q}{\frac{B_g}{B_b} - 1} \tag{18}$$

$$X_2 = (X_b \pm B_b Q) \tag{19}$$

$$Q = \sqrt{\frac{B_g}{B_b} - 1 + \frac{X_g^2}{B_b B_g}} \tag{20}$$

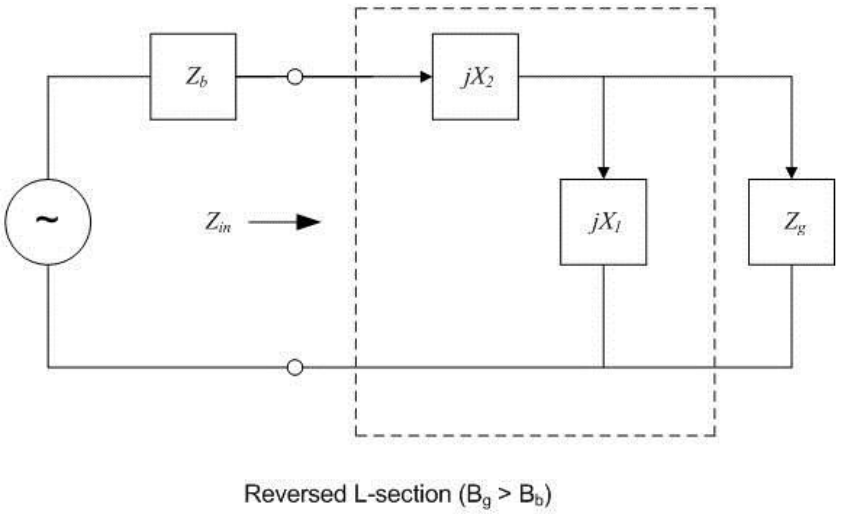

Fig. 36. L-section Controller

L-sect tuning did lower the heave velocity to values much lower than ternary optimal control and wideband control, but it wasn't much different than binary optimal control.

Advantages

The advantages of this control scheme are that arbitrary load and source impedances can be optimally matched and that allowing the generator dampening to be greater than the natural buoy dampening may favorably reduce the buoy heave velocity.

Disadvantages

The disadvantages of the L-section Controller are that it is more complex and actually provides a narrow-band response.

4.7.2 Wide-bandwith Controller

WEC controllers in the literature primarily match impedances to maximize power absorption. But when it was observed that some frequency content was non-optimally matched and reflected back to the ocean a controller was sought that had a better

matched impedance over a wider frequency range. Since several controllers have a natural band pass response, the idea was to purposely control the bandwidth response. The Cauer bandpass filter topology was chosen to actively design the bandpass region. The Cauer topology was also chosen since due to its 'T' topology the buoy dynamic coefficients could actually be used to realize the filter.

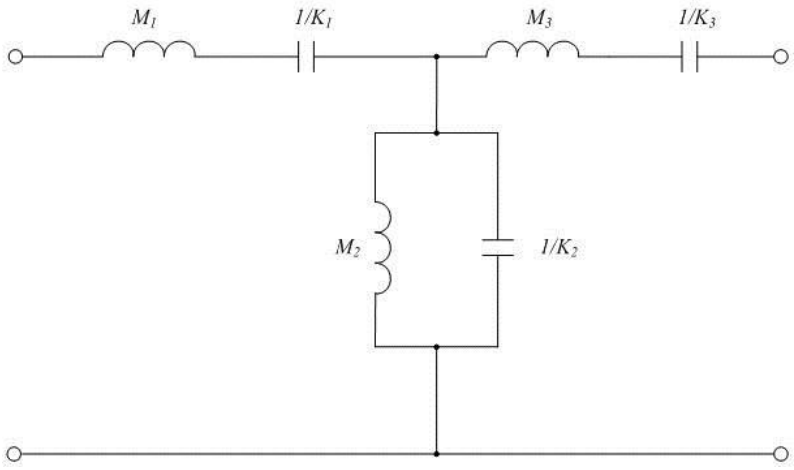

Fig. 37. Cauer Filter Implementation

Utilizing filter design principles, the design methodology first designs a prototype low-pass filter (LPF) normalized to 1 rad/sec. The prototype LPF consists of the series elements M_1 and M_3, and the parallel element K_2.

The filter transfer function:

$$H(s) = \frac{\frac{B_g K_2}{M_1 M_3}}{s^3 + \frac{B_g}{M_3}s^2 + \frac{K_2}{M_1 M_3}(M_1 + M_3)s + \frac{B_g K_2}{M_1 M_3}} \tag{21}$$

is matched with the Butterworth prototype polynomial:

$$s^3 + 2s^2 + 2s + 1 \tag{22}$$

The added mass terms are converted to series resonators utilitzing the filter term Q to specify bandwidth. The normalized frequency is also converted.

$$M_{1/3} = \frac{\omega_c' Q}{\omega_o} M_{1/3}' \tag{23}$$

$$K_{1/3} = \omega_0 \omega_c' Q\left(1/M_{1/3}'\right) \tag{24}$$

The hydrodynamic stiffness term is converted to a parallel resonator by:

$$K_2 = 1/(\omega_c' Q/\omega_o) \cdot (1/K_2') \tag{25}$$

$$M_2 = 1/(\omega_c' Q \omega_o) \cdot K_2' \tag{26}$$

The complete controller is shown in Fig. 38.

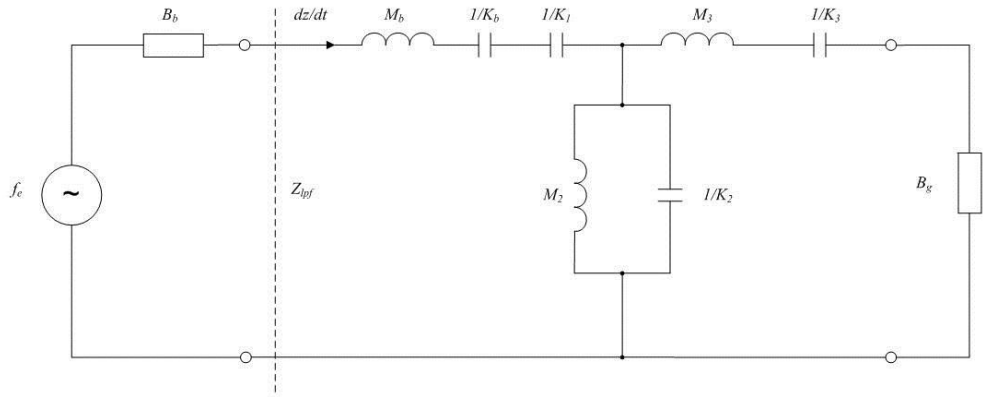

Fig. 38. Buoy and Control System

Since the buoy dynamic terms M_b and K_b are utilized the actual controller realized in the WEC control system is shown in Fig. 39.

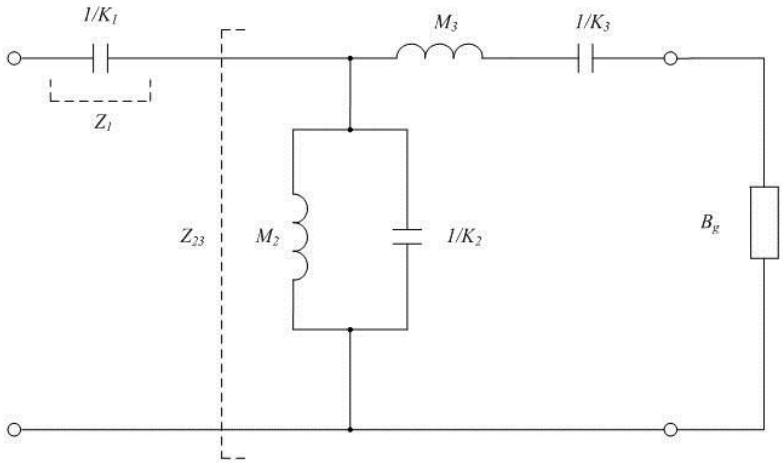

Fig. 39. Proposed Wideband Controller

Of particular importance is that the controller only requires position sensing since it has the form:

$$Z(s) = \frac{a_4 s^4 + a_3 s^3 + a_2 s^2 + a_1 s + a_0}{s(b_4 s^4 + b_3 s^3 + b_2 s^2 + b_1 s + b_0)} = \frac{1}{s} \cdot Z'(s) \tag{27}$$

Advantages

The advantage of this control scheme is that it provides a wide-band response possibly allowing for the capture of a wider frequency range of ocean energy.

Disadvantages

This controller, though, is the most complicated passive controller introduced. Since it consists of several 'reactive' elements it may tend to oscillate and may have numerical issues since it essentially is a high order filter.

4.8 Simulation Results

4.8.1 WEC Frequency Response

Each WEC system was simulated in the frequency domain with the buoy dynamics and proposed controllers. The results with the optimal tuning frequencies matching each of the three location's dominant frequency in the ocean spectra is shown in Fig. 40. Controller Frequency Response, NW Hawaii

, Fig. 41, and Fig. 42.

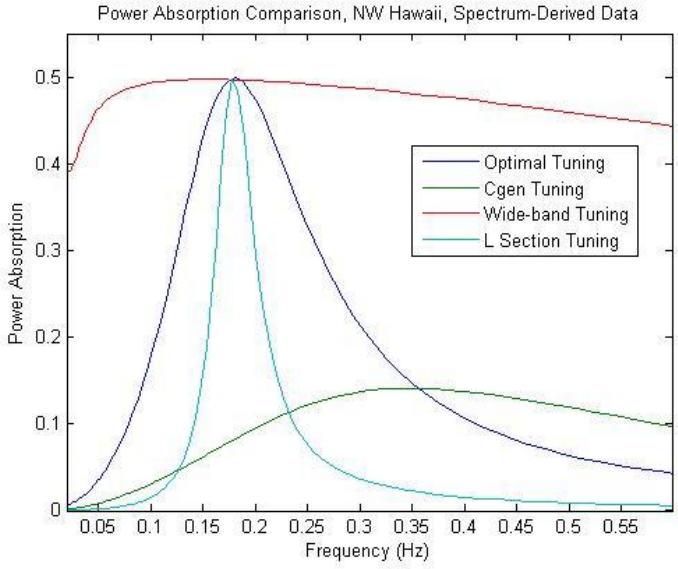

Fig. 40. Controller Frequency Response, NW Hawaii

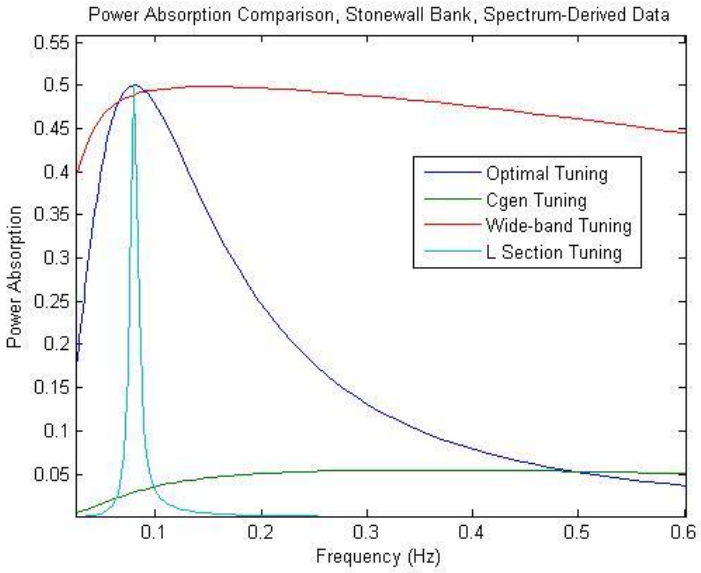

Fig. 41. Controller Frequency Response, Stonewall Banks, OR

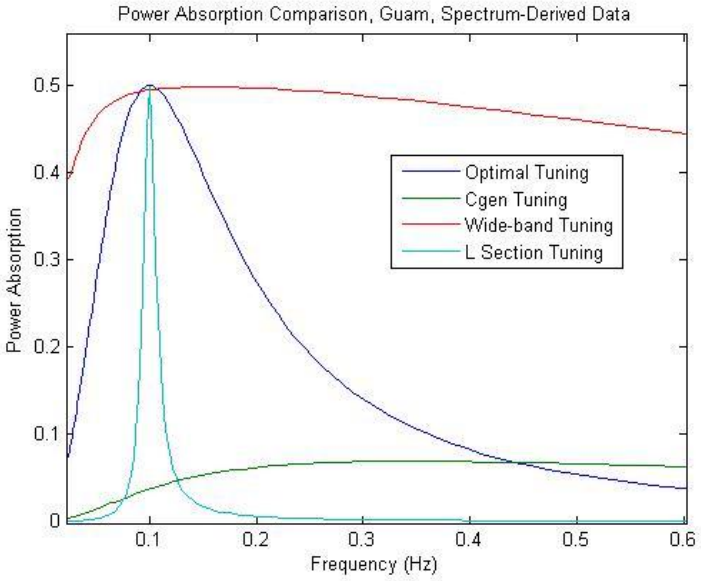

Fig. 42. Controller Frequency Response, Ipan, Guam

The following can be concluded from the frequency response simulations:

The Wideband Controller has the largest ‘power capture width’ of the four controllers simulated. It also seems that it may be able to have a realization that doesn’t have to be tuned, i.e., the controller doesn’t have to constantly sense the maximum power point or dominant frequency and tune to it.

The Binary Optimal Controller has the next best frequency response characteristic and the L-section the third. As suspected the L-section matching is actually narrow-band. These schemes do at least provide for maximum power transfer when tuned appropriately to the dominant wave frequency.

The Matched Impedance Controller does not achieve maximum power transfer and its maximum power absorption frequency does not match the frequency of the dominant wave.

4.8.2 Time-Domain and Power Absorption Simulation

A time-domain simulation was constructed by connecting the irregular wave energy spectrum to a multi-harmonic forcing function. The multi-harmonic forcing function was constructed by constructing the time-series from the magnitude of the frequency spectra with a random phase difference. Though this is not the exact representation of the signal [13] the error is only usually 3-4% and is deemed sufficient for this study.

The proposed Wideband Controller performed well in simulation compared to other control schemes [8,9,11,14]. For the ocean spectra with the largest frequency distribution (NW Hawaii) it can absorb up to 15% more relative power than the Binary Optimal Control buoy system.

Table 2. Power Absorption vs. Control Scheme

	Stonewall Banks	**Northwest Hawaii**	**Ipan, Guam**
Binary Optimal Control	39.9%	28.7%	31.4%
Wideband Control	45.2%	43.6%	43.0%
Matched Non-Reactive	6.8%	11.8%	9.7%
L-section Control	13.7%	14.2%	9.3%

4.9 Conclusions

This paper has quantitatively demonstrated that there potentially can be greater power absorption is real-world, frequency-rich ocean locations if the frequency response of the buoy-controller system is designed to and optimized for a wide ocean energy frequency range. In simulation, power capture of greater than 10% is realized in two of the three locations. The wideband response of the proposed controller may even be wide enough that no active tuning based on the wave dominant frequency may even be needed.

The paper has contributed a proposed control scheme that does not require acceleration feedback. In fact, it only requires position sensing, which may be indigenous to the electrical power take-off section of the generator already. The control is causal [15] and leverages off of classic filter design theory.

Future work will involve the physical implementation of the WEC system and testing to validate the concepts presented.

4.10 References

[1] T. Brekken and A. von Jouanne “ECCE Wave Energy Tutorial”, Energy Conversion Conference and Exposition, Sept 2009

[2] J. Falnes, *Ocean Waves and Oscillating Systems: Linear Interactions Including Wave-Energy Extraction*, Cambridge University Press, 2002.

[3] M. Langeliers, E. Agamloh, A. von Jouanne, A. Wallace, "A Permanent Magnet, Rack and Pinion Gearbox for Ocean Energy Extraction," *44th AIAA Aerospace Science Meeting and Exhibit*, Reno, NV, Jan. 2006, AIAA-2006-999.

[4] K. Rhinefrank, E.B. Agamloh, A. von Jouanne, A.K. Wallace, J. Prudell, K. Kimble, J. Aills, E. Schmidt, P. Chan, B. Sweeny, A. Schacher, "Novel Ocean Energy Permanent Magnet Linear Generator Buoy", *Elsevier Renewable Energy Journal*, Vol. 31, Issue 9, July 2006, pg. 1279-1298

[5] Z. Nie, P.C.J. Clifton, Y. Wu, and R.A. McMahon, "Emulation and Power Conditioning of Outputs from a Direct Drive Wave Energy Converter," *International Conference on Sustainable Energy Technologies*, Nov. 2008, pg. 1129-1133.

[6] M.E. McCormick, *Ocean Wave Energy Conversion*, Dover Publicatons, 2007.

[7] M. Patel, *Dynamics of Offshore Structures*. Butterworth-Heinemann, 1989.

[8] J.K.H. Shek, D.E. Macpherson, M.A. Mueller, "Phase and Amplitude Control of a Linear Generator for Wave Energy Conversion" *4th conference on Power Electronics, Machines, and Drives*, April 2008, pg. 66-70.

[9] J.K.H. Shek, D.E. Macpherson, M.A. Mueller, J. Xiang, "Reaction Force Control of a Linear Electrical Generator for Direct Drive Wave Energy Conversion", *lET Renewable Power Generation*, 2007,1, (1), pp. 17-24.

[10] T. Lewis, A. von Jouanne, T. Brekken, "Per-Unit Wave Energy Converter System Analysis," Digest for *IEEE Energy Conversion Congress and Exposition 2011*.

[11] Schacher, A.V. Meulen, D. Elwood, P. Hogan, K. Rhinefrank, T. Brekken, A. von Jouanne, S. Yim, "Novel Control Design for a Wave Energy Generator," *46th AIAA Aerospace Science Meeting and Exhibit*, Reno, NV, Jan. 2008, AIAA-2008-1305.

[12] S.J. Orfanidis, *Electromagnetic Waves and Antenna*, ECE Department, Rutgers University, 2011. Site: *www.ece.rutgers.edu/~orfanidi/ewa/*

[13] M.J. Tucker, P.G. Challlenor, D.J.T. Carter, "Numerical Simulation of a Random Sea: A Common Error and its Effect Upon Wave Group Statistics," look up …..

[14] E. Tedeschi, M. Molinas, M. Carraro, P. Mattavelli, "Analysis of Power Extraction from Irregular Waves by All-Electric Power Take-off", IEEE Energy Conversion Congress and Expo, Sept. 2010, pp. 2370-2377.

[15] T.K.A. Brekken, B. Batten, E. Amon, "From Blue to Green," *Control System Magazine,* to be published Fall 2011

MODELING AND CONTROL OF A SLACK-MOORED TWO-BODY WAVE ENERGY CONVERTER WITH FINITE ELEMENT ANALYSIS

Timothy M. Lewis, Annette von Jouanne, Ted K.A. Brekken

School of Electrical Engineering and Computer Science

1148 Kelley Engineering Center

Oregon State University

Corvallis, USA

lewisti@eecs.oregonstate.edu

Energy Conversion Conference and Exposition

Raleigh, NC

September 15-20, 2012

5 Modeling and Control of a Slack-Moored Two-Body Wave Energy Converter with Finite Element Analysis

Abstract - Wave energy converter (WEC) detailed design and hydrodynamic analysis is unique, in some respects, because the analysis in dependent on the WEC's integral power-take-off (PTO) control which changes the physical properties of the device and the environment. This raises the complexity when using standard off-shore industry finite element analysis (FEA) tools. It is especially true of autonomous WECs that are smaller and have different design requirements then utility power generation WECs or other larger off-shore structures. This paper first quantifies the design requirements for an autonomous WEC, highlights the design choices that are crucial to the WEC control and analysis, then presents results from the WEC FEA analysis that uses integrated optimal control to maximize power absorption. A proposed equivalent linear circuit is compared against these FEA results[1].

5.1 Introduction

Wave energy is recognized as a potential source for energy harvesting. Direct energy from the immediate ocean environment may be of particular interest for remote or isolated ocean applications since the local wave energy source is persistent, predictable, has a high power density, and maintains a minimum power level in most ocean environments [1]. Typical ocean device designs will have phases of finite element analysis and scaled wave tank validation before a design is committed to. But for a Wave Energy Converter (WEC) any finite element analysis (FEA) design should include the active, real-time power-take-off control since this changes the WEC's physical characteristics and interaction with the ocean wave forcing function which changes the device's radiated forces into the sea environment [2]. This work extends the previous research for axi-symmetric, heave-only, power absorbers [3,4,5,6] and correlates FEA analysis results, with active control, with an expanded two-body WEC

[1] The authors acknowledge support for this work from the US Department of Energy (Award Number DE-FG36-08GO18179) for the Northwest National Marine Renewable Energy Center.

equivalent circuit. This work is also specific to a remote, or isolated, power converter that is intended for unattended ocean sensing. Since it is intended to operate autonomously it is termed an autonomous wave energy converter (AWEC).

The WEC is designed to provide an electrical source to sensing packages on this remote, autonomous buoy. The WEC is intended to remain near-vertical in most sea conditions with a target power output of 200W. The target power level was derived from currently stated remote, autonomous buoy requirements [7] that typically exceed the power output of battery backed photovoltaic power sources that are used on other ocean environmental monitoring systems.

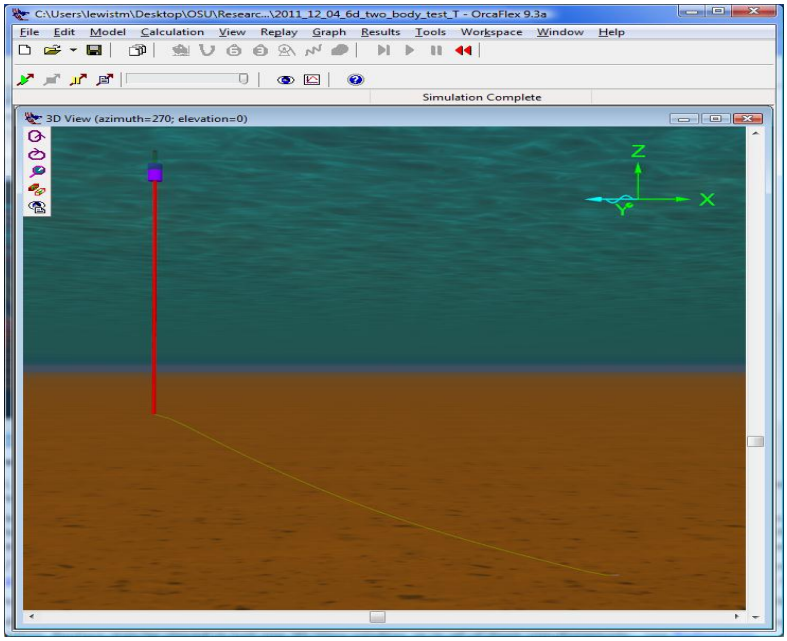

Fig. 43. Slack-Moored WEC in FE Program

It is intended to be relatively inexpensive and to employ a simple slack-moored system. This simple slack-mooring system, chosen for the perceived ease of deployment, results in a system in which both the spar and the float bodies move under ocean forces. Fig. 43 shows the slack-moored, two-body WEC moored to the ocean floor.

A survey of near coastal United States locations was conducted to obtain a representative ocean wave environment that the AWEC would need to operate in. The representative seabed depth, wave periods, and wave heights are shown in Table 3.

Table 3. Minimum Wave Conditions

Name	**Depth (m)**	**APD (sec)**	**DPD (sec)**	**Hs Mean (m)**	**Hs SD (m)**
Columbia River, OR	135	7.5	11.0	1.4	0.5
Stonewall Banks, OR	128	8.3	12.0	1.5	0.5
St. Georges, CA	48	8.2	11.0	1.6	0.7
Cape Cod, MA	156	3.8	4.0	0.9	0.4
Long Island, NY	40	4.4	6.0	1.0	0.4
Virginia Beach, VA	95	5.3	10.0	1.0	0.4
Charleston, SC	38	5.1	6.0	1.0	0.4
Gray's Reef, GA	18	4.8	6.0	0.8	0.4
Galveston, TX	14	3.9	5.0	0.7	0.4

In Table 3 *APD* is the average wave period and *DPD* is the dominant wave period. H_s is the significant wave height and *SD* is the standard deviation, at yearly, minimum wave conditions. For wave period it was chosen to target waves centered at 6 seconds.

The minimum significant wave height of 0.92 m was targeted, and knowing that the significant wave height is approximately four times the root-mean-square of the water surface elevation time-series, yields a peak-to-peak wave height of 0.65 m. The incoming wave energy from a monochromatic wave of this wave height and a period of 6 seconds is then 0.65 m from [9]:

$$P = \frac{\rho g^2 H^2 T}{32\pi} \; [Wm^{-1}] \tag{1}$$

where P is the output power per unit wave width; ρ the density of sea water; g the gravitational constant; H the peak-to-peak wave height; and T the wave period.

Extending the axi-symmetric research from [3,4,5,6], the WEC is designed with a center cylindrical spar with a cylindrical float around it. Either the float or spar must be "stiff" to provide relative motion for the extraction of power with the power take-off (PTO) assembly. It is difficult to get the resonant frequency of a semi-submerged cylindrical float very low [14] so the float's resonant frequency is chosen to be higher than the wave frequency range of interest.

The float size was initially estimated from the derived power per volume approximation in [9].

$$\frac{P_o}{V} < \frac{\pi \rho g H}{4T} \tag{2}$$

with P_o being the output power and V the body volume.

It was chosen then to provide a long vertical spar that is resistant to pitch and to set the resonance frequency of this spar to be lower than the wave frequency range of interest. The resonant frequency for a long spar is approximated by (3) [13].

$$\omega_o = \sqrt{\frac{K}{M}} = \sqrt{\frac{\rho g A_{wp}}{m+A}} \approx \sqrt{\frac{1}{l}} \tag{3}$$

where ω_o is the natural resonance of the body; K is the body hydrodynamic stiffness; M is the body mass plus added mass, $m + A$; A_{wp} is the horizontal water plane area; and l is the spar length.

The float is electromagnetically connected to the spar which houses the generator, control electronics, and sensing payload. Details of the design concepts are provided in previous research [5]. Often a heave plate is used in the design of the spar [11] but this results in a large non-linear drag force in the system [12] and it provides little hydrostatic dampening or stiffness against pitch. Though provisions will be made for incorporating and experimenting with a heave plate for future wave tank testing of the design, the FEA analysis in this paper does not include one.

The outer buoy contains the back-iron for a contact-less force transmission system (CFTS). The CFTS is used to couple the outer moving buoy to an internal spar mechanism. The internal spar mechanism consists of a structure with an electromagnet system that provides contact-less holding torque with the outer float in addition to minimizing the dampening between the float and spar. The electromagnet system is rigidly attached to a central roller screw nut. The electromagnet is energized to make this inner spar structure move vertically which turns the roller lead screw mechanism. On the cylindrical electromagnet assembly an accelerometer is mounted and is used for potential future compensation schemes.

At the end of the roller screw a PM machine is mounted which is controlled in a generating mode. The machine is directly coupled to the lead screw so the electric machine rotates in a bidirectional manner with the vertical oscillatory motion of the float. The machine is a 3-phase PM machine. The control electronics consists of a 6-switch AC/DC converter to rectify and condition the DC output power. Heave acceleration is sensed with an accelerometer on the inner spar cylindrical assembly. Heave position is derived from the sensed commutation resolver position and lead screw pitch. Generator force is sensed through the controlled quadrature current in the PM machine.

The resulting device that is proposed for this application as a remote, autonomous WEC is shown in Fig. 44.

.

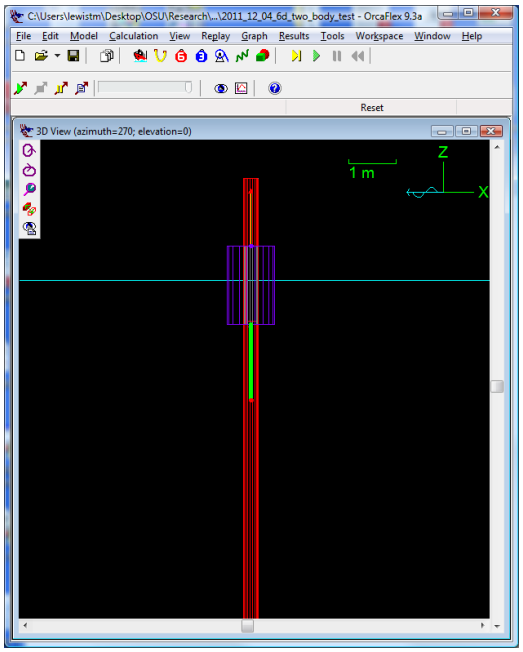

Fig. 44. Proposed WEC Device

The resulting AWEC has a float that is 1.64 m in height, with an outer diameter of 1.0 m, and an inner diameter of 0.3m. The spar is 23.0 m in length.

5.2 Linearized Wave Equation

For a WEC system the force balance is described by:

$$F_e + F_r + F_b + F_{gen} = m\ddot{z}_B \tag{4}$$

in which F_e is the excitation force, F_r is the radiation force generated by the object in the water, F_b is the buoyancy force of the object in the water, F_{gen} is the generator force, m is the mass of the object, and $\ddot{z}_B$ is the acceleration in the heave (vertical) direction for a one dimensional WEC converter.

Wave action can be approximated and is typically described in the literature by using a linearization of the Morrison wave equation [5]. The hydrodynamic equations involving an object moving at velocity v, in a flow with velocity u, is:

$$(\dot{u} - \dot{v})A + (u - v)^2 \hat{B} + F_{ext} = m\dot{v} \quad (5)$$

A dampening term, *B*, is used to linearize $(u - v)^2$ for small $(u - v)$ or $(\dot{z}_w - \dot{z}_b)$ for a heave reference system. With the definition of the added mass term, *A*, the linearization is:

$$(\ddot{z}_w - \ddot{z}_b)A + (\dot{z}_w - \dot{z}_b)B + (z_w - z_b)K + F_{gen} = m\ddot{z}_b \quad (6)$$

Grouping:

$$F_e = A\ddot{z}_w + B\dot{z}_w + Kz_w \quad (7)$$

$$F_r = -A\ddot{z}_b - B\dot{z}_b \quad (8)$$

$$F_b = -Kz_b \quad (9)$$

yields the system linearization:

$$F_e + F_{gen} = M\ddot{z}_b + B\dot{z}_b + Kz_b \quad (10)$$

where F_e is the excitation force from the wave; *M* is the system mass, *m*, plus the added mass, *A*; *B* is the viscous damping of the mechanical system, *K* is the hydrostatic stiffness, and z_b is the displacement of the buoy.

This linearization is the standard first order approximation in the literature. It yields a linear differential equation that is more suitable for analysis and control techniques than the partial differential equations that usually result from wave theory.

In the following equivalent circuits that extend from this, the subscript *b* will denote the single float for a one-body system, or the outer float for a two-body WEC; *s* the inner spar; and *g* the power take-off (PTO) generator coupled between the two.

5.3 Taut-Moored Equivalent Circuit

For a taut-moored system the spar is assumed to be fixed and only the float moves in the heave, or *z*, direction. The electrical equivalent is formulated and shown in Fig.

45. In this equivalent, the input force is analogous to voltage and the buoy velocity state variable ($\dot{z}_b$) is analogous to current. For the system's linear time-invariant coefficients, the mass (*M*) terms are analogous to inductance, the dampening (*B*) terms are analogous to resistance, and the hydrostatic stiffness (*K*) terms are analogous to inverse capacitance. The generator impedance is the summation of forces proportional to buoy heave acceleration ($\ddot{z}_b$), velocity ($\dot{z}_b$), and position (z_b).

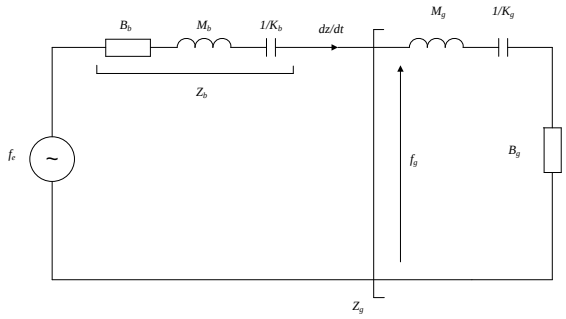

Fig. 45. Taut-Moored Equivalent Circuit with Matching Control

Since the hydrodynamic solution of the Morrison model is similar to a mass-spring-damper system with a periodic input, the concept of formulating a generator equivalent is often used to extract power with active control [9]. This is because the solution for power extraction can be arrived at by matching the impedance of the incident hydrodynamic input with that of the generator control system.

The generator force can use complex conjugate matching to extract maximum power [8,9,10]. Details of the utilized control is explained in the next section.

5.4 Single Body Radiation Forces and Two-Body Cross-Coupled Forces

When a body moves in a fluid it also produces a radiation force into the fluid. This radiation force, F_r, is determined by the convolution of the radiation impulse response function, k_r, with the body's velocity $\dot{z}$ [12].

$$F_r = \int_{-\infty}^{t} k_r(t-\tau)\dot{z}\,(\tau)d\tau \tag{11}$$

This radiation force, in essence, changes the ocean forcing function near the submerged body. FEA programs deal with this term in different ways. OrcaFlex [15] does not alter the ocean forcing function and stipulates that if it is a significant effect, the damping term, which is proportional to velocity, be altered empirically from wave tank test data, to account for it. This approach does allow for faster simulation, and the package is mostly targeted at analyzing stationary off-shore structures. Another hydrodynamic analysis program, AQWA [16], does actually compute this convolution integral of the body and it is accounted for.

There are also additional cross-coupled radiation terms since the system has two bodies moving in the fluid. The form of this force, for example the radiation from a body 2 onto a body 1, due to movement of the second body is [12]:

$$F_{r12} = \int_{-\infty}^{t} k_{r12}(t-\tau)\,\dot{z}_2(\tau)d\tau + A_{12}(\infty)\ddot{z}_2 \tag{12}$$

Neither OrcaFlex nor AQWA account for these cross-coupled forces. Since Orcaflex was utilized for this study this term is neglected, though it is assumed that with no overlap of the bodies physically in the heave direction, that these forces may be minimal. Future wave tank testing will be used to validate or investigate this assumption.

Another force that is neglected in this particular analysis is the force due to the mooring. Since the system is slack-moored and both bodies move in the hydrodynamic environment, it is assumed that this force is minimal, thus neglected.

5.5 Slack Moored Equivalent Circuit

Since the WEC is slack-moored both bodies move with the inner spar (subscript *s*) and outer float (subscript *b*) subject to some proportional amount of the total wave force. An extension of the single-body equivalent electrical representation, Fig. 46, is

proposed. This equivalent circuit is essentially two independent bodies heaving with a 'tuned' power take-off (PTO) between them. The relative velocity of the PTO will be $\dot{z}_b - \dot{z}_s$. Maximum power will be extracted by the PTO when the impedance of the generator is tuned to the complex conjugate of the Thevenin equivalent of the two-body system.

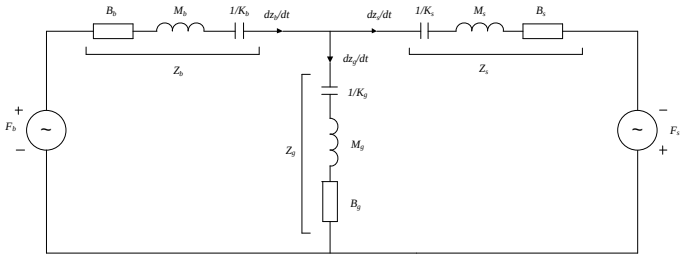

Fig. 46. Slack-Moored Equivalent Circuit with Matching Control

The goal of the equivalent circuit is to provide a valid linear model for the AWEC system at a specific operating point. This will be used for the characterization and controller design for the WEC system.

Also, since the WEC operates predominantly in the vertical heave direction, the water plane areas of both the spar and float will remain fairly constant. This will also aid in the linearity of the resulting motion responses. Linearity is desirable since maximum power absorption is dependent on the active control of the WEC and a more linear system lends itself to easier and more robust control.

5.6 Control Strategies Utilized in Study

For power absorption to occur in a WEC the control essentially makes the WEC system's controlled plus natural mechanical frequency match the natural frequency of the ocean wave from which power is extracted. The control compensates when the natural mechanical frequency does not match the wave, keeping the WEC system in resonance with the ocean wave to extract power.

Under Binary Optimal Control the generator coefficients are controlled such that these parameters are the complex conjugate of the hydrodynamic input. Under this control scheme, as realized in [7,8], the dampening (B_g) and reactive (X_g) generator terms are controlled and the generator mass term is set to zero. The control is set up such that:

$$B_g = B_{WEC} \tag{13}$$

$$K_g = M_{WEC} \cdot \omega^2 - K_{WEC} \tag{14}$$

There will therefore be two components, or binary, control of the generator current command: a dampening force proportional to the velocity which provides amplitude control and the conservation of real power, and a hydrodynamic stiffening force proportional to displacement that provides phase control.

For the slack-moored, two body equivalent circuit in Fig. 47, the matched Thevenin equivalent can be seen in xx with the dominant wave period being the impedance frequency.

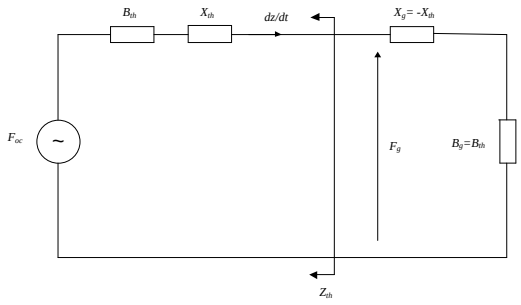

Fig. 47. Matched Thevenin Impedance

5.7 Finite Element Analysis of Two-body WEC

The finite element model consists of the spar; the float; the slack-mooring line; a vertical, virtual, connecting rod to keep the spar and float co-linear axially; and a power link that provides the spring-damping control. The FEA tool used was OrcaFlex by Orcina, Ltd. [14]. An OrcaFlex feature allows the spring control part to be non-linear and the coefficients can be reversed to provide the opposite reactive control. This allows for either 'inductive' (mass dominant) or 'capacitive' (stiffness dominant) matching control to be used.

The environmental conditions described in Section II were utilized.

5.7.1 Float-Only Finite Element Analysis

The first use of the finite element analysis was to attempt to validate the theoretical parameters for the WEC model. The individual spar and float parameters were derived in the following way. First the spar was anchored to the seabed, Fig. 48, and the power link damping-spring control is adjusted to find the maximum power point. The maximum power point was found by running multiple finite element simulations and sweeping damping control and reactive control. At this maximum power point, the generator tuning parameters are the complex conjugate of the float's parameters. This method was used because there is little literature regarding a closed form solution for the damping of a body in a fluid and approximations of added mass are empirical in nature [14]. Fig. 49 shows the results.

Fig. 48. AWEC with Spar Rigidly Coupled to the Seabed

Since under binary optimal control the reactance term is composed of both the stiffness and mass terms, an assumption is needed to determine the two parameters. Since the stiffness is predominately defined by the water plane area, see Eqn. (3), it is assumed to be more accurate. The water plane area also is fairly constant if the WEC operates with little pitch. This allows for the damping and other 'reactive' component, the mass component, to be solved for since at the maximum power point the generator is tuned to the complex conjugate 'impedance'.

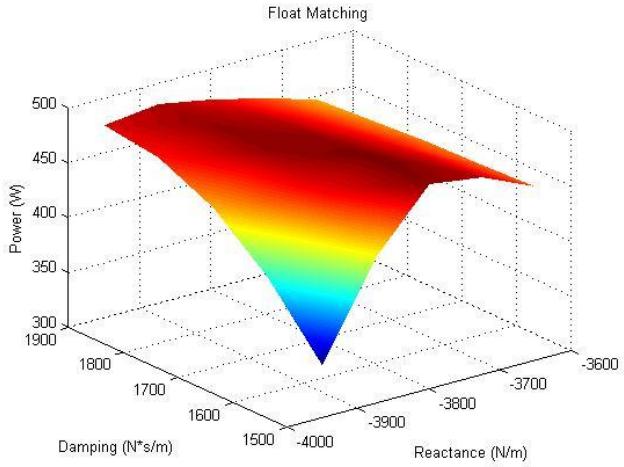

Fig. 49. Single-Body Float Maximum Power

Fig. 50 shows the matching and extraction of the parameters. B_g and X_g are the matching terms for the float under binary optimal control and using K_b, the parameter, M_b is derived. The tuning and relationship between the stiffness and mass makes sense intuitively since the larger diameter float is dominated by the water plane area versus the mass.

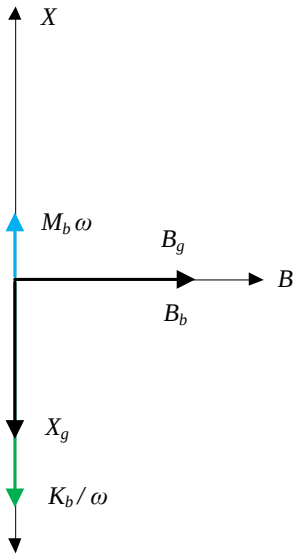

Fig. 50. Float Complex Conjugate Matching

5.7.2 Spar-Only Finite Element Analysis

This same procedure was carried out with the finite element model with the float anchored to the seabed so that only the spar moves. From the simulations, the maximum power point of the spar is shown in Fig. 51. The extraction of the spar parameters is demonstrated in Fig. 52. This too makes sense since the mostly submerged spar is dominated by its mass and not its water plane area.

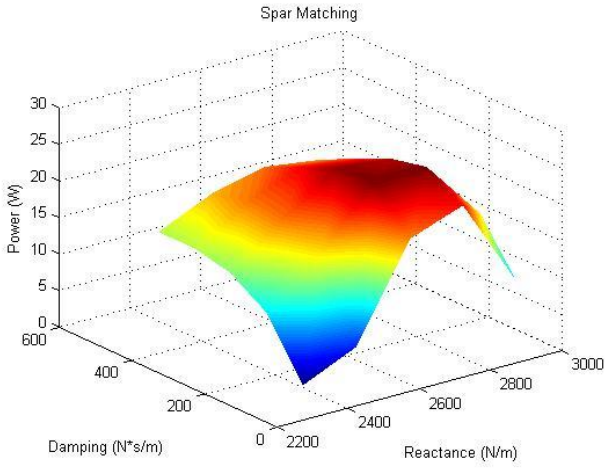

Fig. 51. Single-Body Spar Maximum Power

The extracted parameters for the float and spare are shown in Table 2.

Table 2. AWEC Parameters

	M (kg)	**B (kg/s)**	**K (kg/s^2)**
Float	2785	1600	7221
Spar	3023	125	715

The individual spar and float parameters can then be used to derive a Thevenin equivalent circuit of the two-body WEC. This yielded a two-body WEC impedance of:

$$Z_{WEC} = B_{WEC} + j \cdot X_{WEC} = 1930 + j \cdot 4200 \quad (15)$$

where the subscript *WEC* refers to the two-body equivalent.

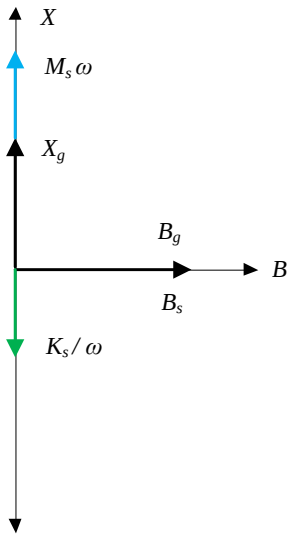

Fig. 52. Float Complex Conjugate Matching

5.7.3 Two-Body Finite Element Analysis

Simulations were then run to find the maximum power point of the slack-moored, two-body WEC. First, validation that the power requirement of 200W was achieved is shown in Fig. 53. Also, note the instantaneous power. It both extracts power from the ocean and returns power to the ocean over an entire wave period. This is consistent with the literature for a WEC controlled with binary optimal control. Additionally the wave period was varied, under the constraint of constant input power, to assess the

tuning. In Fig. 54 it can be seen that the WEC is indeed tuned close to 6 second waves and it exhibits the expected band-pass response that is characteristic of binary optimal control [6].

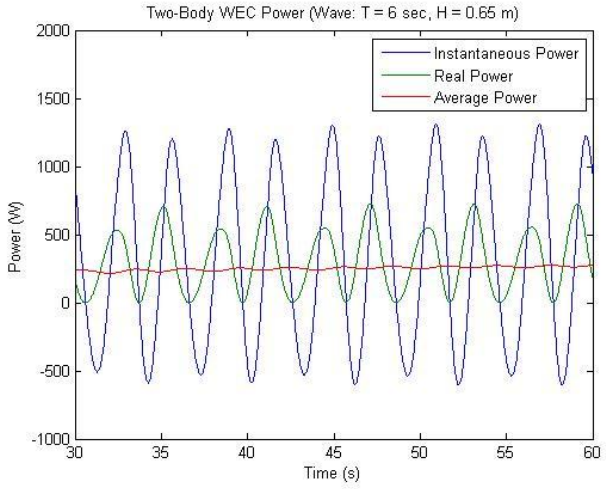

Fig. 53. Optimally Controlled Buoy Power Absorption

The results of the sweeps for damping and reactance for the two-body WEC are shown in Fig. 55. This resulted in a damping term of 2000 N/m and a stiffness term of 5500 N·s/m. This yields a Thevenin equivalent from the FEA analysis of:

$$Z_{WEC} = B_{WEC} + j \cdot X_{WEC} = 2000 + j \cdot 5240 \tag{16}$$

Comparing the Thevenin equivalents it is seen that the damping terms match well, with the reactive terms approximately 20% off.

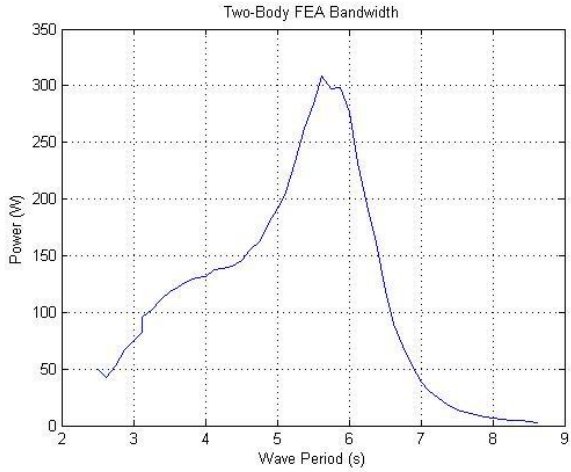

Fig. 54. Two-Body WEC Frequency Response

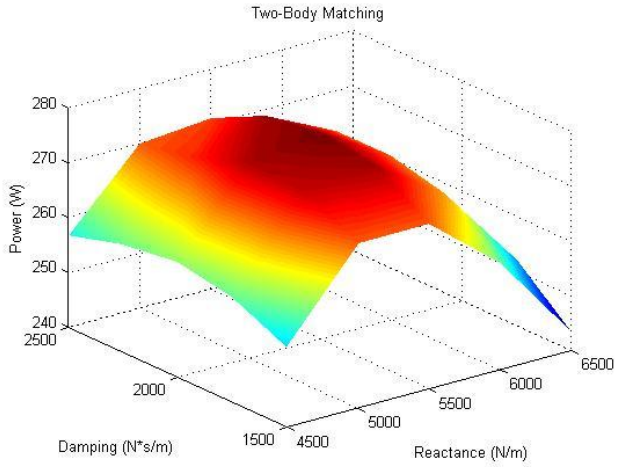

Fig. 55. Two-Body WEC Maximum Power Point

5.8 Parameter Variation Under Differing Wave Conditions

There is still the question regarding the validity and linearity of the model. This is hard to completely answer at this stage of design because there has not yet been any validation of the model itself with wave tank testing. It is well understood that wave

tank validation is a critical phase of any hydrodynamic design [15]. Initial FEA models have been shown to have mismatches of WEC parameters of 20-50% initially [16]. In addition, with the OrcaFlex FEA tool many drag and damping coefficients are entered directly and are expected to be tuned to match tank testing. With that in mind, two FEA analyses were performed before wave tank testing can be done to try to give insight that the equivalent circuit model matches the FEA analysis approximately.

The first test swept the system with matched optimal tuning through different wave heights. Wave height theoretically has no effect on the maximum power point equivalent circuit parameters. Thus the parameter damping and stiffness theoretical values are constant, Fig. 56. The FEA analysis outputs consist of individual points from simulations at the maximum power point for each wave height with dashed lines that are fitted curves for the data. The resulting curves are somewhat constant and in the proper range, but the tuned stiffness and dampening terms vary with wave height so there is some dependence and the parameter coefficients are not linear, time-invariant.

Intuitively it is known that a more varying plot will result from the second test performed which swept wave period. Since reactive modeling components are frequency dependent and the two-body WEC Thevenin equivalent impedance is quite complex, the theoretical curves in Fig. 57 vary quite a bit with wave period.

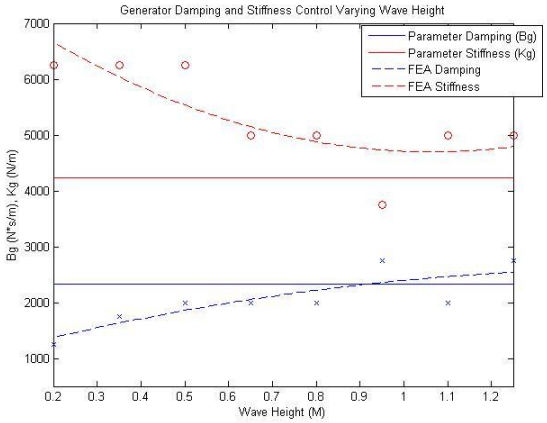

Fig. 56. WEC Parameters Varying with Wave Height

Again a set of FEA simulations were performed to find the tuning parameters at the maximum power point with now different wave periods. The FEA values and the resulting fitted dashed curves approximately match in shape with respect to wave period. It is felt that the validation of the model structure is close due the curves peaking and dipping at the same wave period values and that adding additional model fidelity with wave tank testing should be done to reduce error in this area.

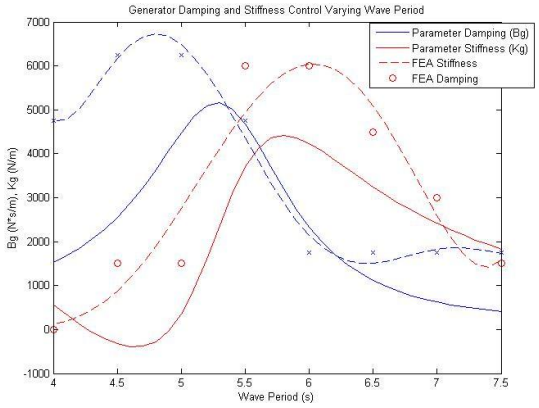

Fig. 57. WEC Parameters Varying with Wave Period

5.9 Conclusions

An autonomous WEC design and analysis with finite element simulations were performed. The FEA utilized active control of the power-take-off system – an aspect that is crucial to high fidelity WEC analysis. A two-body WEC equivalent circuit to use for linear control and analysis was proposed and a method for deriving the equivalent circuit parameters from FEA output was utilized. Further simulations were performed to test aspects of the model's linearity with respect to wave height and wave period.

The proposed equivalent circuit for the slack-moored, two-body WEC shows good correlation, though crucial wave tank testing is required and planned to advance this work further.

5.10 References

[1] T. Brekken and A. von Jouanne "ECCE Wave Energy Tutorial," *IEEE Energy Conversion Conference and Exposition*, San Jose, CA, Sept. 2009.

[2] K. Rhinefrank, A. Schacher, J. Prudell, C. Stillinger, D. Naviaux, T. Brekken, A. von Jouanne, D. Newborn, S. Yim, D. Cox, "High Resolution Wave Tank Testing of Scaled Wave Energy Devices," *29th International Conference on Offshore Mechanics and Arctic Engineering (OMAE),* 2010.

[3] E. Agamloh, "A Direct-Drive Wave Energy Converter with Contactless Force Transmission System," School of Electrical Engineering and Computer Science, Oregon State University, Corvallis, OR, Oct. 2005.

[4] K. Rhinefrank, E. Agamloh, A. von Jouanne, A.K. Wallace, J. Prudell, K. Kimble, J. Aills, E. Schmidt, P. Chan, B. Sweeny, A. Schacher, "Novel Ocean Energy Permanent Magnet Linear Generator Buoy," *Elsevier Renewable Energy Journal*, Vol. 31, Issue 9, July 2006, pg. 1279-1298.

[5] T. Lewis, A. von Jouanne, T. Brekken, “Per-Unit Wave Energy Converter System Analysis,” *IEEE Energy Conversion Congress and Exposition*, Phoenix, AZ, Sept. 2011.

[6] T. Lewis, A. von Jouanne, T. Brekken, “Wave Energy Converter with Wideband Power Absorption,” Digest for *IEEE Energy Conversion Congress and Exposition*, Phoenix, AZ, Sept. 2011.

[7] Office of Naval Research (ONR), http://www.dtic.mil/descriptivesum/ Y2008 / Navy/0603747N.pdf

[8] M. Patel, *Dynamics of Offshore Structures*, Butterworth-Heinemann, 1989.

[9] J. Falnes, Ocean Waves and Oscillating Systems: Linear Interactions Including Wave-Energy Extraction, Cambridge University Press, 2002, ISBN-13 978-0-521-01749-7.

[10] J.K.H. Shek, D.E. Macpherson, M.A. Mueller, "Phase and Amplitude Control of a Linear Generator for Wave Energy Conversion," *4thCconference on Power Electronics, Machines, and Drives*, April 2008, pg. 66-70.

[11] J.K.H. Shek, D.E. Macpherson, M.A. Mueller, J. Xiang, "Reaction Force Control of a Linear Electrical Generator for Direct Drive Wave Energy Conversion," *lET Renewable Power Generation*, 2007,1, (1), pp. 17-24.

[12] K. Ruehl, T.K. Brekken, B. Bosma, P. Paasch, “Large-Scale Ocean Wave Energy Plant Modeling,” *IEEE Conference on Innovative Technologies for an Efficient and Reliable Electricity Supply (CITRES)*, 2010, pp. 379-386.

[13] H. Eidsmoen, “Simulation of a Slack-Moored Heaving-Buoy Wave Energy Converter with Phase Control,” Division of Physics, Norwegian University of Science and Technology, Trondheim, Norway, May 1996.

[14] M. McCormick, *Ocean Wave Energy Conversion*, Dover Publications, 2007, ISBN-13 978-0-486-46245-5.

[15] OrcaFlex, Version 9.3a, Orcina Ltd., Daltergate, UK, www.orcina.com.

[16] AQWA, ANSYS Inc., www.ansys.com.

[17] J. Cruz, *Ocean Wave Energy*, Springer Series in Green Energy and Technology, 2008, ISBN-13 978-3-540-74894-6.

[18] Z. Zhang, "Development of Adaptive Damping Power Take-Off Control for a Three-Body Wave Energy Converter with Numerical Modeling and Validation," School of Electrical Engineering and Computer Science, Oregon State University, Corvallis, OR, Dec. 2011.

MODELING A TWO-BODY WAVE ENERGY CONVERTER DRIVEN BY SPECTRAL JONSWAP WAVES

Timothy M. Lewis, Bret Bosma, Annette von Jouanne, Ted K.A. Brekken

School of Electrical Engineering and Computer Science

1148 Kelley Engineering Center

Oregon State University

Corvallis, USA

lewisti@eecs.oregonstate.edu

Energy Conversion Conference and Exposition

Denver, CO

September 15-19, 2013

6 Modeling a Two-Body Wave Energy Converter Driven by Spectral JONSWAP Waves

Abstract - Wave Energy Converter (WEC) design strives to produce as much power as possible across differing wave conditions. It is especially true of autonomous WECs (used, for example, to power an ocean buoy sensing system) because they are smaller and they need to maximize the amount of power produced under minimal wave energy conditions. This is because the electrical power required is considered a constant load. Autonomous WECs (AWECs) also tend to operate near shore where the wave spectral content spans a larger frequency range. This paper describes the type of spectral waves to be used during the design and simulation stage, then presents results from the WEC hydrodynamic finite element analysis (FEA) that uses integrated optimal control with both monochromatic and spectral waves. A comparison is made of these results against a SPICE simulation using a two-body equivalent circuit. Using these results, plus integrating the effects of losses in the power take-off (PTO), conclusions are reached regarding the preferred control method. It was found that damping control may be the preferable control scheme for this application.

6.1 Introduction

Wave energy is recognized as a potential source for energy harvesting. Direct energy from the immediate ocean environment may be of particular interest for remote or isolated ocean applications since the local wave energy source is persistent, predictable, has a high power density, and maintains a minimum power level in most ocean environments [1]. This work extends the previous research for axi-symmetric, heave-only, power absorbers [2,3,4,5] and implements finite element analysis (FEA), with active control, driven by spectral waves that are present in the real world. In the previous work a two-body, slack-moored autonomous WEC (AWEC) system had been designed and analyzed, but just with monochromatic waves [6,7,8]. An equivalent circuit was defined and a means to derive the equivalent circuit parameters using FEA was developed. This further work shows that it is critical to understand and design to

a richer, larger bandwidth wave spectrum in order to maximize power, and to realize the true energy output.

6.2 Autonomous WEC Requirements and Design

The AWEC is designed to provide an electrical source to sensing packages on remote, autonomous buoys. The design is such that the AWEC remains near-vertical in most sea conditions. The target average power output is 200W. The target power level was derived from currently stated remote, autonomous buoy requirements that typically exceed the power output of battery backed photovoltaic power sources that are used on other ocean environmental monitoring systems.

The AWEC is intended to be relatively inexpensive and to employ a simple slack-moored system. A survey of near coastal United States locations has been completed [8] and the wave spectra at NOAA Bouy 42035 off of Galveston, TX, was selected to be used in the analysis. It is representative of a near-shore environment and has a minimum average significant wave height, H_s, of approximately 0.9 m. This equates to a minimum wave power of 2.5 kW/m. For this application the AWEC must provide the specified power at this minimum wave condition.

The AWEC is designed with a center cylindrical spar with a cylindrical float around it. The float is electromagnetically connected to the spar, where the spar houses the generator, control electronics, and sensing payload. Details of the design are provided in [7,8]. The decision was made to provide a long vertical spar that is resistant to pitch and to set the resonance frequency of this spar to be lower than the wave frequency range of interest. This simple slack-mooring system, chosen for the perceived ease of deployment, results in a system in which both the spar and the float bodies move under ocean forces. Fig. 58 shows the modeled slack-moored two-body WEC in the FEA program, OrcaFlex [9].

The resulting AWEC has a float that is 1.64 m in height, with an outer diameter of 1.0 m, and an inner diameter of 0.3m. The spar is 23.0 m in length.

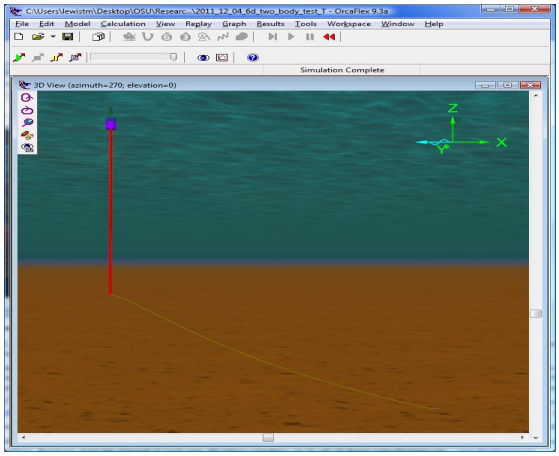

Fig. 58. Slack-Moored WEC in FEA Program

For a WEC system the force balance is described by:

$$F_e + F_r + F_b + F_{gen} = m\ddot{z}_B \tag{1}$$

in which F_e is the excitation force, F_r is the radiation force generated by the object in the water, F_b is the buoyancy force of the object in the water, F_{gen} is the generator force, m is the mass of the object, and $\ddot{z}_B$ is the acceleration in the heave (vertical) direction for a one dimensional WEC converter.

Wave action can be approximated and is typically described in the literature by using a linearization of the Morison wave equation [10,11]. The details of the use of the Morison equivalent circuit with respect to this AWEC design is provided in [8]. This results in a system linearization of:

$$F_e + F_{gen} = M\ddot{z}_b + B\dot{z}_b + Kz_b \tag{2}$$

where F_e is the excitation force from the wave; M is the system mass, m, plus the added mass, A; B is the viscous damping of the mechanical system, K is the hydrostatic stiffness, and z_b is the displacement of the buoy. This linearization is the standard first order approximation in the literature.

For the equivalent circuits that are derived from this, the subscript *b* will denote the single float for a one-body system, or the outer float for a two-body WEC; *s* the inner spar; and *g* the power take-off (PTO) generator coupled between the two.

6.3 Taut-Moored Equivalent Circuit

For a taut-moored system the spar is assumed to be fixed and only the float moves in the heave, or *z*, direction. The electrical equivalent is formulated and shown in Fig. 59. In this equivalent, the input force is analogous to voltage and the buoy velocity state variable ($\dot{z}_b$) is analogous to current. For the system's linear time-invariant coefficients, the mass (*M*) terms are analogous to inductance, the dampening (*B*) terms are analogous to resistance, and the hydrostatic stiffness (*K*) terms are analogous to inverse capacitance. The generator impedance is the summation of forces proportional to buoy heave acceleration ($\ddot{z}_b$), velocity ($\dot{z}_b$), and position (z_b).

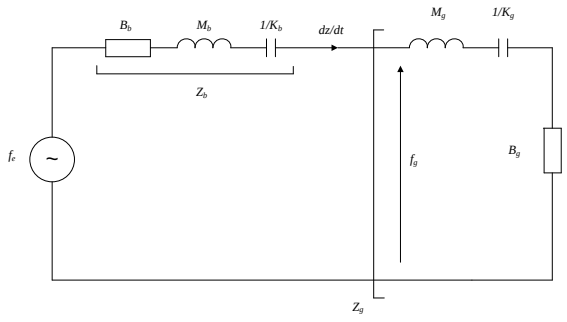

Fig. 59. Taut-Moored Equivalent Circuit with Matching Control

Since the hydrodynamic solution of the Morison model is similar to a mass-spring-damper system with a periodic input, the concept of formulating a generator equivalent is often used to extract power with active control [9]. This is because the solution for power extraction can be arrived at by matching the impedance of the incident hydrodynamic input with that of the generator control system.

The generator force can use complex conjugate matching to extract maximum power [8,12,13]. Details of the utilized control is explained in the next section.

6.4 Slack-Moored Equivalent Circuit

Since the WEC is slack-moored both bodies move with the inner spar (subscript *s*) and outer float (subscript *b*) subject to some proportional amount of the total wave force. An extension of the single-body equivalent electrical representation, Fig. 60, was proposed [8]. This equivalent circuit is essentially two independent bodies heaving with a 'tuned' PTO between them. The relative velocity of the PTO will be $\dot{z}_b - \dot{z}_s$. Maximum power will be extracted by the PTO when the impedance of the generator is tuned to the complex conjugate of the Thevenin equivalent of the two-body system.

The goal of the equivalent circuit is to provide a valid linear model for the AWEC system at a specific operating point. This will be used for the characterization and controller design for the AWEC system.

It is noted that the cross-coupling forces [14,15] between the bodies are neglected. An explanation of these forces and the rationale for neglecting them is provided in [8]. It is assumed that with no overlap of the bodies physically in the heave direction, that these forces may be minimal. Future wave tank testing will be used to validate or investigate this assumption.

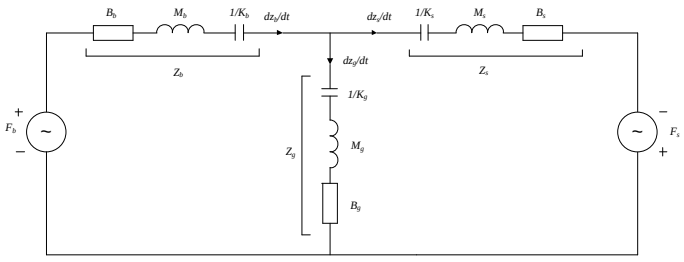

Fig. 60. Slack-Moored Equivalent Circuit with Matching Control

Another force that is neglected in this particular analysis is the force due to the mooring. Since the system is slack-moored and both bodies move in the hydrodynamic environment, it is assumed that this force is minimal, thus neglected.

6.5 WEC Control Strategies

Control of a WEC is usually based on a scheme for matching the Morison linearized model, or equivalent circuits, shown above. The matching control can be simpler, for example, by just using the damping term. This type of control is also called Matched Non-Reactive Control. Attempting to fully match the linearized Morison equivalent is termed WEC Optimal Control, with Binary Control being a version of this that uses a damping term and one reactive term.

6.5.1 Damping or Matched Non-Reactive Control

Matched Non-Reactive Control is detailed in [5]. (This literature cites this as C_{gen} control). Only the damping term is utilized and the control is set up as:

$$B_g = |\bar{Z}_{WEC}(j\omega)| = \left|B_{WEC} + j\omega \cdot M_{WEC} + \frac{K_{WEC}}{j\omega}\right| \quad (3)$$

The damping force term is proportional to the relative velocity of the power take-off.

The goal of this control is simplicity, plus it also limits the velocity due to reactive control swing [6]. Power is also always absorbed. There is no regenerated power during a wave cycle.

6.5.2 Binary Control

For maximum power absorption to occur in a WEC the control attempts to make the WEC system's total response match the natural frequency of the ocean wave from which power is extracted. The control compensates when the natural mechanical frequency does not match the wave, keeping the WEC system in resonance with the ocean wave to extract power. This requires both reactive and resistive components in the control.

Under Binary Optimal Control (BOC) the generator coefficients are controlled such that these parameters are the complex conjugate of the hydrodynamic input. Under this control scheme, as realized in [11,12,13], the dampening (B_g) and reactive (X_g)

generator terms are controlled and the generator mass term is set to zero. The control is set up such that:

$$B_g = B_{WEC} \tag{4}$$

$$K_g = M_{WEC} \cdot \omega^2 - K_{WEC} \tag{5}$$

There will therefore be two components, or binary, control of the generator current command: a dampening force proportional to the velocity which provides amplitude control and the conversion of real power, and a hydrodynamic stiffening force proportional to displacement that provides phase control.

For the slack-moored, two body equivalent circuit represented by Fig. 60, the matched Thevenin equivalent and generator can be seen in Fig. 61. The impedance frequency is the inverse of the dominant wave period, converted to radians.

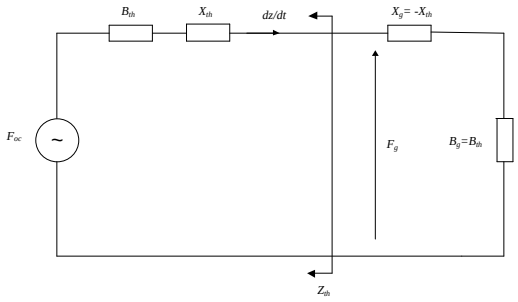

Fig. 61. Matched Thevenin Impedance

6.6 Finite Element Analysis of Two-Body WEC

The finite element model consists of the spar; the float; the slack-mooring line; a vertical, virtual, connecting rod to keep the spar and float co-linear axially; and a power link that provides the spring-damping control. The FEA tool used was OrcaFlex by Orcina, Ltd. [9]. An OrcaFlex feature allows the spring control part to be non-linear and the coefficients can be reversed to provide the opposite reactive

control. This allows for either ‘inductive’ (added mass) or ‘capacitive’ (stiffness dominant) matching control to be used.

In previous work a method was developed to obtain the equivalent circuit parameters of the two-body model in Fig. 59. The method involved alternating fixing the float then the spar to the seabed. For each case the model was stimulated by monochromatic waves at the wave period of interest. The maximum power point was found by running multiple finite element simulations and sweeping damping control and reactive control. At this maximum power point, the generator tuning parameters are the complex conjugate of the float’s parameters. With the assumption that the stiffness can be derived from first principles [16] the resulting equivalent circuit parameters can be extracted.

The extracted parameters with a 6 sec. wave period for the float and spar are shown in Table 4. AWEC Parameters.

Table 4. AWEC Parameters

	M (kg)	**B (kg/s)**	**K (kg/s^2)**
Float	2785	1600	7221
Spar	3023	125	715

The individual spar and float parameters can then be used to derive a Thevenin equivalent circuit of the two-body WEC. This yielded a two-body WEC impedance of:

$$Z_{WEC} = B_{WEC} + j \cdot X_{WEC} = 1930 + j \cdot 4200 \quad (6)$$

where the subscript *WEC* refers to the two-body equivalent.

6.7 Two-Body Finite Element and SPICE Simulation results With Monochromatic Waves

Simulations in OrcaFlex were then run to find the maximum power point of the slack-moored, two-body WEC. Both damping-only and binary control was used. For these first simulations a monochromatic wave at the target wave period of 6 sec. was used. The purpose of first using a monochromatic was to tune the control at the maximum dominant wave period to then use for later comparison when using spectral waves.

Simulations with the same wave conditions were also run with a SPICE model of the two-body equivalent circuit to validate the equivalent circuit so that it could be used for non-FEA analysis that can be executed much faster. The SPICE model is shown in Fig. 62. SPICE Simulation Circuit.

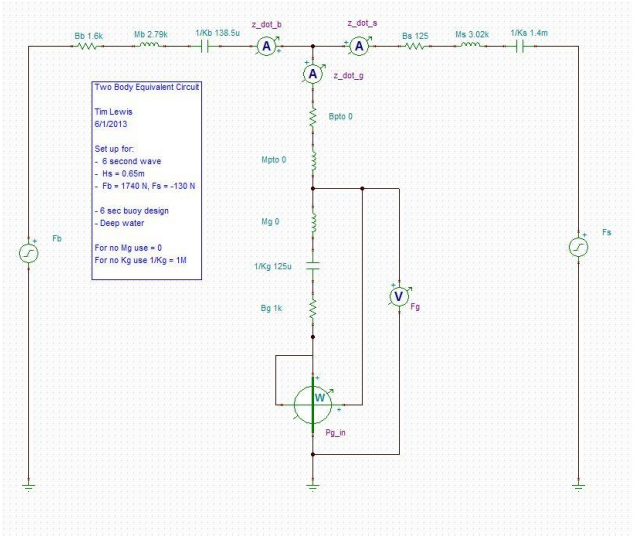

Fig. 62. SPICE Simulation Circuit

6.7.1 Damping Control Results

First, simulations sweeping the damping term only to find the maximum power point were performed. As seen in Fig. 63 the equivalent circuit model tends to over-predict the power output compared to the FEA analysis but it does capture the response shape

as the damping term is swept. Note that with the damping-only control the power output is fairly insensitive to tuning errors around the maximum power point.

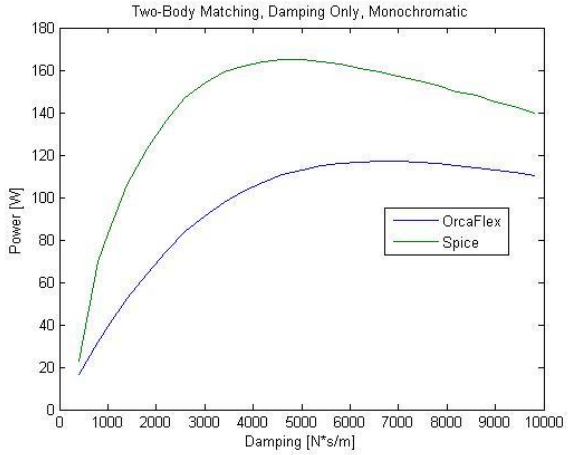

Fig. 63. Damping Control with a Monochromatic Wave

6.7.2 Binary Control Results

The results of sweeping the damping and stiffness terms when using binary control in the FEA package are shown in Fig. 64. To obtain the maximum power point a damping term of 2000 N/m and a stiffness term of 5500 N·s/m would be utilized in the binary control. The maximum average power extracted is approximately 270W which meets the WEC specification.

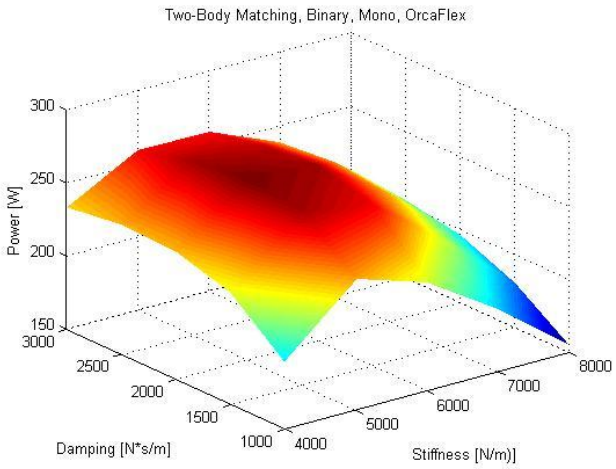

Fig. 64. Binary Control with a Monochromic Wave, OrcaFlex

This yields a Thevenin equivalent from the FEA analysis of:

$$Z_{WEC} = B_{WEC} + j \cdot X_{WEC} = 2000 + j \cdot 5240 \quad (7)$$

Comparing OrcaFlex FEA two-body Thevenin impedance to the Thevenin impedance calculated from the equivalent circuit it is seen that the damping terms match well, with the reactive terms approximately 20% off.

Next the SPICE model was used with binary control, sweeping the same damping and stiffness term ranges. As seen in Fig. 65 the maximum power is approximately 240W which is consistent and the general output characteristics are captured though the tuning parameters are shifted from the FEA simulation.

It is understood that wave tank validation is a critical phase of any hydrodynamic design [17]. Even FEA models have been shown to have mismatches of WEC parameters of 20-50% initially [18]. In addition, with the OrcaFlex FEA tool many drag and damping coefficients are entered directly and are expected to be adjusted to match tank testing.

With this in mind, general conclusions will not be stated as of yet since the SPICE model is a simplified one and at this stage it will only be used for predicting general characteristics and not be used for detailed results. Even the FEA model needs to be corroborated against actual wave tank testing for detailed quantitative conclusions.

The scaled model wave tank testing has been performed but validation against these results is still ongoing.

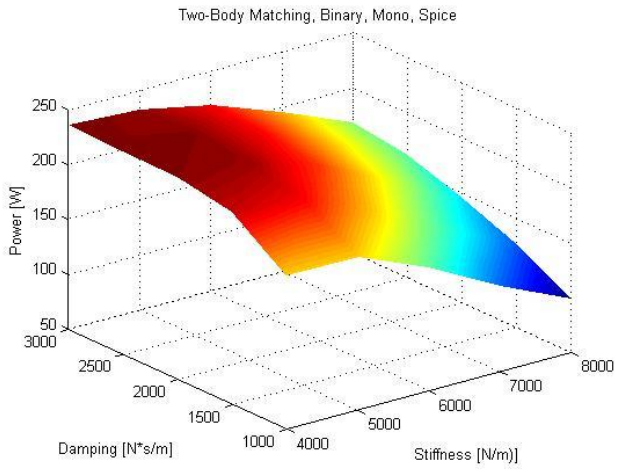

Fig. 65. Damping Control with a Monochromatic Wave, SPICE

6.8 Target Sea Conditions and the Equivalent Wave Representation

To simulate cases similar to wave conditions typically seen by the Galveston 42035 Buoy it was chosen to investigate fitting both the Pierson-Moskowitz and JONSWAP wave distributions. This is appropriate since the Pierson-Moskowitz (PM) and JONSWAP spectrum are frequently applied for wind seas [19]. The JONSWAP spectrum extends the PM spectrum to include fetch limited seas, thus representing

geographically limited, near-shore areas – areas in which an AWEC would typically be intended to operate. The PM spectrum is given by:

$$S_{PM}(\omega) = \frac{5}{16} \cdot H_s^{\,2} \cdot \omega_p^{\,4} \cdot \omega^{-5} \exp\left(-\frac{5}{4}\left(\frac{\omega}{\omega_p} \right)^{-4} \right) \tag{8}$$

where H_s is the significant wave height and ω_p is the angular spectral peak frequency.

The JONSWAP spectrum is formulated as a modification of the PM spectrum as:

$$S_J(\omega) = A_\gamma S_{PM}(\omega) \gamma \wedge \exp\left(-0.5\left(\frac{\omega - \omega_p}{\sigma \omega_p} \right)^2 \right) \tag{9}$$

where γ is a non-dimensional peak shape parameter, σ is a spectral width parameter, and A_γ is a normalizing factor.

Fig. 66 shows the Galveston buoy spectral data along with the PM spectrum and the JONSWAP spectrum with the best fit value of γ equal to 5.0, and σ equal to a typical empirical value.

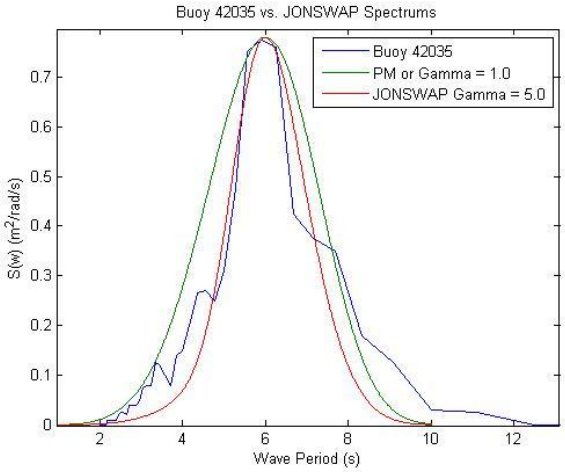

Fig. 66. Spectral Wave Representation

For the spectral simulations the more basic PM spectrum will be utilized. This spectrum is viewed as covering more sea environments and it was chosen since it was felt that the wave tank testing would be able to more accurately represent this spectrum.

6.9 Two-Body Finite Element Simulation results With Spectral Waves

Simulations were next run to find the maximum power point of the slack-moored, two-body WEC, using the PM spectral input.

6.9.1 Damping Control Results

A sweep over the same parameters used in monochromatic analysis was performed and the results are shown in Fig. 67. The maximum power value is approximately 50% of the equivalent monochromatic wave and it is achieved with a damping value that is significantly higher.

It is known that a WEC has an equivalent power absorption bandwidth [7] but this FEA analysis again validates the need to incorporate this into the WEC design.

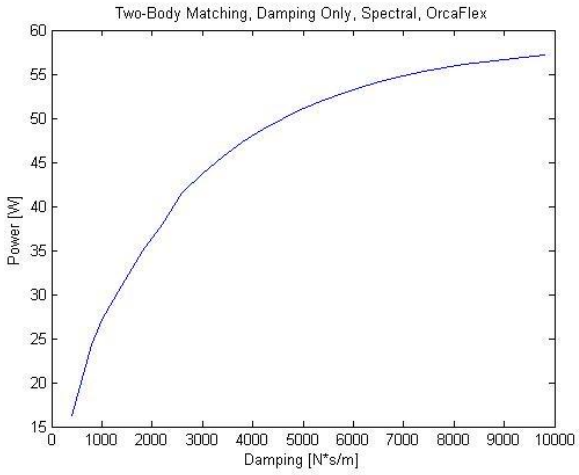

Fig. 67. Damping Control with Spectral Waves

6.9.2 Binary Control Results

The binary control FEA results with the spectral input are shown in Fig. 68. With this control the power output loss is similar, approximately only 55% of the output from the equivalent monochromatic wave. The control tuning does shift a bit also but not quite as dramatically and the damping-only control. The reactive tuning is about the same with the damping tuning for maximum power shifting to approximately 2500 N/m.

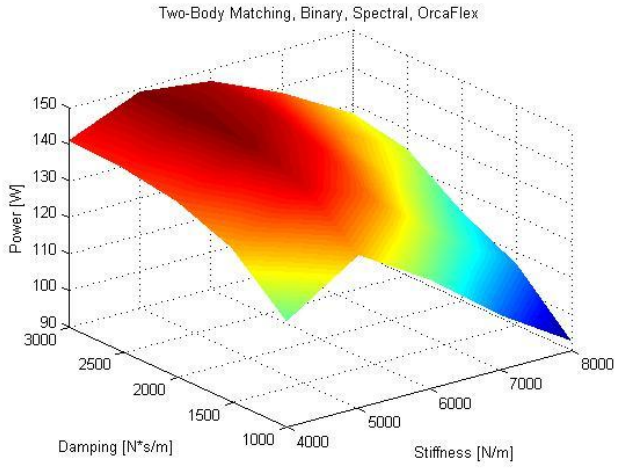

Fig. 68. Binary Control with Spectral Waves

An additional set of FEA simulations was performed to obtain the power absorption bandwidth of the WEC when using binary control and to compare this to the input spectral wave energy. In this set of simulations the wave period was swept to obtain the power output vs. wave period. A normalized version of these results is plotted on the same scale as the wave spectral input to show the mismatch in the waveforms. It can be seen that a large amount of the wave spectral power is outside of the absorption bandwidth of the WEC. Fig. 69 shows these results.

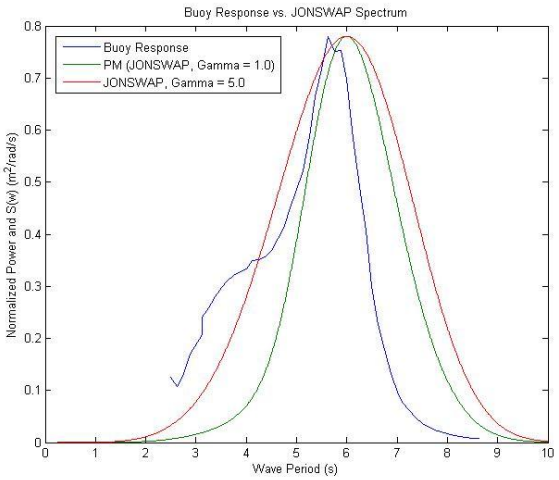

Fig. 69. Buoy Power Response vs. Wave Spectrum

Note also that with the spectral wave input the results with damping-only control is about half that of when the WEC is under binary control.

6.10 Alternate Controller Design and Factors Affecting Controller Choice

6.10.1 Ternary Controls

To try to re-capture some of the lost spectral wave energy due to WEC power absorption bandwidth limitations an alternative three term, or ternary controller, was constructed. The goal of the controller can intuitively be seen from Fig. 61. The idea was to provide impedance matching to both the stiffness and added mass terms. In terms of the taut-moored controller the reactive terms could completely cancel thus resulting in a wide bandwidth controller.

This control would then be:

$$B_g = B_{WEC} \tag{10}$$

$$K_g = -K_{WEC} \tag{11}$$

$$M_g = -M_{WEC} \tag{12}$$

with the damping term (B_g) applied to the relative velocity difference between the two bodies (i.e., the PTO velocity), the stiffness term (K_g) applied to the relative position difference, and the added mass term (M_g) applied to the relative acceleration difference.

Though it is known that the two-body realization has a much more complex Thevenin equivalent to match, a series of bandwidth sweeps adjusting the generator stiffness and added mass control terms was performed. The bandwidth sweeps plotted the bandwidth with damping only control, binary control (K_g, but no M_g control) and five (5) cases of increasing M_g control. With the increasing M_g control, the K_g term was adjusted to retain the overall matched reactive tuning as the M_g term increased. The results are shown in Fig. 70.

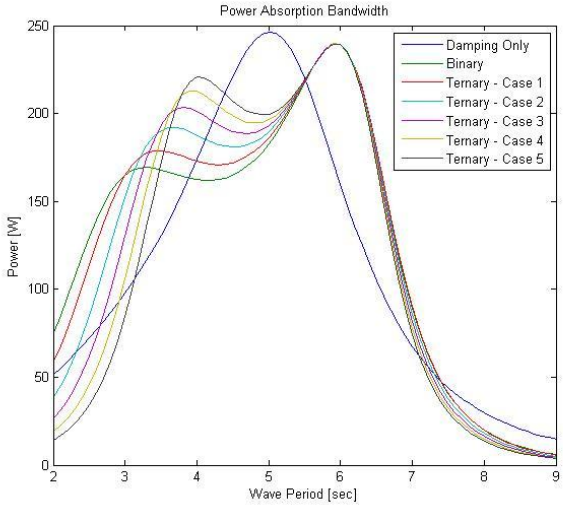

Fig. 70. Power Absorption Bandwidth with Ternary Controls

Two effects can be seen: First, damping-only control does not provide a maximum power point at the wave period of interest, 6 sec. This is obvious from the fact that the reactive component of the equivalent circuit is not compensated for in phase also. The

matched reactive control schemes, though, do indeed provide maximum power at the wave period of interest since the control matches the phase also at this wave frequency. Second, ternary control still provides this matching at the dominant wave period but it does also increase the bandwidth. The bandwidth increases though are very modest, at least with the parameters of the WEC under analysis.

The amount of effort to employ this type of control would have to be compared to the relative performance improvement that may be obtained.

6.11 Effects of Power Take-Off Losses

Another real-world effect that may affect the controller selection is the losses in the power take-off mechanism itself. Since the PTO connection for this WEC is a lead-screw assembly the dominant losses are most likely proportional to velocity, thus can be modeled as a series damping term. This incorporated loss term, B_{PTO}, can be seen in the SPICE model, Fig. 62.

Intuitively the loss term will affect the Thevenin equivalent damping since it is in series. As B_{PTO} increases, for the binary control case, Fig. 71, the generator damping is quickly becoming the dominant term of the control.

Fig. 72 shows the effect of B_{PTO} increasing on the bandwidth of ternary control. Essentially any bandwidth improvements with this control are swamped as the PTO losses increase.

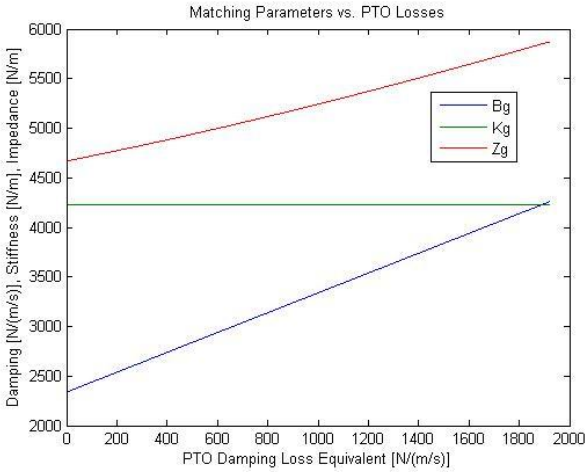

Fig. 71. Effect of Increasing PTO Losses

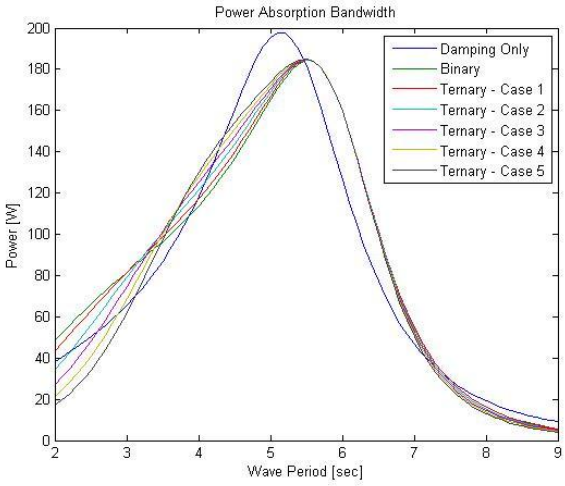

Fig. 72. Effect of PTO Losses on Ternary Control

The results from these analyses show that increasing the controller complexity with a third term of control, and in conjunction with PTO losses, the simpler damping-only control may be the best control strategy to use. Especially when coupled with the known effect of higher kVA requirements of an electrical PTO when using the more complex reactive control [6].

6.12 Conclusions

An autonomous WEC design and analysis with finite element simulation was further extended to include real-world waves with spectral energy content. Both damping-only and binary control were used in the FEA simulation domain to compare the power output of the system. It was found that the power output with the spectral wave input is reduced by about half with both control strategies. The damping-only controlled system also yields a maximum output power that is about half again that of the binary control overall.

Analysis with a more complex, three term reactive controller, was performed and it was shown that there was little increase in the bandwidth of the WEC system, the major cause of less power output with spectral waves.

Although binary control produced the most power with both monochromatic and spectral input it is known to require longer stroke lengths, faster velocities, and a much greater PTO kVA capability. If would have to be judged whether this increase in control complexity and cost is worth the additional power output. In the specific case of an autonomous WEC that must provide a minimum consistent power output, the solution may be to just utilize the less sensitive but less power optimal damping-only control, to size the PTO for this minimum condition, and not have to oversize the PTO to provide the additional reactive power.

6.13 References

[1] T. Brekken and A. von Jouanne "ECCE Wave Energy Tutorial," *IEEE Energy Conversion Conference and Exposition*, San Jose, CA, Sept. 2009.

[2] K. Rhinefrank, A. Schacher, J. Prudell, C. Stillinger, D. Naviaux, T. Brekken, A. von Jouanne, D. Newborn, S. Yim, D. Cox, "High Resolution Wave Tank Testing of Scaled Wave Energy Devices," *29th International Conference on Offshore Mechanics and Arctic Engineering (OMAE)*, 2010.

[3] E. Agamloh, "A Direct-Drive Wave Energy Converter with Contactless Force Transmission System," School of Electrical Engineering and Computer Science, Oregon State University, Corvallis, OR, Oct. 2005.

[4] K. Rhinefrank, E. Agamloh, A. von Jouanne, A.K. Wallace, J. Prudell, K. Kimble, J. Aills, E. Schmidt, P. Chan, B. Sweeny, A. Schacher, "Novel Ocean Energy Permanent Magnet Linear Generator Buoy," *Elsevier Renewable Energy Journal*, Vol. 31, Issue 9, July 2006, pg. 1279-1298.

[5] Schacher, A.V. Meulen, D. Elwood, P. Hogan, K. Rhinefrank, T. Brekken, A. von Jouanne, S. Yim, "Novel Control Design for a Wave Energy Generator," *46th AIAA Aerospace Science Meeting and Exhibit*, Reno, NV, Jan. 2008, AIAA-2008-1305.

[6] T. Lewis, A. von Jouanne, T. Brekken, "Per-Unit Wave Energy Converter System Analysis," *IEEE Energy Conversion Congress and Exposition*, Phoenix, AZ, Sept. 2011.

[7] T. Lewis, A. von Jouanne, T. Brekken, "Wave Energy Converter with Wideband Power Absorption," Digest for *IEEE Energy Conversion Congress and Exposition*, Phoenix, AZ, Sept. 2011.

[8] T. Lewis, A. von Jouanne, T. Brekken, "Modeling and Control of a Slack-Moored Two Body Wave Energy Converter," *IEEE Energy Conversion Congress and Exposition*, Raleigh, NC, Sept. 2012.

[9] OrcaFlex, Version 9.3a, Orcina Ltd., Daltergate, UK, www.orcina.com.

[10] M. Patel, *Dynamics of Offshore Structures*, Butterworth-Heinemann, 1989.

[11] J. Falnes, Ocean Waves and Oscillating Systems: Linear Interactions Including Wave-Energy Extraction, Cambridge University Press, 2002, ISBN-13 978-0-521-01749-7.

[12] J.K.H. Shek, D.E. Macpherson, M.A. Mueller, "Phase and Amplitude Control of a Linear Generator for Wave Energy Conversion," *4thCconference on Power Electronics, Machines, and Drives*, April 2008, pg. 66-70.

[13] J.K.H. Shek, D.E. Macpherson, M.A. Mueller, J. Xiang, "Reaction Force Control of a Linear Electrical Generator for Direct Drive Wave Energy Conversion," *lET Renewable Power Generation*, 2007,1, (1), pp. 17-24.

[14] K. Ruehl, T.K. Brekken, B. Bosma, P. Paasch, "Large-Scale Ocean Wave Energy Plant Modeling," *IEEE Conference on Innovative Technologies for an Efficient and Reliable Electricity Supply (CITRES)*, 2010, pp. 379-386.

[15] H. Eidsmoen, "Simulation of a Slack-Moored Heaving-Buoy Wave Energy Converter with Phase Control," Division of Physics, Norwegian University of Science and Technology, Trondheim, Norway, May 1996.

[16] M. McCormick, *Ocean Wave Energy Conversion*, Dover Publications, 2007, ISBN-13 978-0-486-46245-5.

[17] J. Cruz, *Ocean Wave Energy*, Springer Series in Green Energy and Technology, 2008, ISBN-13 978-3-540-74894-6.

[18] Z. Zhang, "Development of Adaptive Damping Power Take-Off Control for a Three-Body Wave Energy Converter with Numerical Modeling and Validation," School of Electrical Engineering and Computer Science, Oregon State University, Corvallis, OR, Dec. 2011.

[19] Det Norske Veritas, "Environmental Conditions and Environmental Loads", Recommended Practice DNV-RP-C205, October 2010.

WAVE LAB TESTING OF A TWO-BODY AUTONOMOUS WAVE ENERGY CONVERTER

Timothy M. Lewis, Bret Bosma, Annette von Jouanne, Ted K.A. Brekken

School of Electrical Engineering and Computer Science

1148 Kelley Engineering Center

Oregon State University

Corvallis, USA

lewisti@eecs.oregonstate.edu

To be submitted to:

Energy Conversion Conference and Exposition

Pittsburg, PA

September 14-18, 2014

7 Wave Lab Testing of a Two-Body Autonomous Wave Energy Converter

Abstract - Wave Energy Converter (WEC) design strives to produce as much power as possible across differing wave conditions. It is especially true of autonomous WECs (AWECs), used, for example, to power an ocean buoy sensing system, because they are smaller and they need to maximize the amount of power produced under low-energy wave energy conditions. An AWEC is a wave energy device that is not tied to a land-based electric utility. This paper describes the testing results and conclusions from actual wave lab testing of a WEC intended for autonomous applications, i.e., an AWEC. The results are compared to previous WEC hydrodynamic finite element analysis (FEA) that used integrated optimal control with both monochromatic and spectral waves. Conclusions are drawn with respect to the power absorption capability of the AWEC when the wave source is a monochromatic wave versus richer frequency spectral waves.

7.1 Introduction

Wave energy is recognized as a potential source for energy harvesting. Direct energy from the immediate ocean environment may be of particular interest for remote or isolated ocean applications since the local wave energy source is persistent, predictable, has a high power density, and maintains a minimum power level in most ocean environments [1,2]. This work extends the previous research for axisymmetric, heave-only, power absorbers [3,4,5,6,7,8] with wave lab testing and compares the FEA [9], with active control, driven by spectral waves that are present in the real world. This work validates analysis quantifying the reduction in power achievable in spectral waves compared to simplified analysis with monochromatic waves. This work validates the need to understand how critical it is to understand and design to this richer, larger wave spectrum in order to maximize power.

7.2 O.H. Hinsdale Wave Research Lab Description

The O.H. Hinsdale Wave Research Lab (HWRL) is one of two wave facilities at Oregon State University. The 2D wave flume was utilized. It has a flume depth of 15 feet and it is approximately 342 feet long, including the rear sloping beach. The AWEC was moored with a draft of 11 feet and located between markers 6 and 7. Fig. 73 [12] shows the location of the AWEC in the flume along with the utilized wave gauges and PhaseSpace optical sensing system. It also shows the HWRL coordinate system's reference origin.

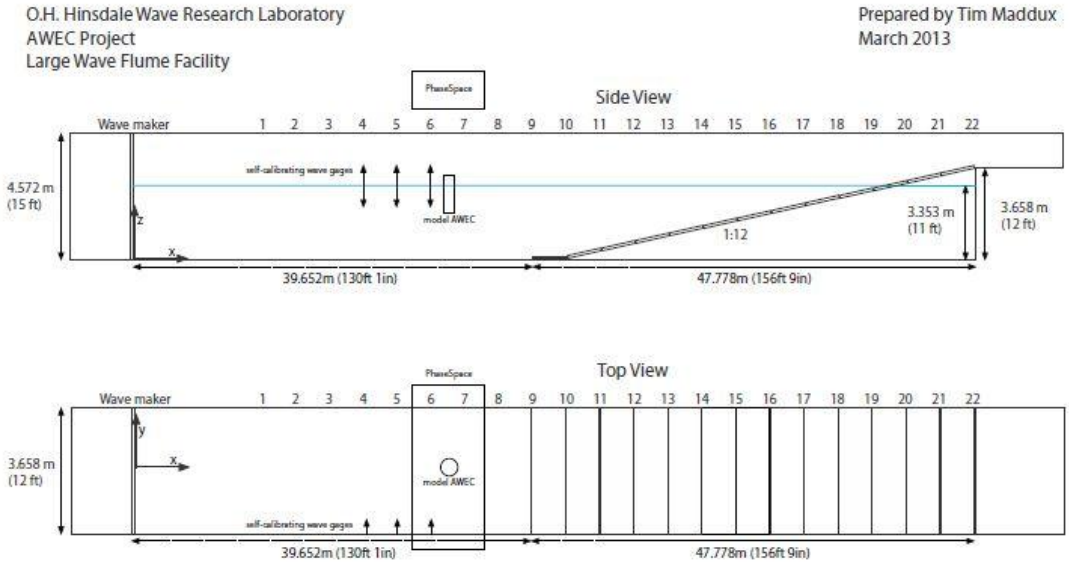

Fig. 73. O.H. Hinsdale Wave Research Lab Wave Flume

Fig. 74 shows an end view of the flume before the water fill and AWEC placement. The mooring system must be placed into the flume before the flume is filled since it is below the water line.

Fig. 74. Longitudinal View Down the Wave Flume

data column	sensor name	cable to driver	driver	driver channel	cable to DAQ	DAQName	DAQHardwareChannels
wmstart	wmstart	NA	LWF-WM	AO1	CX-70-256 + CX-58-077 + CX-05-187	pxi3	SC1Mod1/ai0
wmdisp	TMPO-LWM	NA	LWF-WM	AO2	CX-70-257 + CX-59-198	pxi3	SC1Mod1/ai1
wmwg	RWG-LWM	NA	LWF-WM	AO3	CX-70-258 + CX-58-066	pxi3	SC1Mod1/ai2
level	PRES-8482	NA	SG-SC-6381	1	CX-62-199	pxi3	SC1Mod1/ai3
wg1	RWG-2260-01	WG-25-52	RWG-2260	1	CX-05-134	pxi3	SC1Mod1/ai4
wg2	RWG-2260-02	WG-25-49	RWG-2260	2	CX-05-026	pxi3	SC1Mod1/ai5
wg3	RWG-2260-03	WG-50-23	RWG-2260	3	CX-05-025	pxi3	SC1Mod1/ai6
escon_cur_cmd	NA	NA	AWEC-DA	1	CX-15-226	pxi3	SC1Mod1/ai7
escon_en	NA	NA	AWEC-DA	2	CX-15-049	pxi3	SC1Mod2/ai0
nut_pos	NA	NA	AWEC-DA	3	CX-15-048	pxi3	SC1Mod2/ai1
nut_vel	NA	NA	AWEC-DA	4	CX-15-230	pxi3	SC1Mod2/ai2
nut_acc	NA	NA	AWEC-DA	5	CX-15-228	pxi3	SC1Mod2/ai3
k_gen	NA	NA	AWEC-DA	6	CX-15-044	pxi3	SC1Mod2/ai4
b_gen	NA	NA	AWEC-DA	7	CX-15-234	pxi3	SC1Mod2/ai5
m_gen	NA	NA	AWEC-DA	8	CX-15-231	pxi3	SC1Mod2/ai6
escon_cur	NA	NA	AWEC-ADC	6	CX-15-200	pxi3	SC1Mod2/ai7
escon_vel	NA	NA	AWEC-ADC	5	CX-16-212	pxi3	SC1Mod3/ai0
pwr_sup_cur	NA	NA	AWEC-ADC	1	CX-15-045	pxi3	SC1Mod3/ai1
load_cur	NA	NA	AWEC-ADC	3	CX-15-236	pxi3	SC1Mod3/ai2
sup_load_volt	NA	NA	AWEC-ADC	2	CX-15-235	pxi3	SC1Mod3/ai3
lc_fore_star	643296	NA	SG-SC-9860	1	CX-07-052	pxi3	SC1Mod3/ai4
lc_fore_port	686604	NA	SG-SC-9860	2	CX-07-051	pxi3	SC1Mod3/ai5
lc_aft	640915	NA	SG-SC-9860	3	CX-08-159	pxi3	SC1Mod3/ai6
Notes:							
1. pxi3 is located along the E wall of the LWF at Bay 5							
2. wmstart routed through DAQ-SC-ALD1 ch1							
3. PhaseSpace is triggered by wmstart routed through DAQ-SC-ALD1 ch2 on CX-03-160							

Fig. 75. Data Collected with the HWRL Acquisition System

Fig. 75 shows the instrumentation that was interfaced with the HWRL primary data acquisition equipment. The captured signals are:

wmstart: Discrete signal indicating the wave maker start. This was utilized to trigger the AWEC control and data acquisition system.

wmdisp: Wave maker displacement

wmwg: Wave height at the wave maker

level: Pressure transducer to detect tank water level

wg1,2,3: Wave gauges for measuring wave height.

escon_curr_cmd: Signal sent by the AWEC control system current through the WEC electric power take-off (PTO)

escon_en: Signal indicating the PTO's 4-quadrant power electronics drive is enabled (pulse width modulation (PWM) control active)

nut_pos: Signal indicating the PTO relative distance between float and spar after initial zeroing

nut_vel: Signal indicating the PTO relative velocity between the float and spare (encoder based)

nut_acc: Signal indicating the PTO relative acceleration between the float and spar

k_gen: Signal indicating the AWEC feedforward force term (proportional to position)

b_gen: Signal indicating the AWEC feedforward force term (proportional to velocity)

m_gen: Signal indicating the AWEC feedforward force term (proportional to acceleration)

escon_curr: Signal indicating the measured current through the PTO

escon_vel: Signal indicating the velocity from the 4-quadrant drive

pwr_sup_cur: Signal indicting the power supply voltage output

load_curr: Signal indicating he current flow through the load resistor

sup_load_volt: Signal indicating the voltage across the load resistor

lc_fore_star: Signal indicating the force on the forward, starboard mooring line

lc_fore_port: Signal indicating the force on the forward, port mooring line

lc_fore_aft: Signal indicating the force on the aft mooring line

data column	sensor name	coord space	placement (X)	placement (Y)	placement (Z)
wmstart	wmstart	Large Wave Flume			
wmdisp	TMPO-LWM	Large Wave Flume		0.000	
wmwg	RWG-LWM	Large Wave Flume		0.000	
level	PRES-8482	Large Wave Flume	13.966	-1.480	0.318
wg1	RWG-2260-01	Large Wave Flume	21.370	-1.280	
wg2	RWG-2260-02	Large Wave Flume	25.040	-1.273	
wg3	RWG-2260-03	Large Wave Flume	36.004	-1.279	
escon_cur_cmd	NA	Large Wave Flume			
escon_en	NA	Large Wave Flume			
nut_pos	NA	Large Wave Flume			
nut_vel	NA	Large Wave Flume			
nut_acc	NA	Large Wave Flume			
k_gen	NA	Large Wave Flume			
b_gen	NA	Large Wave Flume			
m_gen	NA	Large Wave Flume			
escon_cur	NA	Large Wave Flume			
escon_vel	NA	Large Wave Flume			
pwr_sup_cur	NA	Large Wave Flume			
load_cur	NA	Large Wave Flume			
sup_load_volt	NA	Large Wave Flume	28.582	1.683	2.812
lc_fore_star	643296	Large Wave Flume	28.582	1.683	2.812
lc_fore_port	686604	Large Wave Flume	28.610	-1.690	2.810
lc_aft	640915	Large Wave Flume	32.433	0.072	2.822

Fig. 76. Physical Location of Sensors with Hinsdale Reference System

Fig. 76 then shows the physical location of the sensors relative to the 2D wave flume reference system.

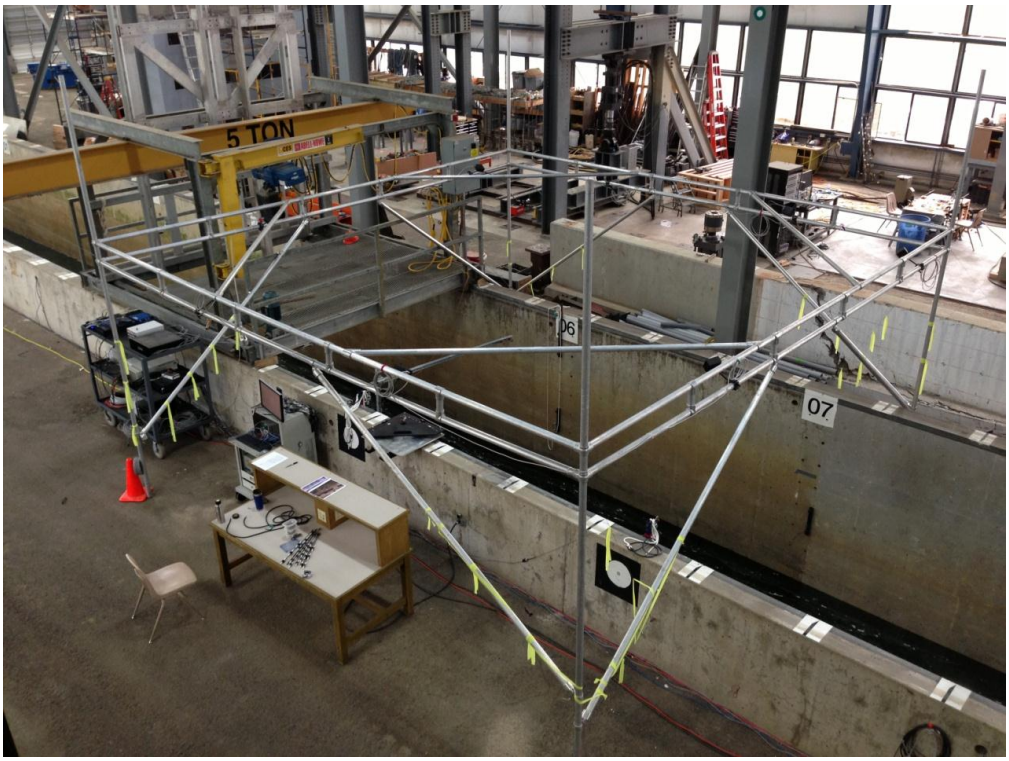

Fig. 77. PhaseSpace Scaffolding System

The PhaseSpace system was also utilized to optically track the two bodies of the AWEC buoy. The sytem utilizes LED strings on the float and spar and in conjuction with it's LED reference system it can track the movement of bodies in 3D space at a rate of 480 Hz. Fig. 77 show the scafolding that the optical motion tracking cameras are mounted to. The cameras are mounted on the top edge of the scaffolding and can view both the AWEC and the LED reference system.

Fig. 78 shows one of the eight optical tracking cameras and Fig. 79 shows the PhaseSpace program output after the calibration LED wand was used during system configuration.

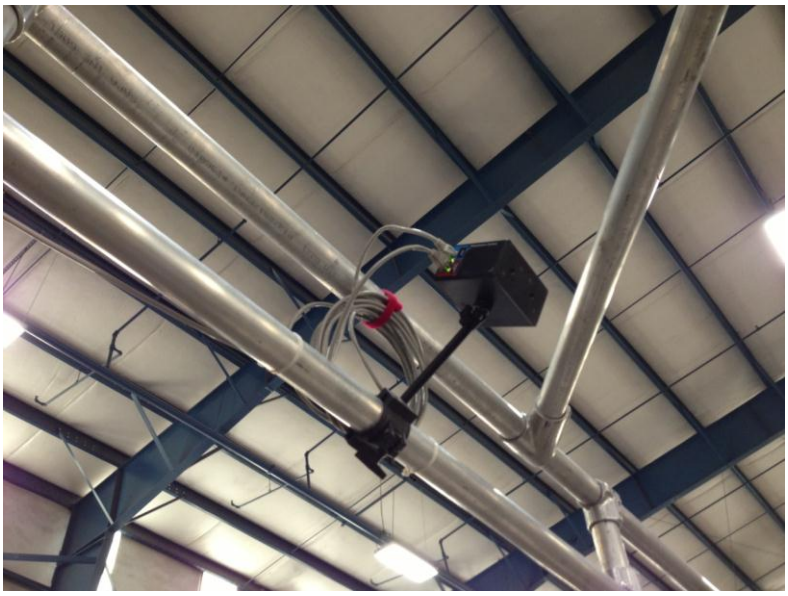

Fig. 78. PhaseSpace Optical Camera

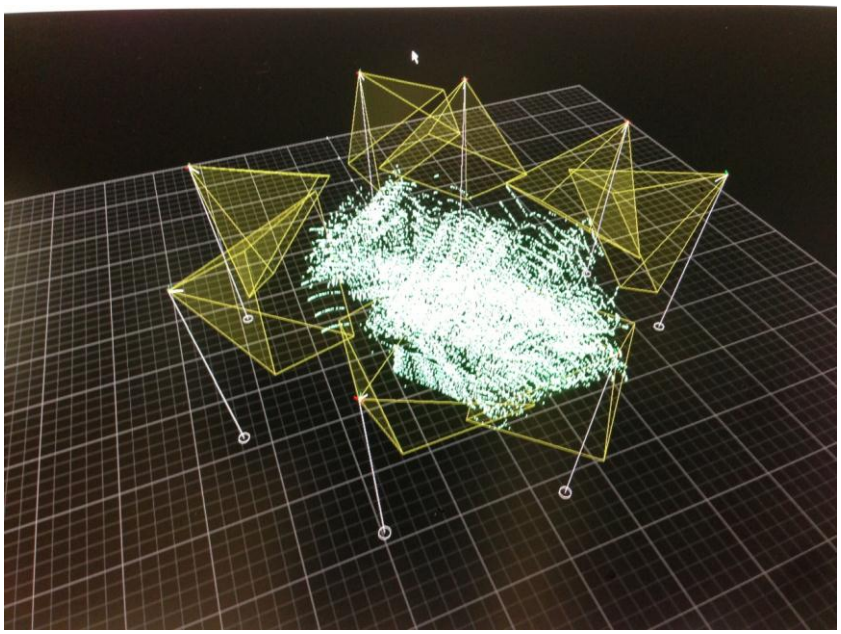

Fig. 79. PhaseSpace Calibration Output

7.3 Autonomous WEC Design and Wave Lab Restrictions

The WEC is designed to provide an electrical source to sensing packages on remote, autonomous buoys. It is designed with a center cylindrical spar with a cylindrical float around it. The float, in the full-scale design, is electromagnetically connected to the spar, where the spar houses the generator, control electronics, and sensing payload. Details of the design are provided in [7]. The design is such that the WEC remains near-vertical in most sea conditions. The long vertical spar is designed such that it is resistant to pitch and the heave resonance frequency is lower than the wave frequency range of interest thus providing a stiff platform for relative motion [10]. The target average power output is 200W. It is intended to be relatively inexpensive and to employ a simple slack-moored system. For this application the WEC must provide the specified power at the minimum, summer, wave strength.

The AWEC fabricated for test had to be scaled to be tested within the physical constraints of the lab. A 1:4 geometric scaling was used. Scaling of the AWEC properties following the Froude scaling laws are shown in Table 5 [11].

Table 5. Froude Scaling

Quantity	**Scaling**
Wave height and length	s
Wave period	$s^{0.5}$
Linear displacement	s
Linear velocity	$s^{0.5}$
Linear acceleration	1
Mass and linear added mass	s^3
Force	s^3
Torque	s^4
Power	$s^{3.5}$
Linear stiffness	s^2
Linear damping	$s^{2.5}$

The scaling, wave laboratory physical conditions, and practical fabrication restrictions caused a number of changes in the design. Wave energy converter testing is primarily concerned with power output, and the Froude scaling for power forces, the use of lower power electronics, and electric machines that are less efficient negatively impacts the output data scale and error. The scaling of power also forced the use of a much smaller electric power take-off generator which is inherently less efficient. A scale factor of 1:4 was chosen to balance the implications of depth, wave period, and power.

The 2D HWRL wave flume's depth required altering the base conceptual premise of a long, hydrodynamically stiff spar. Even with the shifting the full scale dominant wave period to 4 seconds (2 second, scaled) which was also better to also match the range of the flume wave maker. The flume depth required truncating the spar depth to a length shorter than desired. To try to overcome this a damper plate was installed. But this results in a perceived more non-linear response of the system. The damper plate's close proximity to the float may add 'shadowing' and two-body coupling effects which was not envisioned in the original design.

Due to the need to use more cost effective and available material, the dimensions of the float diameter had to be altered which actually changed the target output power. The use of full scale material at scale also changed basic buoyancy predictions. To cheaply fabricate the AWEC a PVC pipe section with a large diameter was utilized. In addition the PTO had to be mounted externally due to size restrictions and the required alignment bushing did increase the drag friction of the PTO. Fig. 80 shows the device under test in the lab facility.

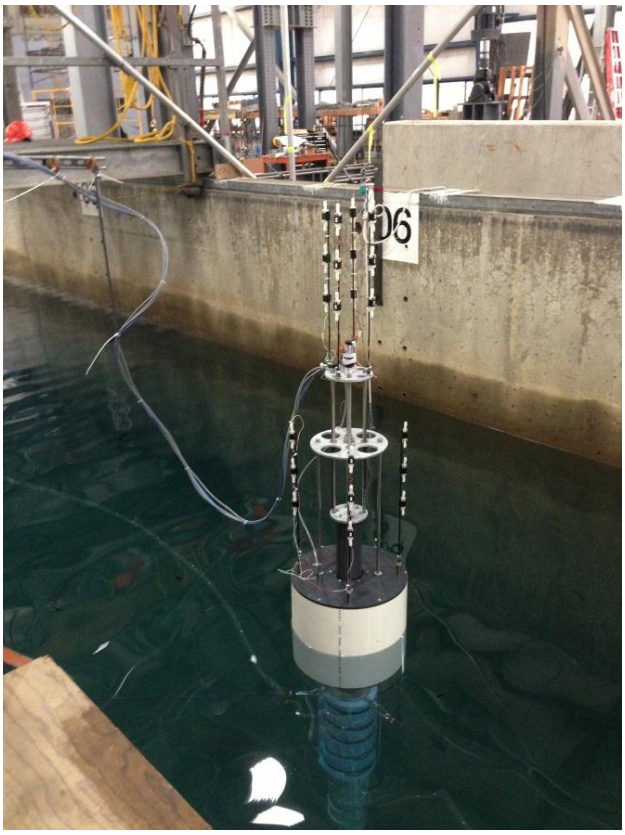

Fig. 80. Two-body WEC in Wave Flume.

Fig. 81 shows the 1:4 scaled AWEC with the limitations incorporated and Fig. 82 shows the ‘full-scale’ equivalent.

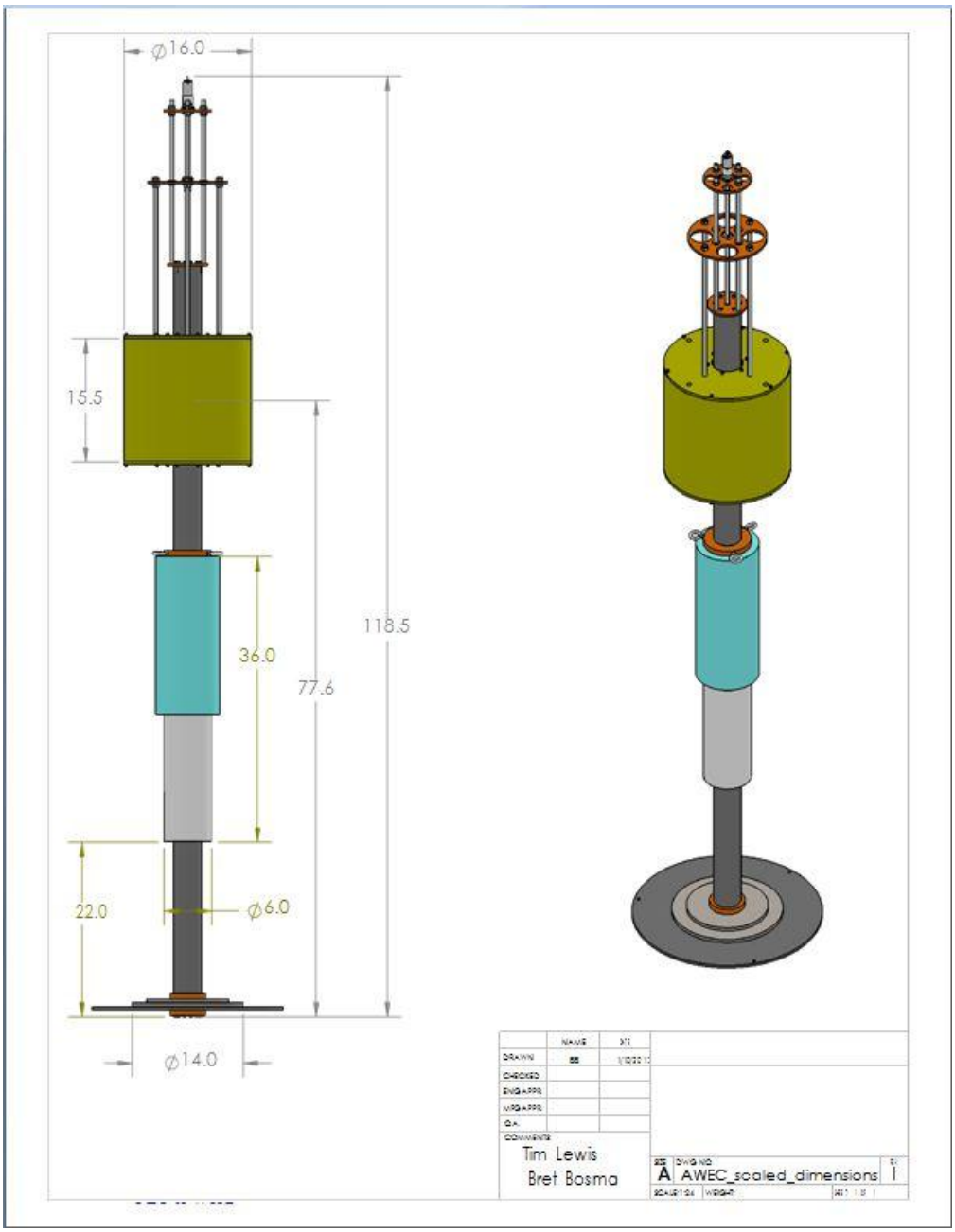

Fig. 81. Scaled AWEC

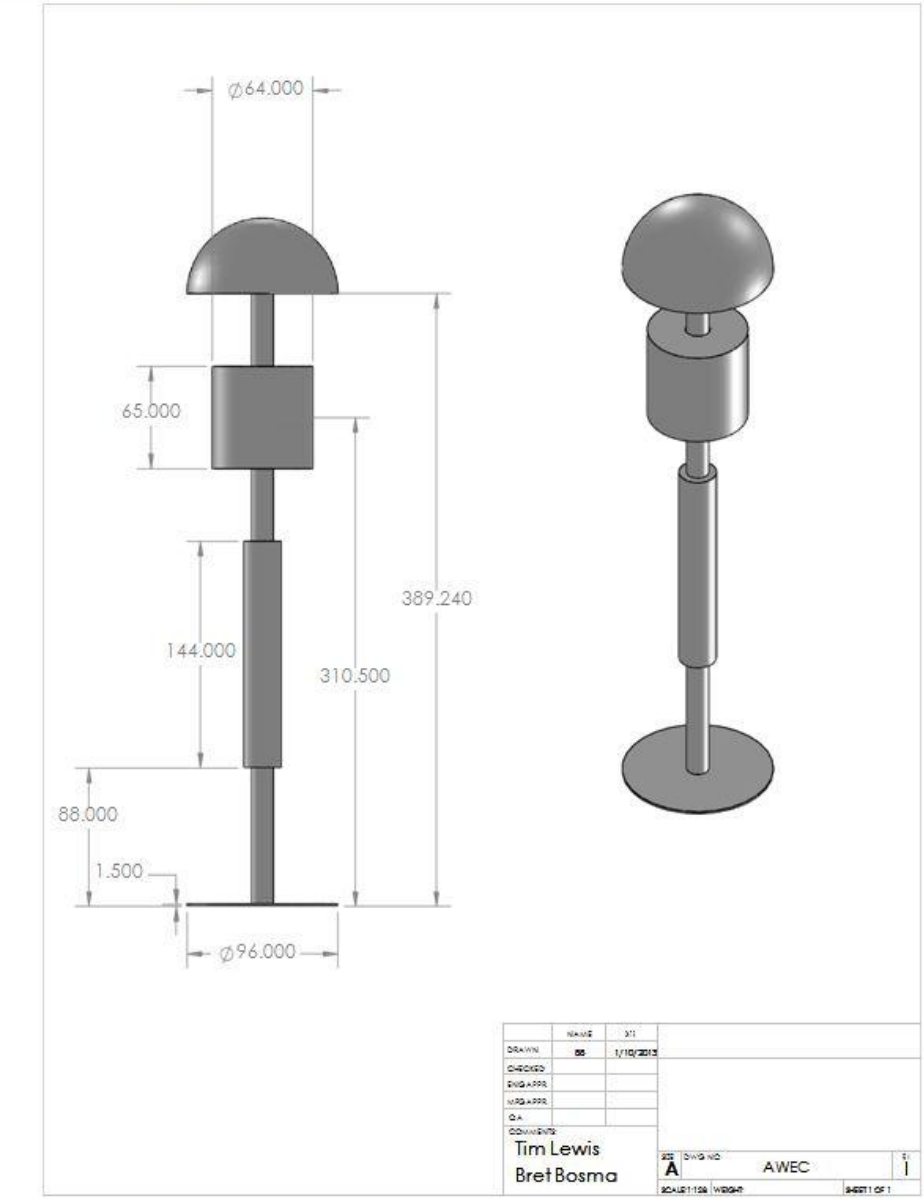

Fig. 82. Full Scale AWEC

Fig. 83Fig. 83. Float Material and Fabrication

shows the float in the middle of fabrication and Fig. 84 shows the external PTO assembly.

Fig. 83. Float Material and Fabrication

Fig. 84. Float with Inverted PTO

7.4 AWEC Mooring

A mooring design was completed by Bret Bosma and is described in detail in [12]. It is a three point taut mooring system. Surgical tubing and line were used as the mooring line material. As seen in Fig. 85 each mooring line was attached to the damper plate and run to the wave tank wall. The two forward lines ran diagonally to the wall and the rear line ran to a turnbuckle and then to one side of the flume. At the wave tank wall the lines run through an eye bolt and then vertically to a tie off point. Above the waterline the line was tied off via a force transducer for measurement.

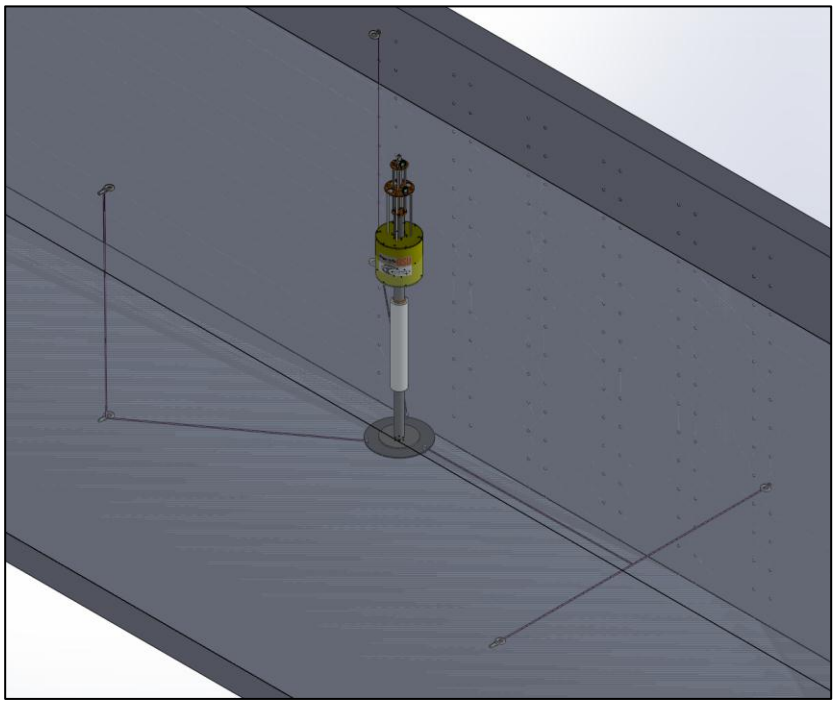

Fig. 85. Mooring View

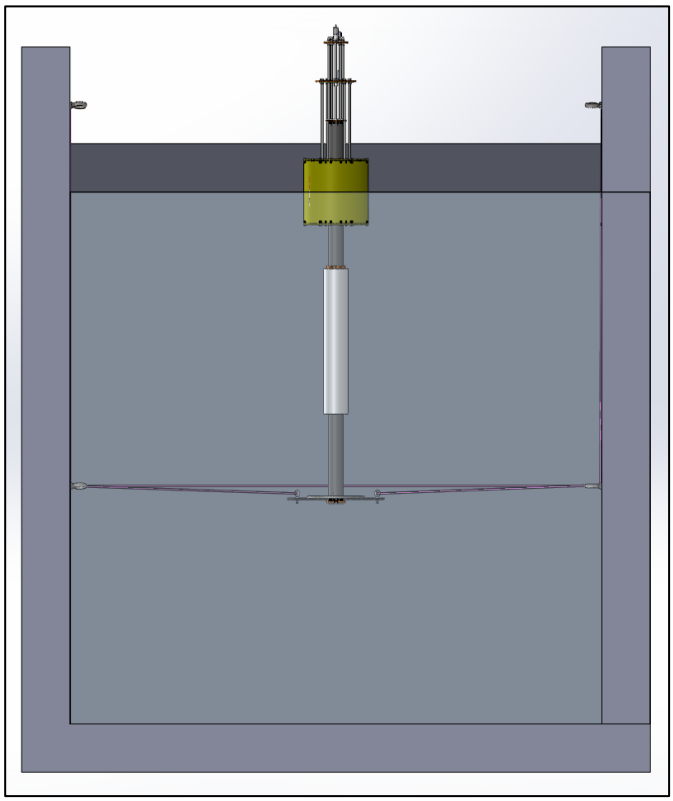

Fig. 86. Mooring Longitudinal View

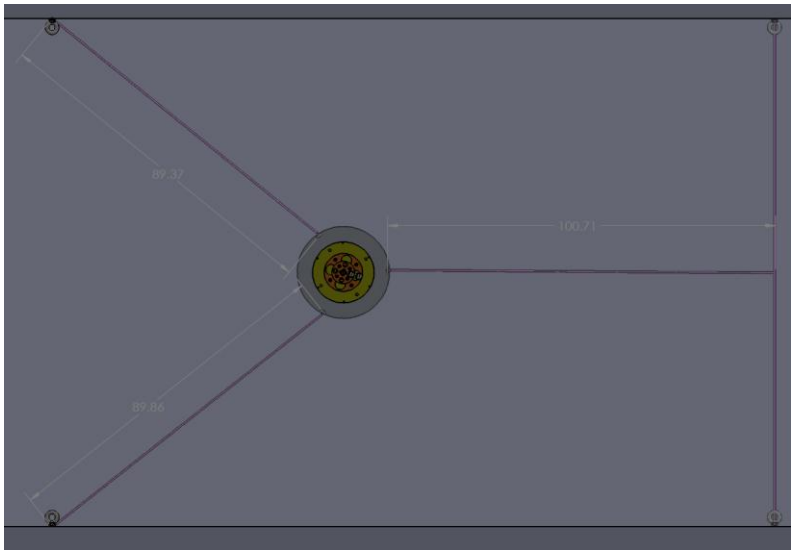

Fig. 87. Mooring Top View

7.5 Target Sea Conditions and the Equivalent Wave Representation

A survey of near coastal United States locations was completed [7] and NOAA Buoy 42035 off of Galveston, TX, was selected to be used in the analysis. It is representative of a near-shore environment and has a minimum average significant wave height, H_s, of approximately 0.9 m. This equates to a minimum wave power of 2.5 kW/m. The dominant wave period of 4 seconds, when scaled, is 2 seconds and was a good central point for the wave lab facility.

To simulate cases similar to wave conditions typically seen by the Galveston 42035 Buoy, it was chosen to use the Pierson-Moskowitz (PM) spectrum. A more complex JONSWAP spectrum could be better fitted [12] but the PM distribution was used for simplicity. The PM spectrum is given by:

$$S_{PM}(\omega) = \frac{5}{16} \cdot H_s^{\,2} \cdot \omega_p^{\,4} \cdot \omega^{-5} \exp\left(-\frac{5}{4}\left(\frac{\omega}{\omega_p} \right)^{-4} \right) \tag{1}$$

where H_s is the significant wave height and ω_p is the angular spectral peak frequency.

An equivalence between the monochromatic and spectral waves was derived by using wave moments to equate monochromatic and spectral effective wave periods. A scale is then derived between the monochromatic peak-to-peak wave height and the lab's use of significant wave height for spectral waves.

7.6 Wave Lab Testing of the Autonomous Wave Energy Converter

The control methods used in the AWEC testing were damping control, binary reactive control, and ternary reactive control [8,13,14,15]. The details of the control methods were previously explained [7,8]. When testing the AWEC with damping control, various wave heights and wave periods where used with both monochromatic and spectral waves. Fig. 88 and Fig. 89 show the power output and motion results of the AWEC under a test monochromatic wave condition (sweepHTDampMono, Trial 24). One investigation compared monochromatic vs. spectral waves with the same equivalent wave power when using damping control. This experiment was run to compare lab results against previous design simulations [8]. FEA analysis with a wave height (scaled) of 0.15 (0.6) m showed this reduction to be about 50%. Table 6 tabulates this reduction in absorbed power and the average for the wave conditions tested is 0.476 which matches the FEA analysis well. In the table 'Note 1' documents the invalid wave runs that had periods of data acquisition losses which negated the run.

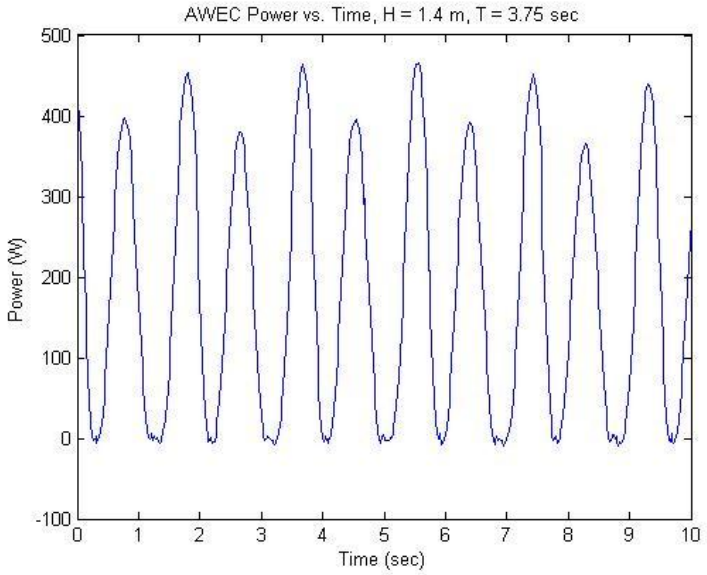

Fig. 88. Power Production with Damping Control and Monochromatic Waves

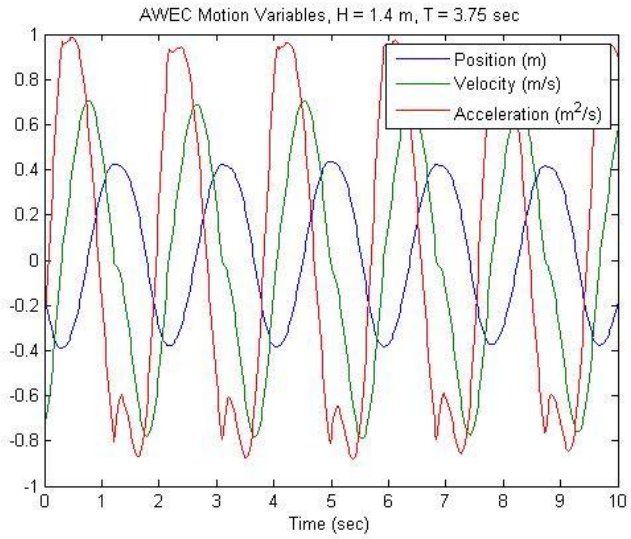

Fig. 89. Motion Parameters with Damping Control and Monochromatic Waves

Table 6. Power Reduction with Spectral Waves and Damping Control

H_s (m)	T_p (s)	Spectral/Monochromatic Power
0.50	3.0	0.484
1.10	3.0	Note 1
1.40	3.0	Note 1
0.50	3.75	0.262
1.10	3.75	Note 1
1.40	3.75	0.542
0.5	4.5	0.420
1.10	4.5	0.191
1.40	4.5	0.408
0.50	5.25	0.608
1.10	5.25	0.313
1.40	5.25	0.693
0.50	6.0	0.766
1.10	6.0	0.429
1.40	6.0	0.602

7.7 PhaseSpace Processing

PhaseSpace results are shown in Fig. 90. It shows the expected trends for the two-body and differential heave but the scaling is incorrect. This section is presented to demonstrate that the PhaseSpace output was obtained and checked. Due to the complex transformations in the HWRL algorithms to extract this data work in this area is cited for future research.

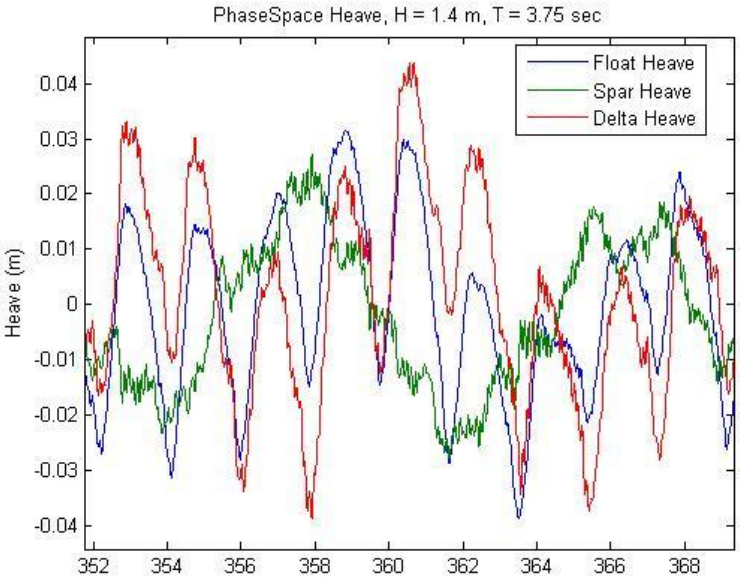

Fig. 90. Phase Space Heave Results

7.8 Laboratory Results with Binary Control

Next, binary reactive control was implemented. When using binary control, the actual power absorption bandwidth of the AWEC is more narrowband, therefore knowledge of the peak spectral wave period and control tuning is critical [7]. Fig. 91 (testBinTerCntrlSpectral, Trial: 18) shows the power output with binary reactive control with a spectral wave input. Reactive control actually has times of power flow back to the water and this can be easily seen. A series of tests were run in which the control tuning was set for one wave period, and then the test wave spectra's peak

period was changed to show the effects of mistuning. As seen in Table 7, the reduction in power absorption can be dramatic. Gains achievable with reactive tuning can be nullified with slight amounts of mistuning.

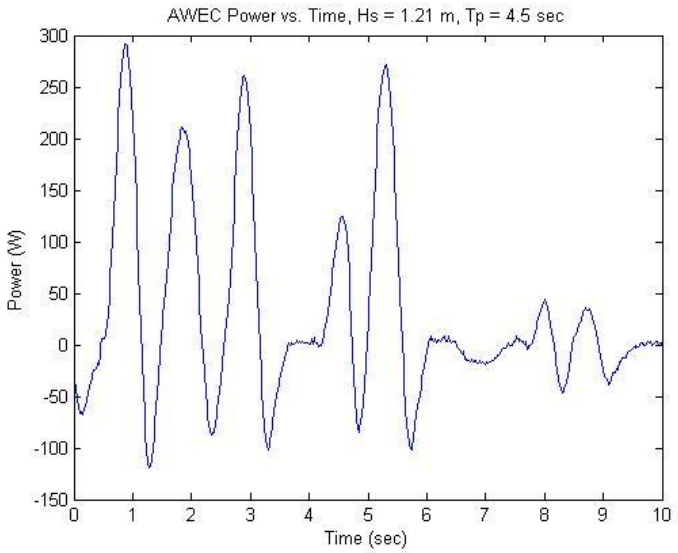

Fig. 91. Power Production with Binary Control and Spectral Waves

Table 7. Loss of Power Output with Mismatched Binary Tuning

H_s (m)	T_p (s)	Power Absorption Ratio
1.47	3.0	0.49
1.32	3.75	0.60
1.21	4.5	1.0
1.11	5.25	0.35

7.9 Ternary Control

The use of ternary (three term) reactive control was implemented even though analysis has shown that this may not be effective with a more complex two-body WEC [8]. Results yielded power levels that were even less than damping control. Fig. 92, Fig.

93, Fig. 94, and Fig. 95 show the results of ternary vs. damping control under spectral conditions.

It is felt that a mistuning of the damping term when using ternary control led to some of the power loss. A damping term was set based on the previous FEA analysis. Especially when testing with spectral waves and long runs are necessary this shows the complexity of tuning with two or three control parameters. After the reactive peak was found, another iteration of adjusting the damping term was necessary.

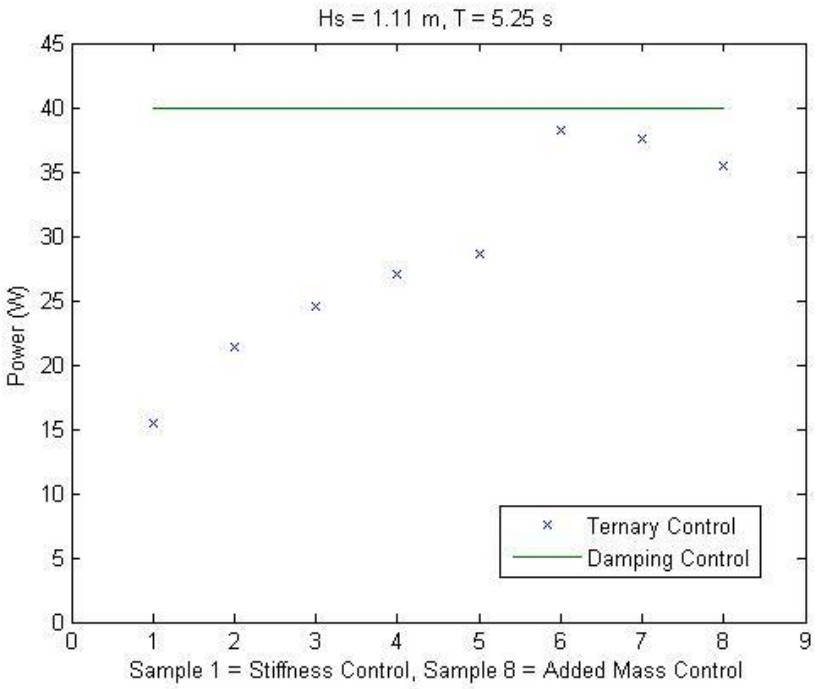

Fig. 92. Ternary Control, T = 5.25 sec

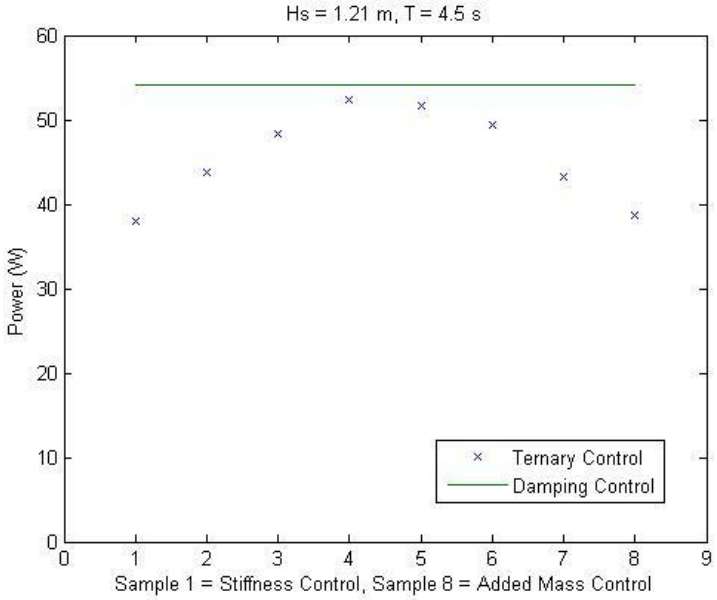

Fig. 93. Ternary Control, T = 4.5 sec

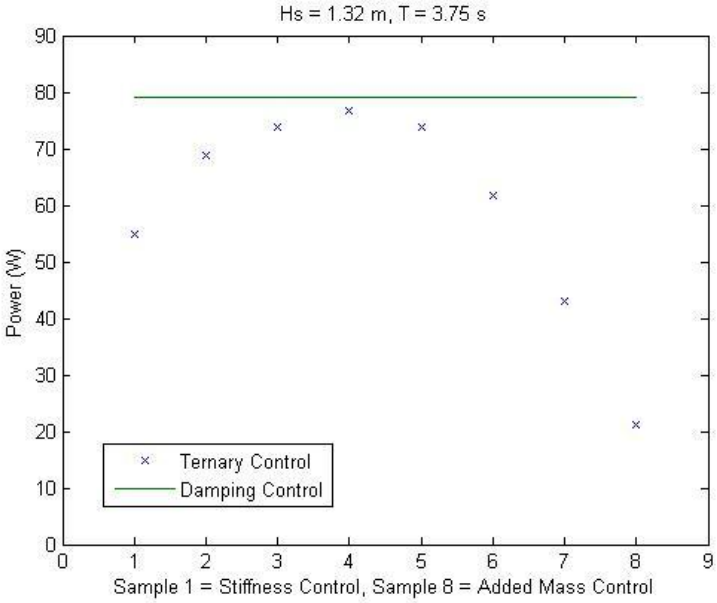

Fig. 94. Ternary Control, T = 3.75 sec

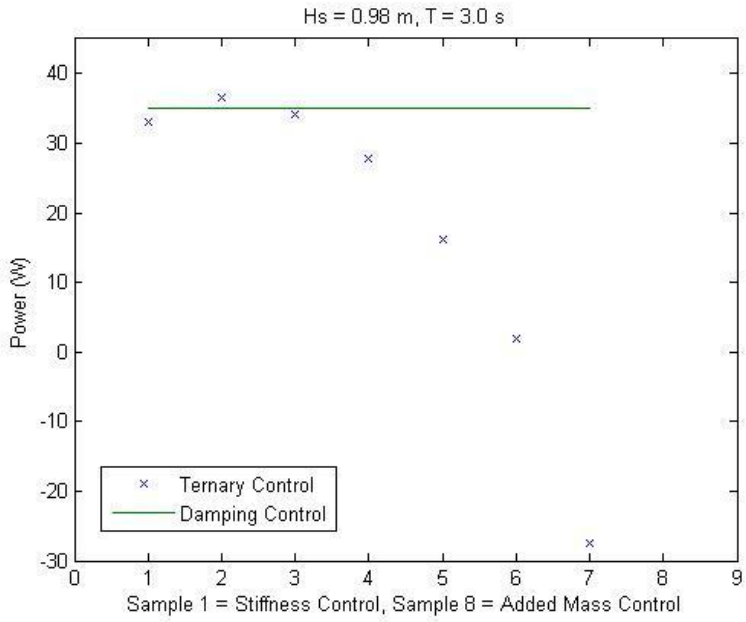

Fig. 95. Ternary Control, T = 3.0 sec

The tuning runs were completed with a fixed value of reactive control that swept from fully using the stiffness term (K); to the use of stiffness, damping, and added mass; to just using the added mass (M) term.

It was interesting to note that the AWEC power absorption bandwidth could be increased by using both components of reactive control (stiffness and added mass). The peak of where this occurred also shifted as expected with differing wave periods.

7.10 Conclusions

Scaled testing of an autonomous WEC design was performed in an instrumented wave lab facility that could apply both monochromatic and spectral wave conditions. Results were obtained that corroborated the trends seen with hydrodynamic FEA analysis. The results confirmed that WEC design must address the inherent power absorption bandwidth of a WEC, especially when utilizing control schemes that require good knowledge of the wave conditions for proper tuning.

It is concluded that for a simpler AWEC damping-only tuning may be preferred. It has a larger power absorption bandwidth, allows for a greater amount of mistuning, and tuning, or optimization, and is simpler with one term. The device may have to be larger but if the PTO efficiency is not high there are diminishing returns of trying to utilize much reactive control.

Because binary control has a narrow bandwidth, mistuning or incorrect system parameters can cause significant power loss.

Ternary control can be used to increase the bandwidth but has the limitation of yet another control parameter to adjust in light of unknown non-linear system parameters.

These methods that rely on knowing the system parameters have all the significant disadvantages without some type of correction, optimizing control, or power point tracking mechanism.

Lastly laboratory limitations, scaling, and the physical realization of a scaled prototype can start to make the lab testing vary significantly from any analysis of the full scale design. The greater this divergence, the less precise analytical analysis and lab results may not match and only trends or general design characteristics obtained.

7.11 References

[1] T. Brekken and A. von Jouanne "ECCE Wave Energy Tutorial," *IEEE Energy Conversion Conference and Exposition*, San Jose, CA, Sept. 2009.

[2] K. Rhinefrank, A. Schacher, J. Prudell, C. Stillinger, D. Naviaux, T. Brekken, A. von Jouanne, D. Newborn, S. Yim, D. Cox, "High Resolution Wave Tank Testing of Scaled Wave Energy Devices," *29th International Conference on Offshore Mechanics and Arctic Engineering (OMAE)*, 2010.

[3] E. Agamloh, "A Direct-Drive Wave Energy Converter with Contactless Force Transmission System," School of Electrical Engineering and Computer Science, Oregon State University, Corvallis, OR, Oct. 2005.

[4] K. Rhinefrank, E. Agamloh, A. von Jouanne, A.K. Wallace, J. Prudell, K. Kimble, J. Aills, E. Schmidt, P. Chan, B. Sweeny, A. Schacher, "Novel Ocean Energy Permanent Magnet Linear Generator Buoy," *Elsevier Renewable Energy Journal*, Vol. 31, Issue 9, July 2006, pg. 1279-1298.

[5] T. Lewis, A. von Jouanne, T. Brekken, "Per-Unit Wave Energy Converter System Analysis," *IEEE Energy Conversion Congress and Exposition*, Phoenix, AZ, Sept. 2011.

[6] T. Lewis, A. von Jouanne, T. Brekken, "Wave Energy Converter with Wideband Power Absorption," *IEEE Energy Conversion Congress and Exposition*, Phoenix, AZ, Sept. 2011.

[7] T. Lewis, A. von Jouanne, T. Brekken, "Modeling and Control of a Slack-Moored Two Body Wave Energy Converter," *IEEE Energy Conversion Congress and Exposition*, Raleigh, NC, Sept. 2012.

[8] T. Lewis, B. Bosma, A. von Jouanne, T. Brekken, "Modeling of a Two-Body Wave Energy Converter Driven by Spectral JONSWAP Waves," *IEEE Energy Conversion Congress and Exposition*, Denver, CO, Sept. 2013.

[9] OrcaFlex, Version 9.3a, Orcina Ltd., Daltergate, UK, www.orcina.com.

[10] M. McCormick, *Ocean Wave Energy Conversion*, Dover Publications, 2007, ISBN-13 978-0-486-46245-5.

[11] G. Payne, "Guidance for the Experimental Tank Testing of Wave Energy Converters," The University of Edinburgh, Vers. 01B, Dec. 22, 2008.

[12] B. Bosma, "On the Design, Modeling, and Testing of Ocean Wave Energy Converters," *PhD Dissertation*, Oregon State University, July 16, 2013.

[13] Det Norske Veritas, "Environmental Conditions and Environmental Loads", Recommended Practice DNV-RP-C205, October 2010.

[14] J. Falnes, *Ocean Waves and Oscillating Systems: Linear Interactions Including Wave-Energy Extraction*, Cambridge University Press, 2002, ISBN-13 978-0-521-01749-7.

[15] J.K.H. Shek, D.E. Macpherson, M.A. Mueller, "Phase and Amplitude Control of a Linear Generator for Wave Energy Conversion," *4th Cconference on Power Electronics, Machines, and Drives*, April 2008, pg. 66-70.

[16] J.K.H. Shek, D.E. Macpherson, M.A. Mueller, J. Xiang, "Reaction Force Control of a Linear Electrical Generator for Direct Drive Wave Energy Conversion," *lET Renewable Power Generation*, 2007,1, (1), pp. 17-24.

8 Conclusions and Future Research

8.1 Conclusions

This body of work spans the investigation, specification, design, performance simulations, fabrication, integration, and wave lab testing of an Autonomous Wave Energy Converter (AWEC). The testing compared several actual wave testing against performance simulations to validate the design. Specifically, with damping control, the approximate loss of power under spectral wave conditions vs. monochromatic wave conditions was validated. Results were shown when using reactive control and although the absolute power numbers differed due to losses and tuning, trends that showed reactive tuning can be used to maximize wave power under spectral conditions was shown. Also, the importance of tuning, or conversely the negative effects of mistuning, was demonstrated at the wave laboratory.

8.2 Future Research

Future research can be extended quite easily from this work. The AWEC was designed and fabricated to be fairly robust with the intent for possible future research. The dSPACE control system allows for rapid control system development. Over 70 GB of O.H. Hinsdale Wave Research Lab and PhaseSpace data was collected.

8.2.1 Full Scale Testing

Now that scaled testing has occurred under both monochromatic and spectral, real world wave conditions the design could be refined and a full scale prototype constructed. The full scale prototype testing could occur at the Pacific Marine Energy Center (PMEC) using the Ocean Sentinal.

8.2.2 System Identification

Two body, six degree of freedom data was collected with the PhaseSpace system. This collection of the motion state space variables with known control and wave stimulus data may be able to be used in another system identification process. The

identification of a suitable linear model could be extracted under different monochromatic wave height and wave period conditions.

8.2.3 Correlation of Data

There could also be further correlation of the data between the O. H. Hinsdale Wave Research Lab collected data and the PhaseSpace system. After the discrepancies in the PhaseSpace data are collected there may be fruitful conclusions linking the motion and control parameters.

In addition to this the correlated data could be compared back to the OrcaFlex FEA analysis. Due to the lab limitations and property constraints the OrcaFlex model would need to be updated to match the wave lab configuration. (It still could remain at the full scale size.) The FEA simulations could then be rerun with the updated model and the actual test wave heights, periods, and spectra to give a more true comparison of the FEA with the lab test results.

8.2.4 Scaling

A scaling mechanism other than Froude scaling with direct physical proportionality could be investigated. The limitations of this scaling, particularly for power, but also for mass/buoyancy and damping, caused increases in inefficiencies, and design and fabrication tradeoffs.

8.2.5 Control

All of the classic control methods and the additional one studied in this research are all essentially feed forward control so they are highly dependent on knowing the system properties. Being able to wrap a control loop around the system and have some amount of adaptations, for example some form of model reference control, could be investigated.

If better system identification is obtained perhaps some sort of inverse transfer function control could be implemented to still investigate obtaining a wider bandwidth response.

Better system identification and control could lead to researching the implementation of some adaptive control, specifically Model Reference Adaptive Control (MRAC) or Model Identification Adaptive Control (MIAC).

During time of low wave energy the full kVA of the power take-off may be able to be exploited even if the AWEC is design for damping control - blended damping and reactive hybrid control approach.

8.2.6 Simulation Software

The OrcaFlex FEA package had limitations, or at least greatly increased complexity, if control any more complex than implemented here were to be attempted. Perhaps there are other packages that are more beneficial to use when researching power take-off and control issues.

9 Bibliography

[1] Andrews, Jelley, Energy Science: Principles, Technologies, and Impacts, Oxford University Press, 2007.

[2] T. Brekken and A. von Jouanne "ECCE Wave Energy Tutorial", Energy Conversion Conference and Exposition, Sept 2009

[3] G. Haggerman, "Wave Energy Systems for Recharging AUV Supplies," Workshop on Autonomous Underwater Vehicles, June 2002, pg. 75-84.

[4] N.J. Baker, "Linear Generators for Direct Drive marine Renewable Energy Converters", University of Durham, PhD. Thesis, 2003

[5] J. Falnes, Ocean Waves and Oscillating Systems: Linear Interactions Including Wave-Energy Extraction, Cambridge University Press, 2002.

[6] M. Patel, "Dynamics of offshore structures," Butterworth and Co. Ltd., 1980.

[7] K. Thorburn, "Electric Energy Conversion Systems: Wave Energy and Hydropower," Digital Comprehensive Summaries of Uppsala Dissertations from the Faculty of Science and Technology 202, Uppsala University, 2006.

[8] H. Polinder and M. Scuotto, "Wave Energy Converters and their Impact on Power Systems," in 2005 International Conference on Future Power Systems, Nov. 2005.

[9] M. Previsic, "Wave Power Technologies", IEEE Conference Proceeding Power Engineering Society General Meeting, 12-16 June 2005, Vol. 2, pg. 2011-2016.

[10] M. Leijon, H. Bernhoff, O. Agren, J. Isberg, J. Sundberg, M. Berg, K. E. Karlsson, and A. Wolfbrandt, "Multiphysics Simulation of Wave Energy to Electric Energy Conversion by Permanent Magnet Linear Generators," in IEEE Transaction on Energy Conversion, Vol. 20, Issue 1, pp. 219-224, Mar 2005.

[11] H. Polinder, B.C. Mecrow, A.G. Jack, P.G. Dickinson, M.A. Mueller, "Conventional and TFPM Linear Generators for Direct-Drive Wave Energy Conversion", IEEE Trans. on Energy Conversion, Vol. 20, No.2, June 2005

[12] M. Langeliers, E. Agamloh, A. von Jouanne, A. Wallace, "A Permanent Magnet, Rack and Pinion Gearbox for Ocean Energy Extraction," 44th AIAA Aerospace Science Meeting and Exhibit, Reno, NV, Jan. 2006, AIAA-2006-999.

[13] K. Rhinefrank, E.B. Agamloh, A. von Jouanne, A.K. Wallace, J. Prudell, K. Kimble, J. Aills, E. Schmidt, P. Chan, B. Sweeny, A. Schacher, "Novel Ocean Energy Permanent Magnet Linear Generator Buoy", *Elsevier Renewable Energy* Journal, Vol. 31, Issue 9, July 2006, pg. 1279-1298

[14] E.B. Agamloh, A.K. Wallace, and A. von Jouanne, "A Novel Direct-Drive Ocean Wave Energy Extraction Concept with Contact-Less Force Transmission System," Renewable Energy, Vol. 33, 2008, pp. 520-529.

[15] J.H. Prudell, "Novel Design and Implementation of a Permanent Magnet Linear Tubular Generator for Wave Energy Conversion," Master's Thesis. Corvallis, OR: Oregon State University, 2007.

[16] M.A. Mueller, "Current and Novel Electrical Generator Technology for Wave Energy Converters," International Electric Machine and Drive Conference, May 2007, pg. 1401-1406.

[17] M.A. Mueller, A.S. McDonald & D.E. Macpherson "Structural Analysis of Low Speed Axial Flux Permanent Magnet Machines", IEE Proceedings on Electric Power Applications, Vol 152, No. 6, pp. 1417-1426, November 2005, ISSN 1350-2352

[18] H. Polinder, M. Damen, and F. Gardner, "Linear PM Generator System for Wave Energy Conversion in the AWS," IEEE Transactions on Energy Conversion, Vol. 19, Issue 3, Sept. 2004, pg. 583-589.

[19] M.A. Mueller, "Electrical generators for direct drive wave energy converters," in Proc. Inst. Elect. Eng. Generation, Transmission and Distribution, vol. 149, 2002, pp. 446–456.

[20] N.J. Baker, M.A. Mueller, E. Spooner, "Permanent magnet air-cored tubular linear generator for marine energy converters"' University of Durham, University of Edinburgh, IEE, 2004

[21] M. Blanco, G. Navarro, M. Lafoz, “Control of Power Electronics Driving a Switched Reluctance Linear Generator in Wave Energy Applications,” 13th European Conference on Power Electronics and Applications, Sept. 1009, pg. 1-9.

[22] P. Cancelliere, F. Marignetti, V. Delli Colli, R. Di Stefano, M. Scarano, “A Tubular Generator For Marine Energy Direct Drive Applications”, DAEIMI-Department of Automation, Faculty of Engineering, University of Cassino, 2005

[23] K. Rhinefrank, T. Brekken, B. Pasch, A. Yokochi, and A. von Jouanne, “Comparison of Linear Generators for Wave Energy Applications,” 46th AIAA Aerospace Science Meeting and Exhibit, Reno, NV, Jan. 2008, AIAA-2008-1335.

[24] Z. Nie, P.C.J. Clifton, Y. Wu, and R.A. McMahon, “Emulation and Power Conditioning of Outputs from a Direct Drive Wave Energy Converter,” International Conference on Sustainable Energy Technologies, Nov. 2008, pg. 1129-1133.

[25] A. Schacher, A.V. Meulen, D. Elwood, P. Hogan, K. Rhinefrank, T. Brekken, A. von Jouanne, S. Yim, “Novel Control Design for a Wave Energy Generator,” 46th AIAA Aerospace Science Meeting and Exhibit, Reno, NV, Jan. 2008, AIAA-2008-1305.

[26] J.K.H. Shek, D.E. Macpherson, M.A. Mueller, "Phase and Amplitude Control of a Linear Generator for Wave Energy Conversion" 4th conference on Power Electronics, Machines, and Drives, April 2008, pg. 66-70.

[27] J.K.H. Shek, D.E. Macpherson, M.A. Mueller, J. Xiang, "Reaction Force Control of a Linear Electrical Generator for Direct Drive Wave Energy Conversion", lET Renewable Power Generation, 2007,1, (1), pp. 17-24.

[28] E. Spooner, P. Tavner, M.A. Mueller, N.J. Baker, "Vernier Hybrid Machines for Compact Drive Applications". lEE Int. Conf. Power Electronics, Machines and Drives, Edinburgh, UK, 2004, pp. 452-457.

[29] T. Lewis, A. von Jouanne, T. Brekken, “Wave Energy Converter with Wideband Power Absorption,” Digest for *IEEE Energy Conversion Congress and Exposition 2011*.

[30] C.A. Gross, S.P. Melipoulos, “Per-Unit Scaling in Electric Power Systems”, *Transactions on Power Systems*, Vol. 7, No. 2, May 1992.

[31] P.C. Krause, O. Wasynczuk, S.D. Sudhoff, *Analysis of Electric Machinery*, McGraw Hill, 1986

[32] M.E. McCormick, *Ocean Wave Energy Conversion*, Dover Publicatons, 2007.

[33] T. Lewis, A. von Jouanne, T. Brekken, “Per-Unit Wave Energy Converter System Analysis,” Digest for *IEEE Energy Conversion Congress and Exposition 2011*.

[34] S.J. Orfanidis, *Electromagnetic Waves and Antenna*, ECE Department, Rutgers University, 2011. Site: *www.ece.rutgers.edu/~orfanidi/ewa/*

[35] E. Tedeschi, M. Molinas, M. Carraro, P. Mattavelli, “Analysis of Power Extraction from Irregular Waves by All-Electric Power Take-off”, IEEE Energy Conversion Congress and Expo, Sept. 2010, pp. 2370-2377.

[36] T.K.A. Brekken, B. Batten, E. Amon, “From Blue to Green,” *Control System Magazine*, to be published Fall 2011

[37] Office of Naval Research (ONR), http://www.dtic.mil/descriptivesum/ Y2008 / Navy/0603747N.pdf

[38] K. Ruehl, T.K. Brekken, B. Bosma, P. Paasch, “Large-Scale Ocean Wave Energy Plant Modeling,” *IEEE Conference on Innovative Technologies for an Efficient and Reliable Electricity Supply (CITRES)*, 2010, pp. 379-386.

[39] H. Eidsmoen, “Simulation of a Slack-Moored Heaving-Buoy Wave Energy Converter with Phase Control,” Division of Physics, Norwegian University of Science and Technology, Trondheim, Norway, May 1996.

[40] OrcaFlex, Version 9.3a, Orcina Ltd., Daltergate, UK, www.orcina.com.

[41] AQWA, ANSYS Inc., www.ansys.com.

[42] J. Cruz, *Ocean Wave Energy*, Springer Series in Green Energy and Technology, 2008, ISBN-13 978-3-540-74894-6.

[43] Z. Zhang, “Development of Adaptive Damping Power Take-Off Control for a Three-Body Wave Energy Converter with Numerical Modeling and Validation,”

School of Electrical Engineering and Computer Science, Oregon State University, Corvallis, OR, Dec. 2011.

[44] T. Lewis, A. von Jouanne, T. Brekken, "Modeling and Control of a Slack-Moored Two Body Wave Energy Converter," *IEEE Energy Conversion Congress and Exposition*, Raleigh, NC, Sept. 2012.

[45] Det Norske Veritas, "Environmental Conditions and Environmental Loads", Recommended Practice DNV-RP-C205, October 2010.

[46] T. Lewis, B. Bosma, A. von Jouanne, T. Brekken, "Modeling of a Two-Body Wave Energy Converter Driven by Spectral JONSWAP Waves," *IEEE Energy Conversion Congress and Exposition*, Denver, CO, Sept. 2013.

[47] G. Payne, "Guidance for the Experimental Tank Testing of Wave Energy Converters," The University of Edinburgh, Vers. 01B, Dec. 22, 2008.

[48] B. Bosma, "On the Design, Modeling, and Testing of Ocean Wave Energy Converters," *PhD Dissertation*, Oregon State University, July 16, 2013.